AD-A046 414 ARMY ENGINEER WATERWAYS EXPERIMENT STATION VICKSBURG MISS F/G 8/8
DESIGN WAVE INFORMATION FOR THE GREAT LAKES: REPORT 4. LAKE HUR--ETC(U)
SEP 77 D T RESIO, C L VINCENT

UNCLASSIFIED WES-TR-H-76-1-4 NL

1 OF 2
ADA
046414

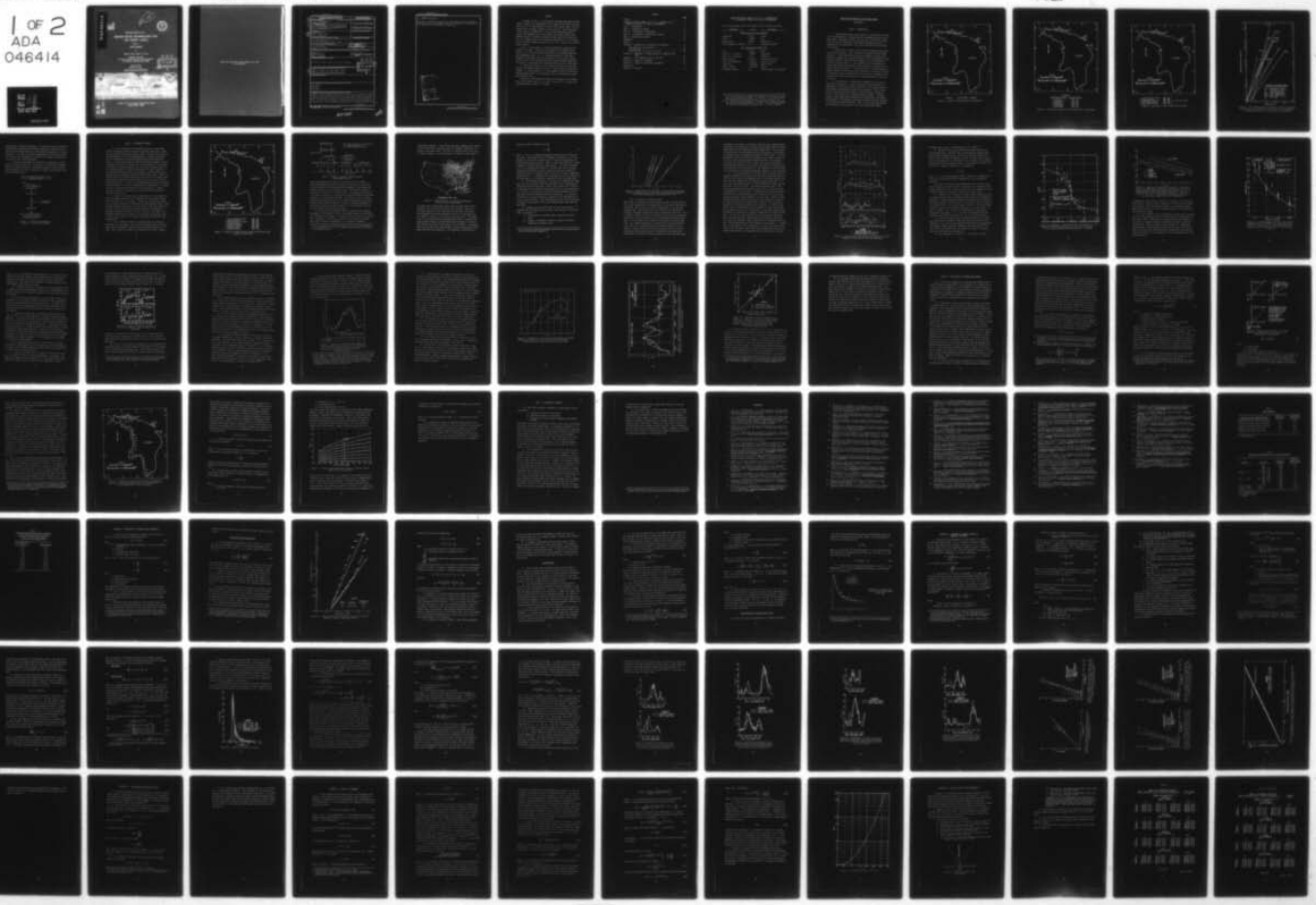

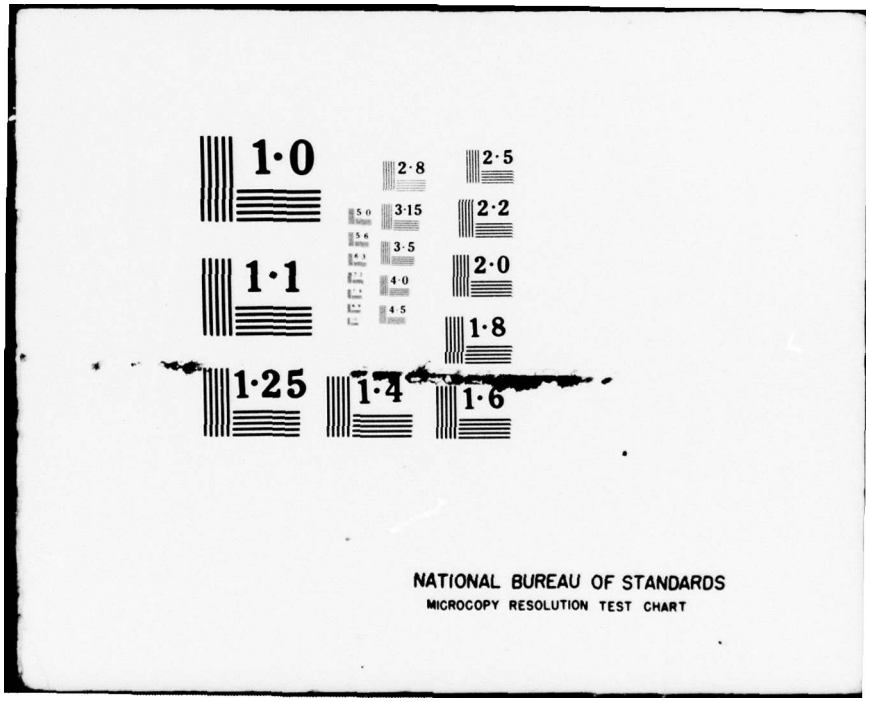
1·0
1·1
1·25
1·4
1·6
1·8
2·0
2·2
2·5
2·8
3·15
3·5
4·0
4·5
5·0
5·6
NATIONAL BUREAU OF STANDARDS
MICROCOPY RESOLUTION TEST CHART

TECHNICAL REPORT H-76-1

DESIGN WAVE INFORMATION FOR THE GREAT LAKES

Report 4

LAKE HURON

by

Donald T. Resio, Charles L. Vincent

Hydraulics Laboratory
U. S. Army Engineer Waterways Experiment Station
P. O. Box 631, Vicksburg, Miss. 39180

September 1977
Report 4 of a Series

Prepared for U. S. Army Engineer Division, North Central
Chicago, Illinois 60605

Destroy this report when no longer needed. Do not return it to the originator.

Unclassified

SECURITY CLASSIFICATION OF THIS PAGE (When Data Entered)

REPORT DOCUMENTATION PAGE

READ INSTRUCTIONS BEFORE COMPLETING FORM

1. REPORT NUMBER: Technical Report H-76-1-4	2. GOVT ACCESSION NO.
3. RECIPIENT'S CATALOG NUMBER	
4. TITLE (and Subtitle): DESIGN WAVE INFORMATION FOR THE GREAT LAKES: Report 4, LAKE HURON.	5. TYPE OF REPORT & PERIOD COVERED: Report 4 of a series
	6. PERFORMING ORG. REPORT NUMBER
7. AUTHOR(s): Donald T. Resio, Charles L. Vincent	8. CONTRACT OR GRANT NUMBER(s)
9. PERFORMING ORGANIZATION NAME AND ADDRESS: U. S. Army Engineer Waterways Experiment Station, Hydraulics Laboratory, P. O. Box 631, Vicksburg, Miss. 39180	10. PROGRAM ELEMENT, PROJECT, TASK AREA & WORK UNIT NUMBERS
11. CONTROLLING OFFICE NAME AND ADDRESS: U. S. Army Engineer Division, North Central, 536 South Clark St., Chicago, Ill. 60605	12. REPORT DATE: September 1977
	13. NUMBER OF PAGES: 153
14. MONITORING AGENCY NAME & ADDRESS (if different from Controlling Office): 12 158p.	15. SECURITY CLASS. (of this report): Unclassified
	15a. DECLASSIFICATION/DOWNGRADING SCHEDULE

16. DISTRIBUTION STATEMENT (of this Report)

Approved for public release; distribution unlimited.

DDC RECEIVED NOV 16 1977 B

17. DISTRIBUTION STATEMENT (of the abstract entered in Block 20, if different from Report)

14 WES-TR-H-76-1-4

18. SUPPLEMENTARY NOTES

19. KEY WORDS (Continue on reverse side if necessary and identify by block number)

Design wave
Great Lakes
Lake Huron
Water waves

20. ABSTRACT (Continue on reverse side if necessary and identify by block number)

This report contains hindcast wave information that is applicable to many planning and design purposes on Lake Huron. Historical wind data from stations along Lake Huron served as input to the numerical hindcast model, and significant wave heights were calculated for 5-, 10-, 20-, 50-, and 100-yr return periods. These results are provided in tabular form for 28 points along the Lake Huron shoreline. The mean significant period for each of these wave heights is →

(Continued)

DD FORM 1 JAN 73 1473 EDITION OF 1 NOV 65 IS OBSOLETE

Unclassified

SECURITY CLASSIFICATION OF THIS PAGE (When Data Entered)

038100

4B

20. ABSTRACT (Continued).

also given. Information is provided for four seasons of the year (January-March, April-June, July-September, and October-December) and is separated into three approach directions relative to shore. ←

PREFACE

A request for the U. S. Army Engineer Waterways Experiment Station (WES) to conduct an investigation of wave heights on the Great Lakes was made by the U. S. Army Engineer Division, North Central (NCD), in a conference held in Chicago, Illinois, on 22 July 1974. Funds were authorized by NCD on 30 August 1974. The study was conducted during the period from September 1974 to June 1976 in the Coastal Branch, Wave Dynamics Division, Hydraulics Laboratory, WES, under the direction of Mr. H. B. Simmons, Chief of the Hydraulics Laboratory, Dr. R. W. Whalin, Chief of the Wave Dynamics Division, and Dr. C. L. Vincent, Chief of the Coastal Branch.

Drs. D. T. Resio and C. L. Vincent conducted the study and also prepared the report. During the investigation, Mrs. Rebecca Brooks and Mr. W. D. Corson were especially helpful in performing analytical and programming tasks. Dr. L. H. Blakey and Messrs. N. Arno and L. Hiipakka of NCD exhibited a keen perception of the priority need and practical use of this information and contributed valuable suggestions to the form of the design wave information required on the Great Lakes.

A significant proportion of the numerical computations were performed on a CDC-7600 computer at the U. S. Army facility in Huntsville, Alabama. Mr. Fred Bourgeois, U. S. Army Engineer Division, Huntsville, assisted significantly in coordinating visits to Huntsville and scheduling computer time.

Directors of WES during the conduct of the study and the preparation of this report were COL G. H. Hilt, CE, and COL J. L. Cannon, CE. Technical Director was Mr. F. R. Brown.

CONTENTS

	Page
PREFACE	1
CONVERSION FACTORS, METRIC (SI) TO U. S. CUSTOMARY AND U. S. CUSTOMARY TO METRIC (SI) UNITS OF MEASUREMENT	3
PART I: INTRODUCTION	4
PART II: ESTIMATION OF WINDS	11
PART III: APPLICATION OF WAVE MODELS	23
PART IV: THE ANALYSIS OF EXTREME WAVE HEIGHTS	33
PART V: DISCUSSION OF RESULTS	43
REFERENCES	45
TABLES 1-5	
APPENDIX A: METHODOLOGY OF OVERLAKE WIND ESTIMATION	A1
Post-1948 Wind Transformations	A2
Pre-1948 Winds	A5
Transformation to Winds Over the Lake	A7
APPENDIX B: TREATMENT OF GENERAL ASPECTS OF NUMERICAL WAVE MODEL	B1
APPENDIX C: WIND INTERPOLATION OVER THE LAKE	C1
APPENDIX D: ANALYSIS OF EXTREMES	D1
APPENDIX E: TABLES OF DESIGN WAVE INFORMATION	E1
TABLES E1-E4	
APPENDIX F: NOTATION	F1

CONVERSION FACTORS, METRIC (SI) TO U. S. CUSTOMARY AND U. S. CUSTOMARY TO METRIC (SI) UNITS OF MEASUREMENT

Units of measurement used in this report can be converted as follows:

Multiply	By	To Obtain
Metric (SI) to U. S. Customary		
centimetres	0.3937	inches
metres	3.28084	feet
square metres	10.7638	square feet
Celsius degrees or Kelvins	9/5	Fahrenheit degrees*
U. S. Customary to Metric (SI)		
feet	0.3048	metres
miles (U. S. statute)	1.609344	kilometres
miles (U. S. nautical)	1.852	kilometres
miles per hour	1.609344	kilometres per hour
knots (international)	0.5144444	metres per second
square feet	0.09290304	square metres
degrees (angle)	0.01745329	radians
Fahrenheit degrees	5/9	Celsius degrees or Kelvins**

* To obtain Fahrenheit (F) temperature readings from Celsius (C) readings, use the following formula: $F = 9/5(C) + 32$. To obtain Fahrenheit readings from Kelvins (K), use: $F = 9/5(K - 273.15) + 32$.

** To obtain Celsius (C) temperature readings from Fahrenheit (F) readings, use the following formula: $C = 5/9(F - 32)$. To obtain Kelvin (K) readings from Fahrenheit readings, use: $K = 5/9(F + 459.67)$.

DESIGN WAVE INFORMATION FOR THE GREAT LAKES

LAKE HURON

PART I: INTRODUCTION

1. The primary purpose of this study is to provide wave information for planned sites of dredged material retaining structures on the Great Lakes. Secondary goals are the provision of wind-field information over the Great Lakes and detailed wave information along U. S. shorelines of the Great Lakes. This report deals with wave conditions on Lake Huron.

2. Past studies of waves on Lake Huron have generally been made on a site-to-site basis. Very few data are available from wave gages (Figure 1). Visual wave observations are available from Coast Guard stations at several shore locations (Figure 2) and from commercial ships for waves offshore. Data from wave hindcasts are also available for several locations (Figure 3). For a specific site, inconsistencies exist between these data that make them unreliable for estimates of recurrence intervals (Figure 4). The sensitivity of economic analyses of optimal design criteria to even small variations in recurrence intervals of large waves clearly demonstrates an acute need for a reliable source of wave data as well as an evaluation of the distribution of errors in these data.

3. The sparseness of reliable wave information is critical for many areas on Lake Huron. Visual observations from shore cannot be extrapolated to other sites along a shore due to the unknown effects of shallow-water transformations and shorelines geometry. Visual observations from ships provide estimates of waves offshore but are difficult to treat properly in a shallow-water environment. Although a network of wave gages might eventually provide good data, the expense involved makes it economically infeasible to provide detailed coverage of the entire Lake Huron shoreline. Even if such a wave gage network were established, there would be a lag time of many years before

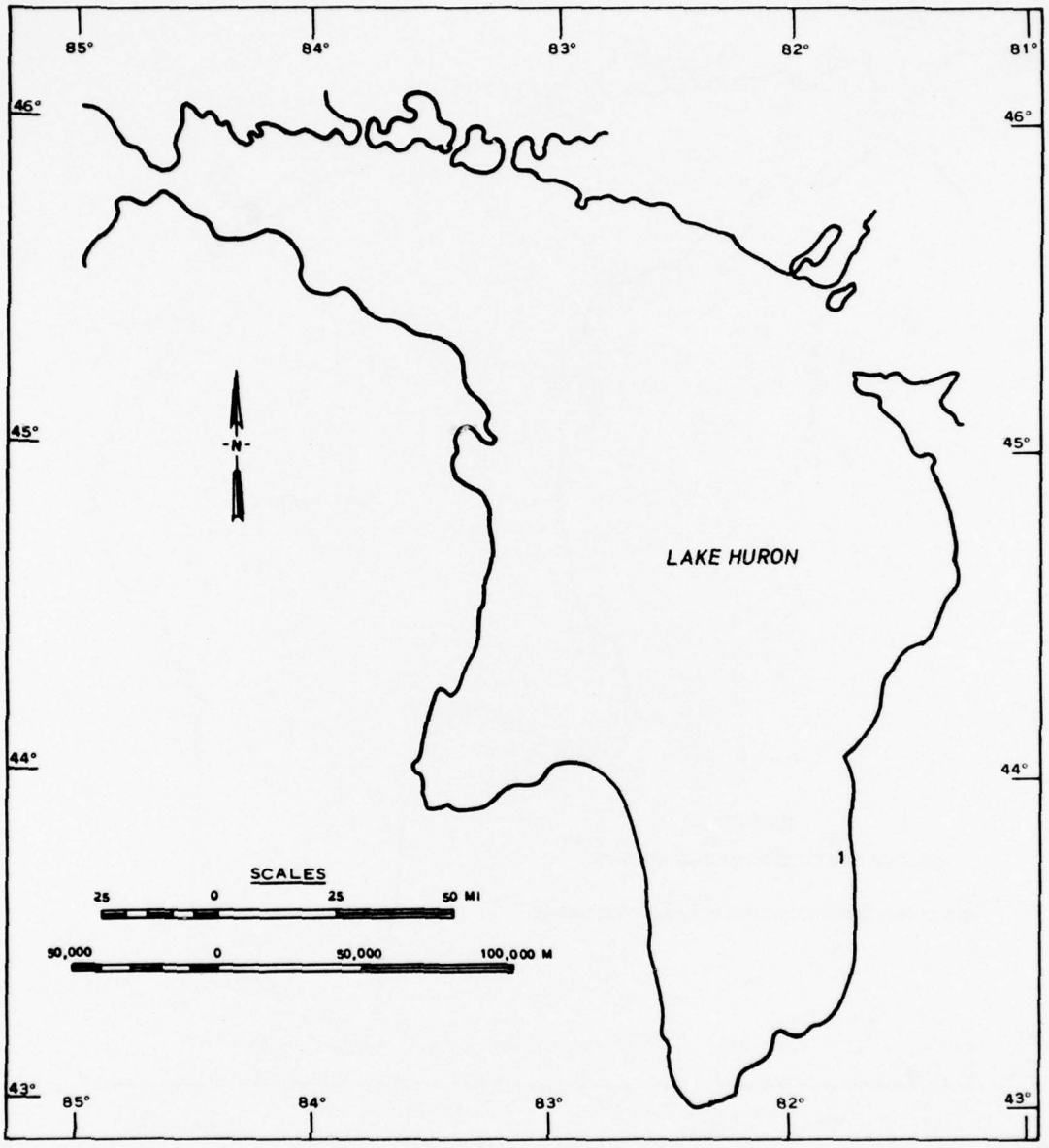

1 GODERICH 1972 SEPTEMBER - DECEMBER

Figure 1. Location of wave gage site on Lake Huron

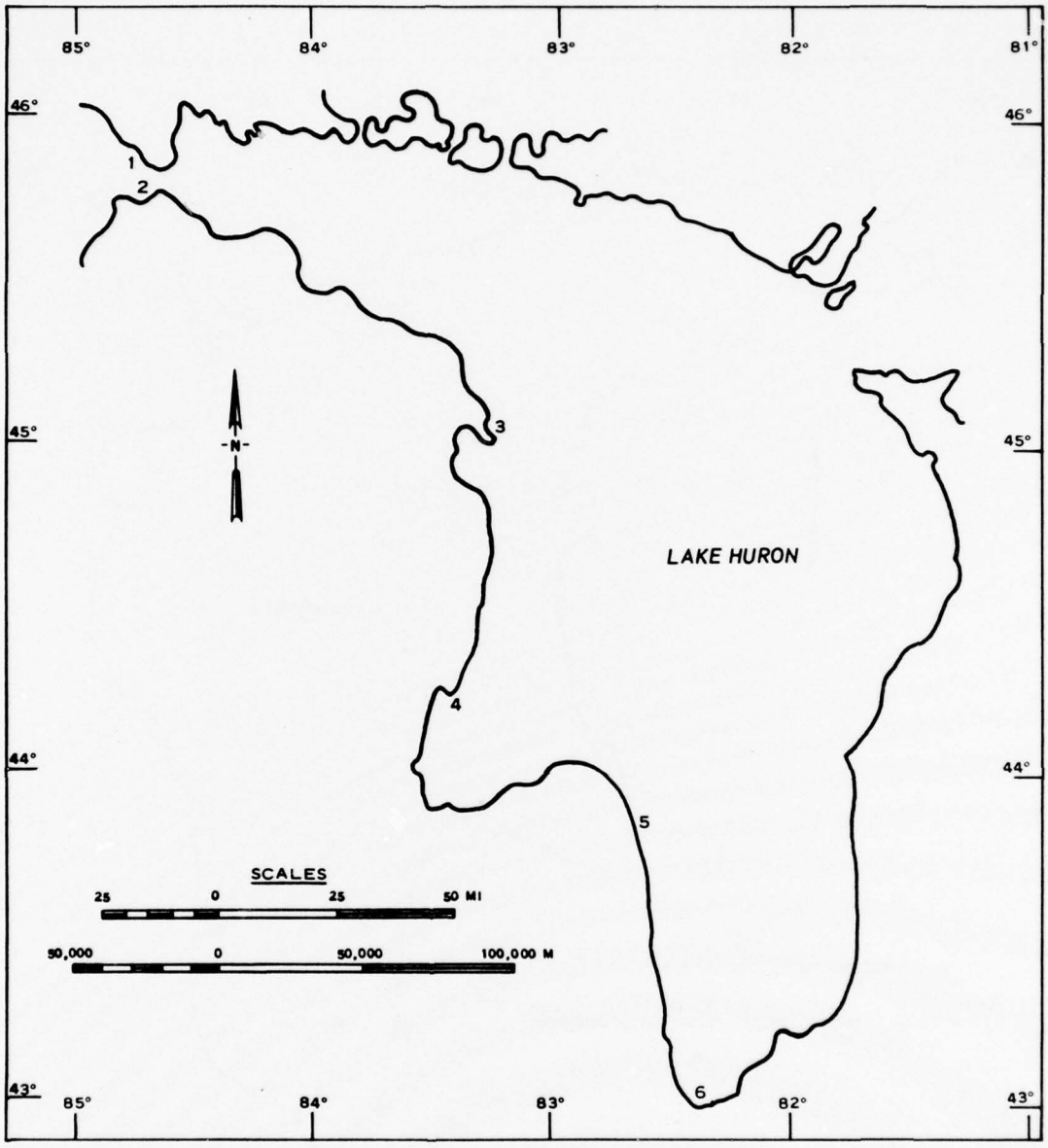

MICHIGAN

COAST GUARD STATIONS	PERIOD OF RECORD
1 ST. IGNACE	1970 – 1971
2 MACKINAW CITY	1914 – 1968
3 THUNDER BAY	1945 – 1971
4 TAWAS POINT	1944 – 1971
5 HARBOR BEACH	1968 – 1971
6 PORT HURON	1941 – 1971

Figure 2. Locations of visual wave observation sites on Lake Huron

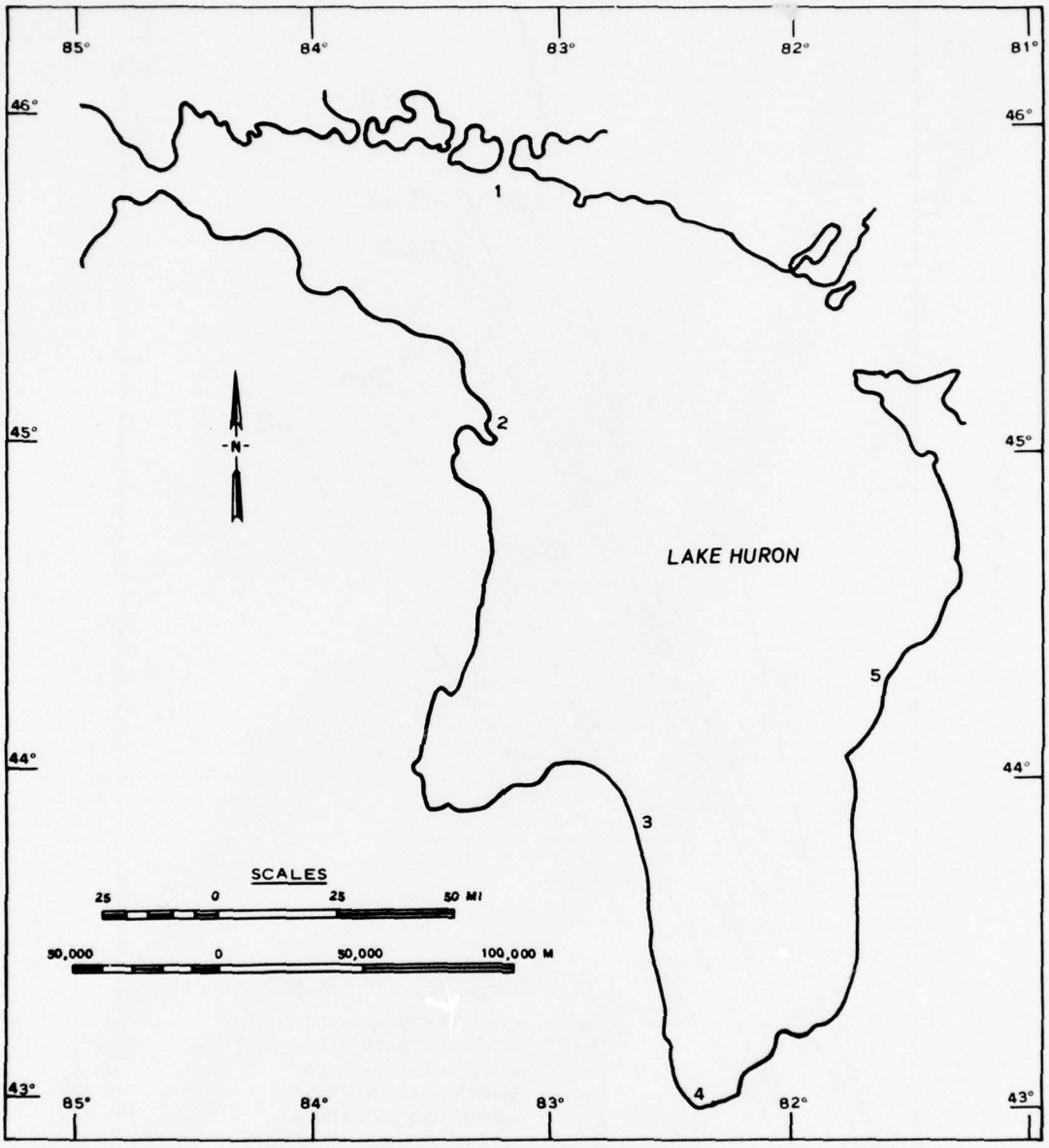

1	COCKBURN ISLAND, ONTARIO	1965 – 1967	COLE AND HILFIKER[1]
2	ALPENA, MICHIGAN	1965 – 1967	
3	HARBOR BEACH, MICHIGAN	1965 – 1967	
4	PORT HURON, MICHIGAN	1965 – 1967	
5	DOUGLAS POINT, ONTARIO	1965 – 1967	

Figure 3. Locations of sites on Lake Huron hindcast

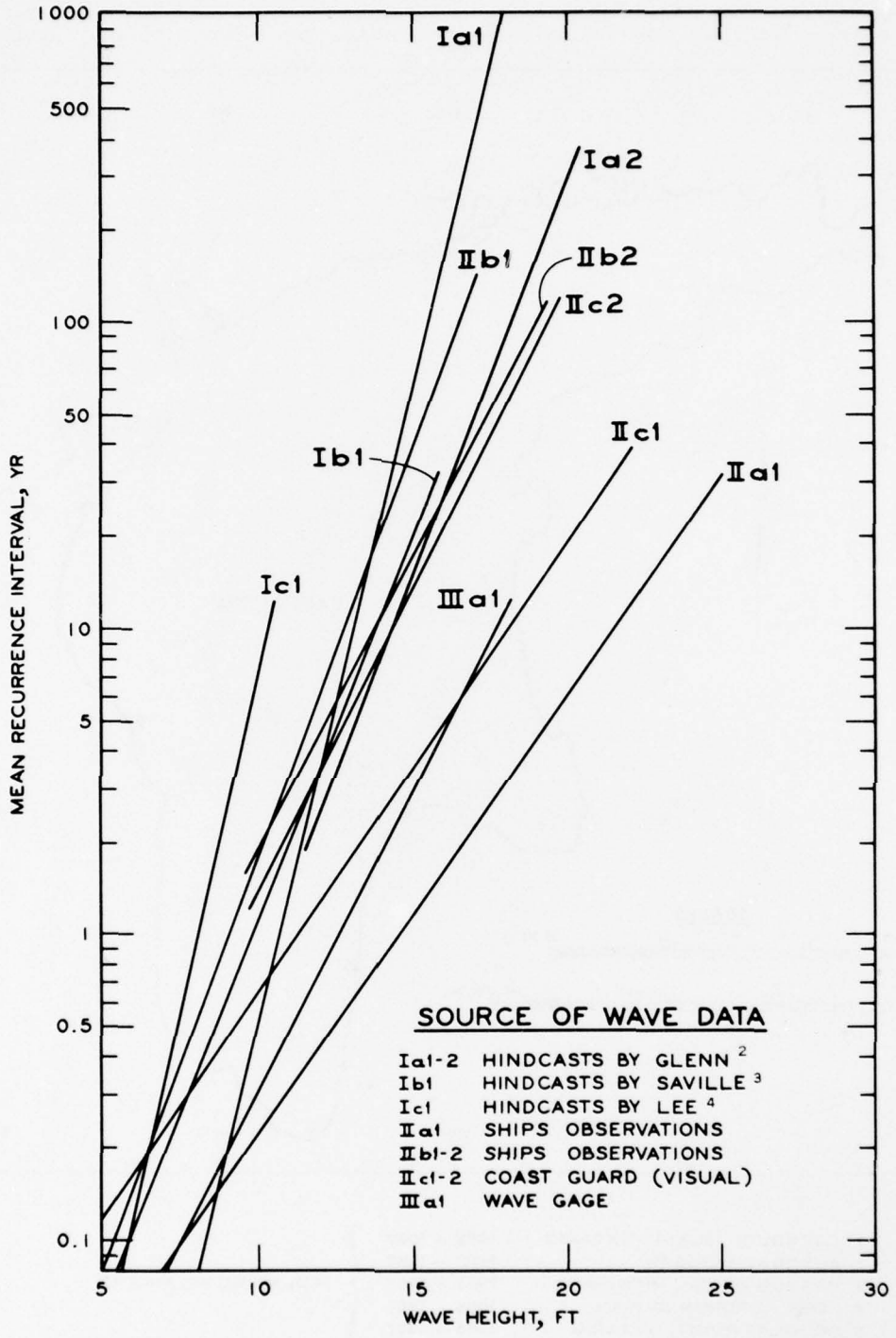

Figure 4. Chart showing range of estimates of design wave heights for Cleveland. Arabic numbers 1 and 2 refer to full population and asymptotic methods of extreme analysis, respectively

sufficient wave information was available for design purposes. Hindcasted waves can provide data along the entire Lake Superior shoreline; however, there are many problems that must be overcome, if reliable hindcasts are to be obtained. The treatment of some of these and the selection of an appropriate wave model will be discussed in detail in Part III, along with comparisons of this numerical wave model to the Sverdrup-Munk-Bretschneider (SMB) technique described in the Shore Protection Manual (SPM).[5]

4. In spite of uncertainties of hindcast methods, the immediate need for wave data on Lake Huron makes an approach via hindcasting the only viable alternative. Historical wind fields can be used to establish a length of record up to 22 yr for Lake Huron. The sparsity of stations and large lake surface area make any effort to hindcast beyond 22 yr dubious.

5. The largest wind-generated waves on the Great Lakes are those produced by synoptic-scale circulation features such as extratropical and tropical cyclones. Smaller-scale wind phenomena, such as individual thunderstorms or squall lines, do not maintain high winds over sufficient fetch to generate waves of comparable height.* Consequently, the study of extreme wave conditions on the Great Lakes is equivalent to the study of extreme synoptic events.

6. The use of a hindcast technique to estimate wave heights assumes that the coupling between the atmospheric boundary layer and waves generated by the motion in this boundary layer is known. Other factors, such as the interaction between waves and the lake bottom and interactions between different spectral wave components, also must be considered. If all these effects can be treated adequately and if the atmospheric motion over a lake is known, then a reliable estimate of waves can be made. In any estimate of wave height, there will always be some error whether the estimate is from a wave gage, visual

---

* This refers only to waves with periods of less than 30 sec. Long waves can be generated by a resonant interaction with a front or squall line, but this is essentially a different process than the growth of wave spectra covered in this report.

observations, or hindcast techniques. The essential question that must be answered for engineering and planning purposes is how much error is there in these methods relative to the requisite accuracies for a given application. In order to facilitate answering this question for potential users of wave information, an effort will be made to include control bands for all results presented.

7. Figure 5 demonstrates an overview of the approach to be followed in the estimation of wave information for the design of dredged material retaining structures. The general approach is valid as well for any application in which information is needed, particularly in the range of extreme values.

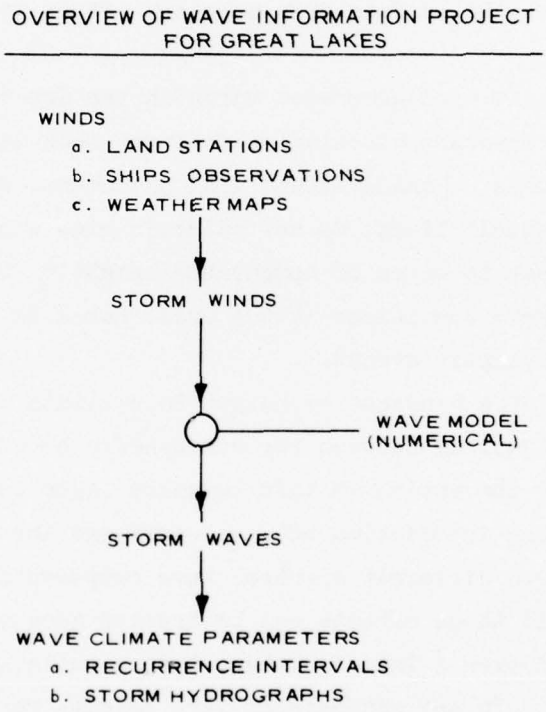

Figure 5. Overview of hindcasting approach to design wave estimates

PART II: ESTIMATION OF WINDS

8. Lack of continuous wind observations over the Great Lakes forces the conclusion that, for practical purposes, winds over a lake must be estimated from other sources of data. Time and space scales of wave generation, as well as the adaptability to computer processing, must be considered in choosing the methodology for these wind estimates. The only three sources of data with sufficient length of record to permit calculation of extremes for the Great Lakes are (a) pressure observations at adjacent land stations, (b) synoptic weather maps, and (c) wind observations at adjacent land stations. Recent studies by Cole and Hilfiker[1] have shown that a network of pressure data around a lake can produce reasonable forecasts of winds over a lake. However, a study by Resio and Vincent[6] demonstrated that the use of suitably transformed overland winds from around a lake can also provide an accurate overlake wind field. The ease of data manipulation and wind field interpolation (Appendix C) in this technique make it advantageous to consider the use of these wind transformations for lake hindcasts. Figure 6 shows the locations of the major sites at which wind data have been recorded on Lake Huron.

9. Reports 1 (Lake Erie) and 2 (Lake Ontario) of this series and WES Miscellaneous Paper H-76-12[6] established the relationship between winds over land and over the lakes. Theoretical and empirical support of the technique employed is detailed in this Miscellaneous Paper. Thus, specific examples presented in this report may be taken from Lakes Erie or Ontario with the data from Lake Huron serving as a supplement to increase the general confidence in earlier results. The concept is to accumulate general data in support of the proposed wind and wave techniques with each report in this series rather than to treat each lake independently.

10. Cole[7] reviewed a number of techniques used for estimating winds over the Great Lakes. His conclusions indicated that none of the presently used techniques correlated well with winds observed over a lake. Table 1 gives the results Cole obtained in his study. Figure 7

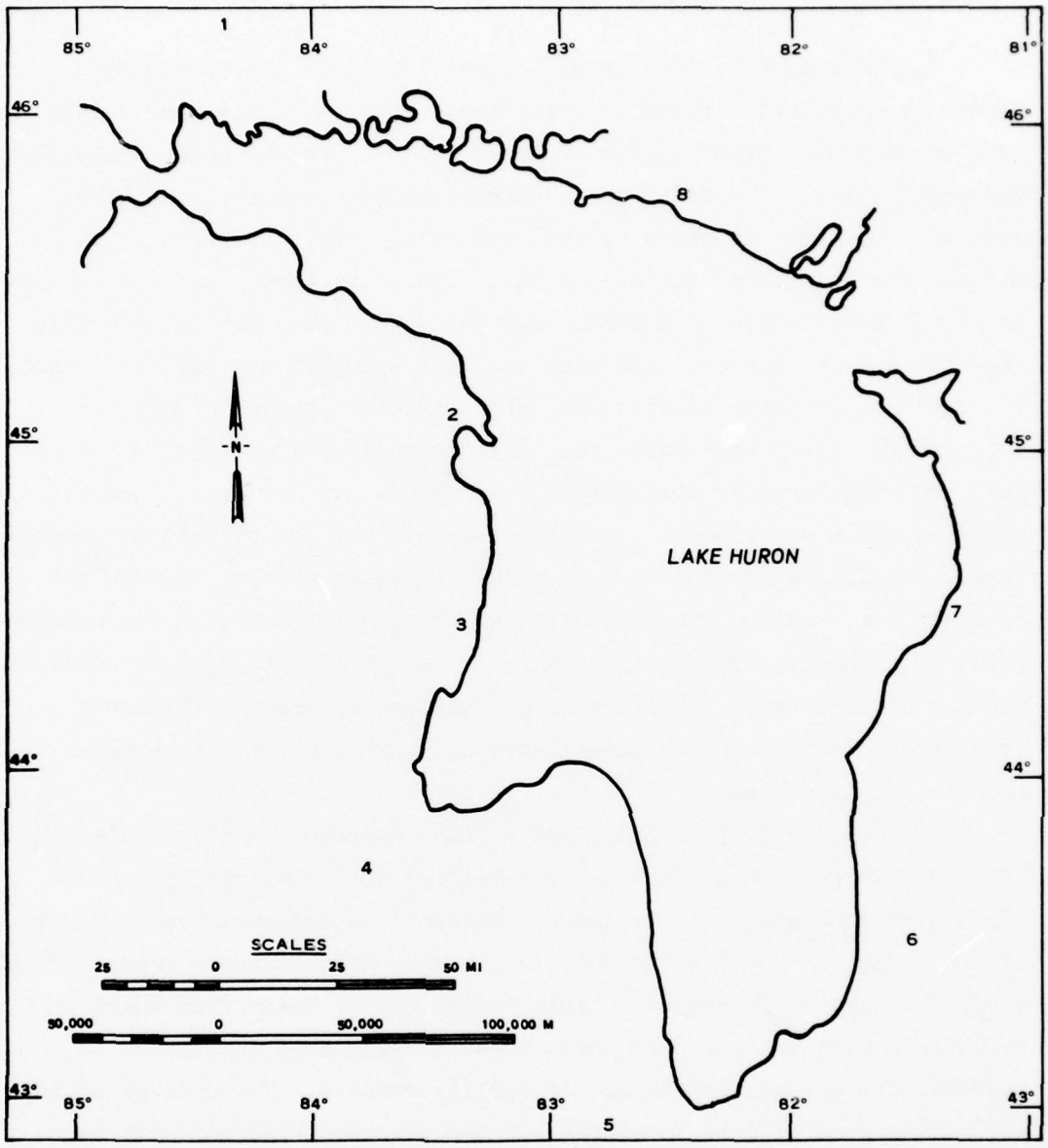

1	SAULT STE. MARIE, MICHIGAN	1948 – 1973
2	ALPENA, MICHIGAN	1959 – 1974
3	OSCODA-WURTSMITH, MICHIGAN	1950 – 1970
4	SAGINAW, MICHIGAN	1948 – 1954
5	SELFRIDGE, MICHIGAN	1949 – 1970
6	CENTRALIA, ONTARIO	1953 – 1966
7	WIARTON, ONTARIO	1953 – 1972
8	GORE BAY, ONTARIO	1953 – 1972

Figure 6. Locations of major sites at which wind data have been recorded for Lake Huron

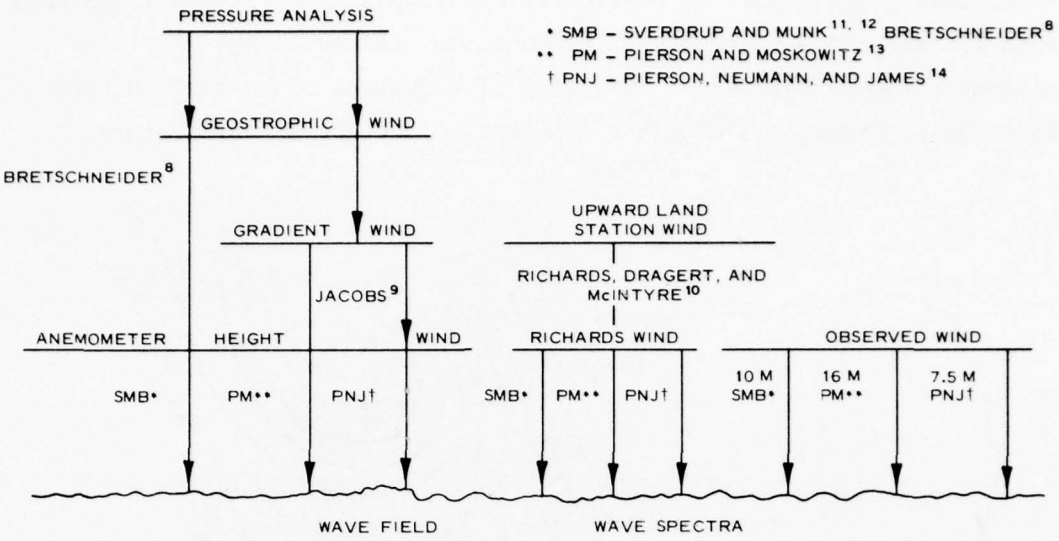

Figure 7. Schematic diagram of wind techniques investigated by Cole[7]

shows the analyses used in each of the methods listed in Table 1. The Bretschneider[8] and Jacobs[9] techniques would have to be taken from weather maps and involve exceedingly large amounts of hand processing. Only the comparison to the Richards et al.[10] technique is relevant to the method to be used in the present study. This comparison indicates a very poor correlation of 0.36 between the 16-m* Richards wind and winds observed at a tower in Lake Michigan. On the basis of such an inadequate wind representation, the use of land-wind information to estimate overlake winds might be dismissed. However, a possible explanation of the lack of correlation in this study will be offered after a more detailed discussion of the general problem.

11. The interaction between a marine surface and the overlying atmosphere is very complex. Only at some large distance from the interface (somewhere in the range of a kilometre) can the effect of the boundary be neglected. At this level, winds at the latitude of the Great Lakes can be treated as geostrophic or, if isobaric curvature is

---

* A table of factors for converting metric (SI) units of measurement to U. S. customary units and U. S. customary units to metric (SI) units is presented on page 3.

significant, gradient. As previously mentioned, synoptic-scale systems, such as extratropical cyclones, produce the dominant large-wave conditions on the Great Lakes. The size of a typical storm of this type is shown in Figure 8. From the patterns of isobars in this figure, it

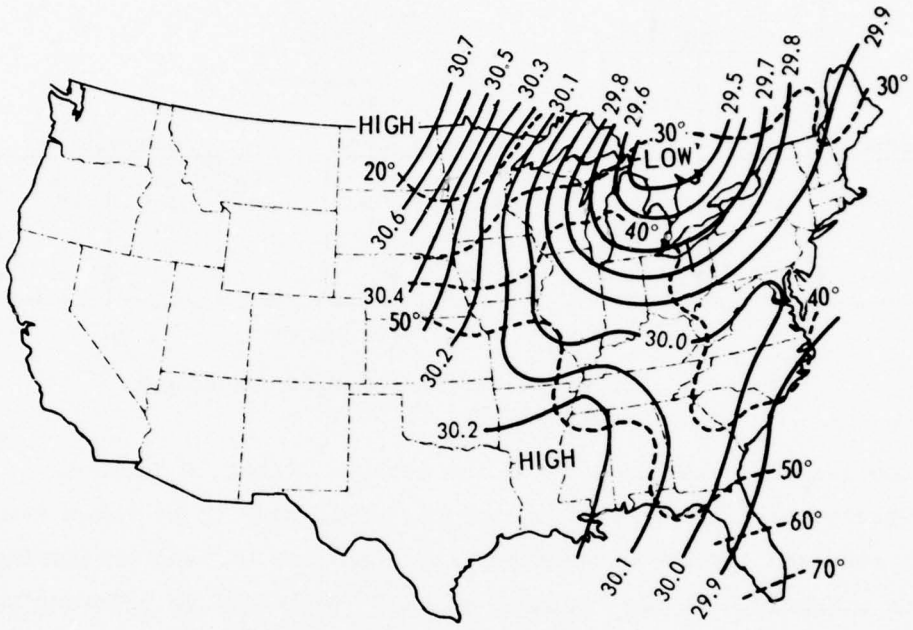

NOVEMBER 19, 1879 3 PM

Figure 8. Isobaric pattern of a typical extratropical low in the Great Lakes region

is evident that the geostrophic winds above the Great Lakes are not different from the winds over adjacent land stations. Hence, the driving mechanism for lower level winds in each case is the same. The fundamental differences between the lower level winds must then be primarily a function of the boundary characteristics. This means that, if the transformations from geostrophic winds to overland winds and geostrophic winds to overlake winds were both known, a relationship between land winds and lake winds could be defined. In practice, this is not an easy task. Most attempts to relate land winds to lake winds have been purely empirical. For comparison of lake winds to

land winds, Hunt[15] proposed the ratio*

$$R = \frac{U_w}{U_\ell} \tag{1}$$

where U_w and U_ℓ represent wind speed over water and over land, respectively. Then Hunt,[15] Lemire,[16] Richards,[17] Richards et al.,[10] and Richards and Phillips[18] used this ratio to study the relationship between land winds and lake winds. Table 2, taken from Reference 18, gives a summary of results obtained in these studies. The study by Richards et al. also documented the effects of over-the-water fetch, air-water temperature differences, and wind velocity on this ratio (Figure 9). From this study, it is apparent that the effect of air-water temperature differences on R is decreased with increasing wind velocity, which, for the investigation of extreme wave conditions, can be very significant.

12. The systematic behavior of the wind ratio suggests that these results are not spurious but actually represent a real relationship between land winds and lake winds. However, the studies do not indicate to what degree the relationship was reproducible in a given application, i.e., there is no correlation coefficient calculated between observed lake winds and winds estimated using the relationship. An evaluation of the error in the wind estimate is essential to the determination of errors in wave hindcasts. Thus, additional empirical work was necessary to complete the evaluation of the relationship between lake winds and land winds.

13. Richards and Phillips[18] points out that the wind ratio R "combines the influences which cause winds over the water to vary from winds on the land; i.e.,

(i) differences in frictional effects created by land and water;

(ii) changes in atmospheric stability created by air-water temperature differences; and

---

* For convenience, symbols and unusual abbreviations are listed and defined in the Notation (Appendix F).

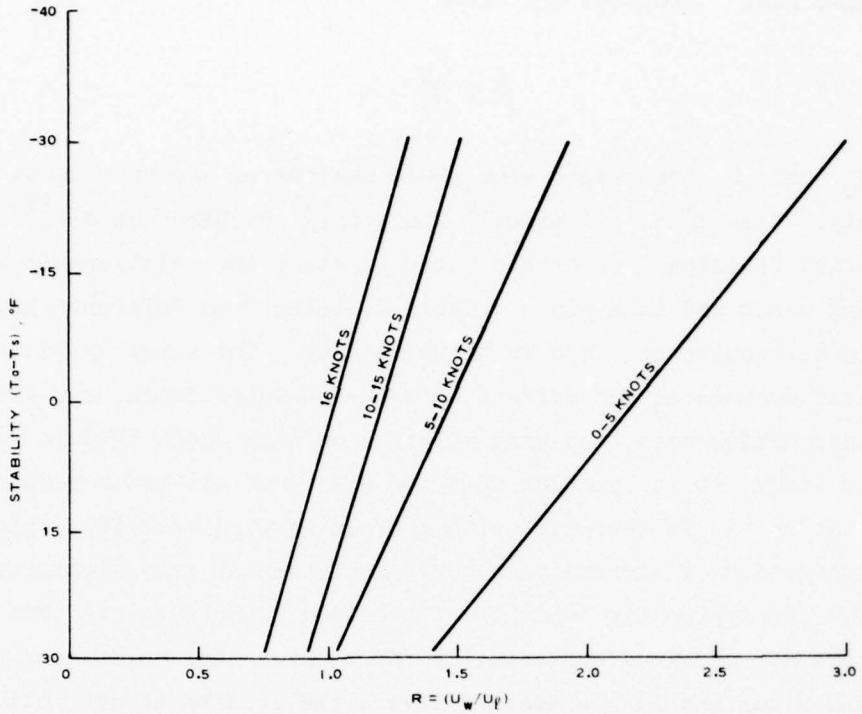

Figure 9. Characteristics of the ratio of overlake wind velocities to overland velocities for various wind speed classes as a function of air-water temperature (after Richards et al.[10])

(iii) the length of overwater fetch."

When errors in estimated winds are examined relative to observed winds over a lake, another factor, inhomogeneities in the wind field, must be considered. Many scales of motion are superimposed in the planetary boundary layer. Any observation of wind speed must be regarded as a statistic containing elements from each of these scales of motion. Thus, a comparison between two winds at different locations must be carefully scrutinized to retain only the scales of motion that are being investigated. In the present study, synoptic-scale features are being examined. If a single land station is correlated with the ships observations, there is no consideration given to spatial gradients in wind velocity. Results from such a correlation analysis can be quite misleading since they contain sources of variability other than those attributable to inherent differences between land winds and lake winds.

To emphasize this point, a correlation coefficient was computed between simultaneous wind observations at Toledo and Cleveland airports (using a random sample of 50 observations during December 1972). The calculated correlation was 0.85, which means that only 72 percent of the variance at Cleveland could be explained using wind data from Toledo. On close examination, much of this difference appears to be related to shifts in the time of peak winds during the passage of storms. For example, a storm moving at 30 mph from west to east along a line from Toledo to Cleveland might take about 3 hr to advect the same wind conditions from the Toledo area to the Cleveland area. The remainder of the difference is most likely due to mesoscale and smaller variations in the wind field.

14. It should be noted that the land winds for airport stations typically represent the average of two 1-min wind observations per hour. Cole[6] does not discuss the averaging length for the winds observed over the lake, which together with the neglect of spatial gradients in the wind field, may explain why the correlation between lake winds and land winds was so low in his study. The ships observations used in this study are approximate winds averaged visually by an observer watching an anemometer for a 1-min period. Deviations from such an observation schedule might be expected during severe weather, but for most observations the quality control appears to be quite high. Figure 10 shows a comparison between several sequences of winds observed at Toledo and Cleveland and simultaneous observations by ships on the lake between longitude 81.5 deg and the western end of Lake Erie. As seen in this figure, there is considerable variance between the ships observations for the same time; yet, if an average wind is calculated from the ships observations, a consistency is apparent between the land winds and lake winds. To test this result with the entire data sample, regressions were run between the ships observations and the mean wind calculated from Toledo and Cleveland. These regressions are stratified by the number of ships observations per 3-hr increment of time (Table 3). Clearly, there is an increase in the correlation as one moves from one observation per time increment. Hence, the actual correlations between a 1-hr average land wind and a 1-hr average lake wind should tend to be well

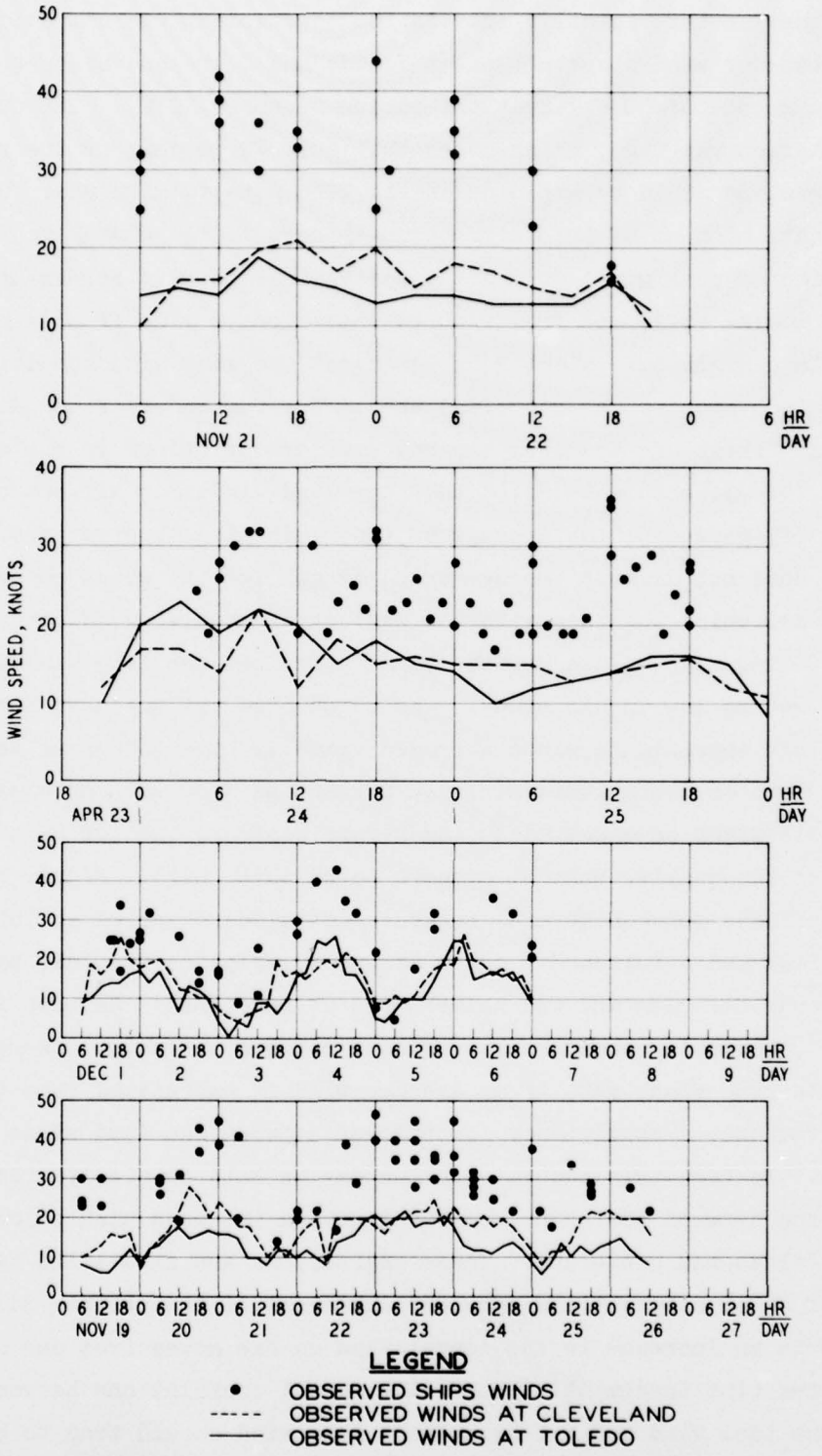

Figure 10. Wind sequences from Toledo and Cleveland (Lake Erie) compared to winds observed over the lake ships

correlated with correlation coefficients of 0.8 or better.

15. Extensive wind data are available for eight stations surrounding Lake Huron: Sault Ste. Marie, Selfridge AFB, Alpena, Oscada Wurtsmith AFB, Saginaw, Wiarton, Gore Bay, and Centralia (Figure 6). These records are stored on magnetic tapes and are thus easily retrievable for the complete 22 yr of hindcasts, but a minimum of four stations was maintained for all hindcast storms. In this report, the basic form for ratio R derived in Reference 6 is expressed as

$$R = \psi_v \Phi_n \tag{2}$$

where ψ_v is a velocity-dependent function (Figure A2 in Appendix A), and Φ_n is a normalized function dependent on air-sea temperature difference.

16. Table 4 presents the root-mean-square (rms) errors of wind speeds estimated from land stations, using Equation 2, compared to wind speeds observed by ships. As seen in this table, the expected rms error for most conditions of interest to hindcasts is under 5 knots.

17. Reports 1 and 2 indicated a linear relation between the ratio of anemometer-level winds to geostrophic winds and air-sea temperature difference. However, analyses documented in Reference 6 have shown that although the portion of curve studied in the earlier reports is linear, the complete curve is of the form shown in Figure 11. The relationship is given in terms of the normalized function Φ_n in this figure. In order to convert V/G, the ratio of anemometer-level wind speed to geostrophic wind speeds, to Φ_n, the curve from Bretschneider[8] was normalized by dividing by the value of V/G for neutral stability.

18. Using a two-layer model of atmospheric motion in the planetary boundary layer, Cardone[19] showed that the linear portion of the variation of Φ_n with air-sea temperature difference was theoretically justifiable. Figure 12 presents empirical data from Bijvoet,[20] H.O. Pub. 604,[12] and Johnson[21] that also support the slope of the linear portion of the curve shown in Figure 11.

19. The dependence of the ratio R on velocity is clearly

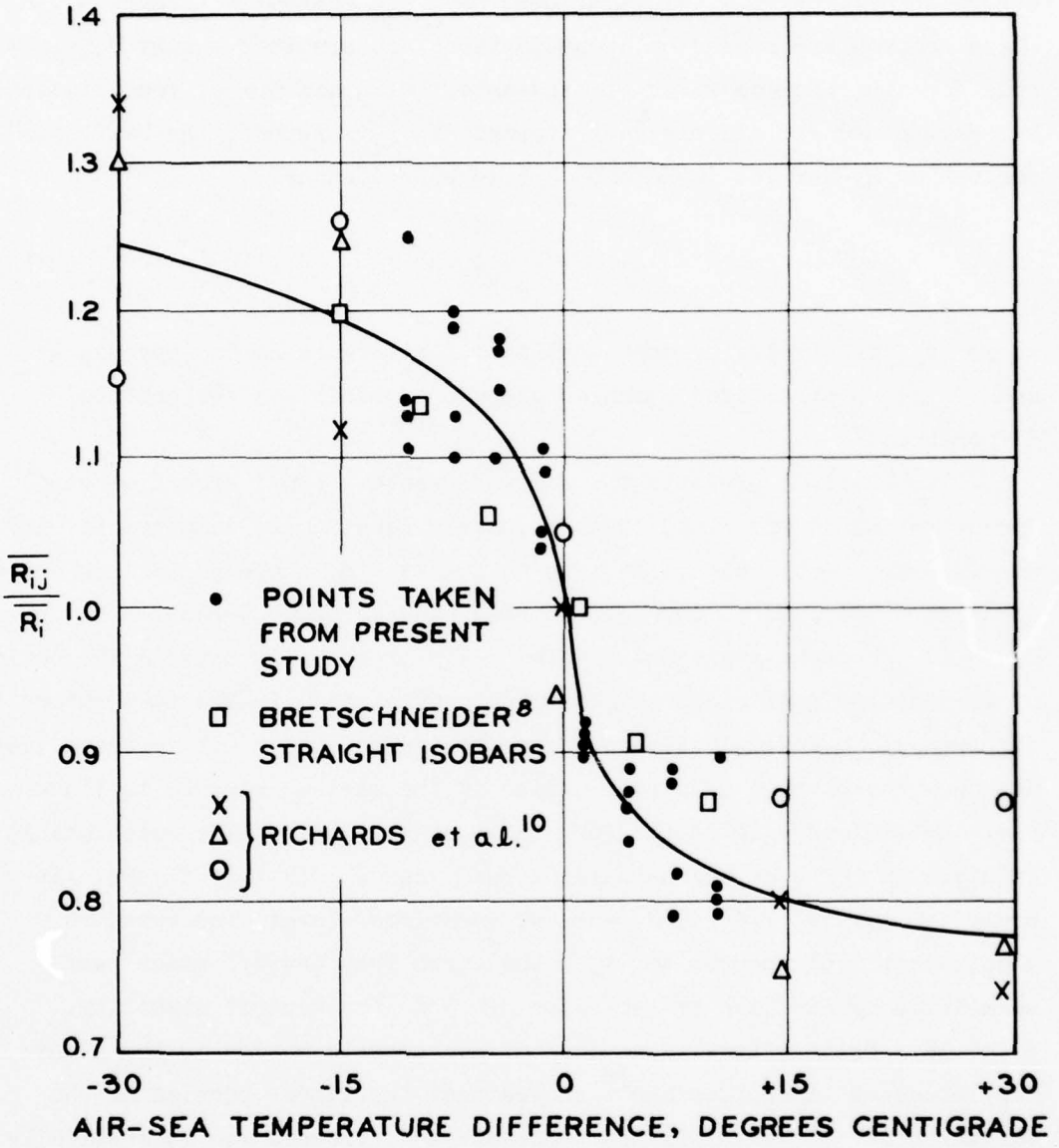

Figure 11. Comparison of empirical results of Richards et al.,[10] Bretschneider,[8] and the present study. The data of Richards et al. and Bretschneider were normalized to 1 at neutral

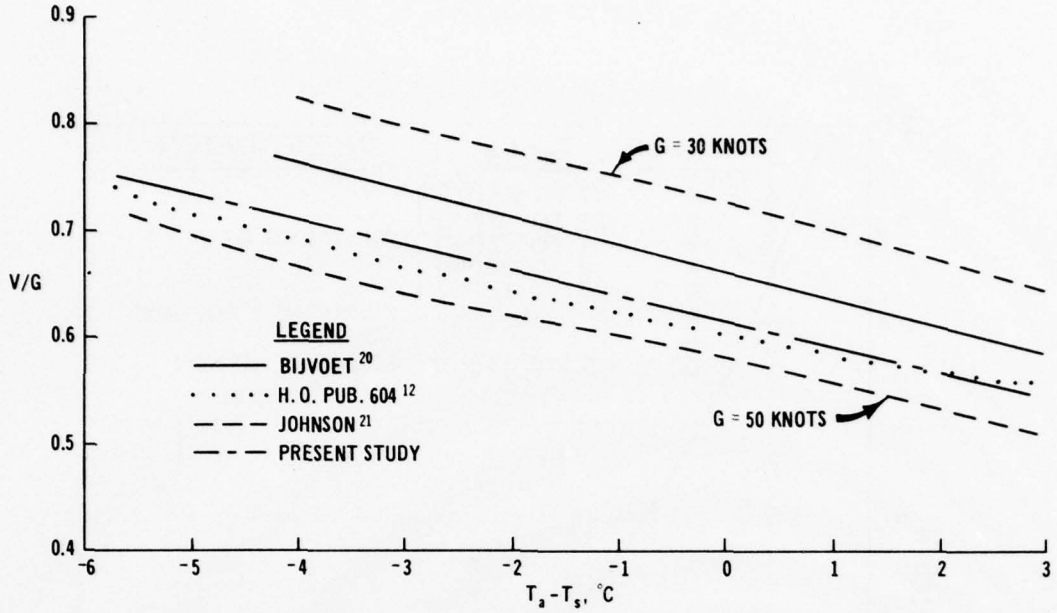

Figure 12. Comparison of relationship between "b" coefficients and air-sea temperature differences as determined in the present study and published empirical relationships of the ratio of anemometer-level wind to geostrophic wind speed. A value of V/G = 0.45 at $T_a - T_s = 0$ was assumed in constructing the line for the present study (from the "b" coefficients)

established in several studies (Johnson,[21] Richards et al.,[10] and Resio and Vincent[6]). Figure 13 shows a comparison of the results from these three studies. When the statistical nature of the different measurements and analyses used in these independent studies is considered, the consistency is striking.

20. The conclusion of this investigation is that the use of winds around the lake perimeter appears to give an adequate representation of winds over a lake. Certainly, the representation is quite limited in its ability to reproduce effects of mesoscale and smaller variations in the wind field. What is obtained in this analysis is a synthesized representation of the synoptic-scale winds over a lake. Only calibration of the wave models using lake winds estimated from land winds can answer the question as to the adequacy of this representation for hindcasting purposes.

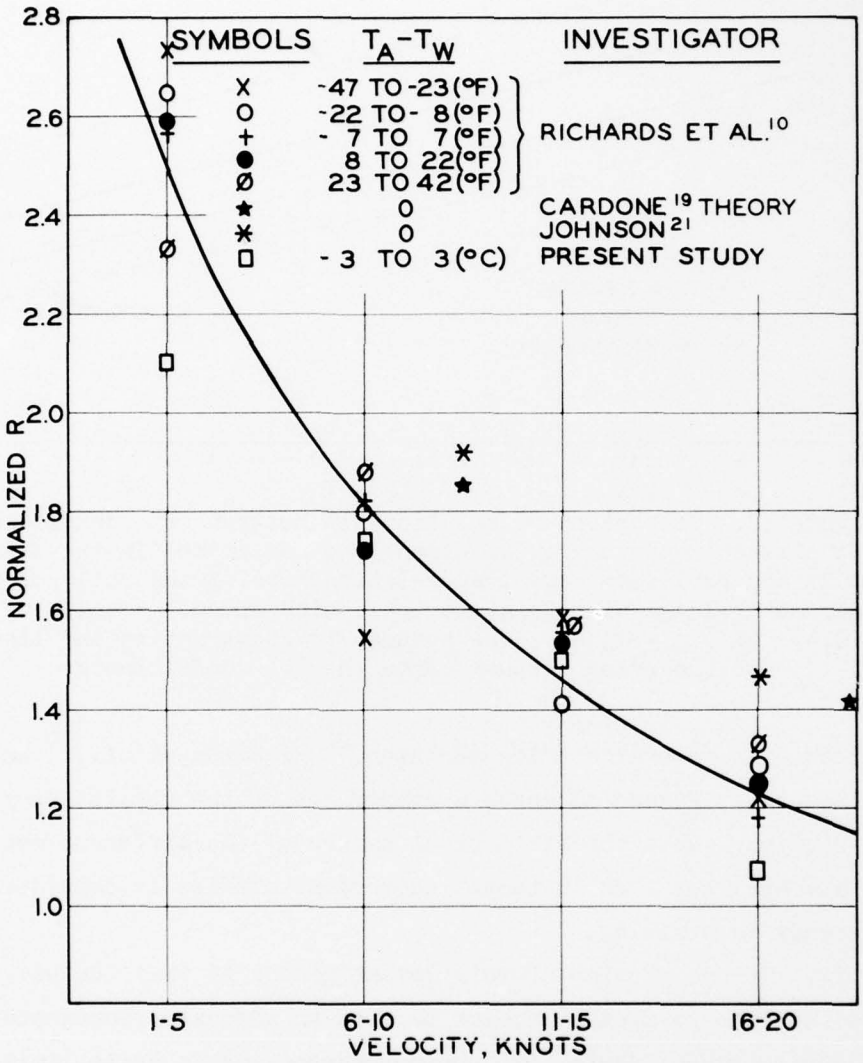

Figure 13. Velocity-dependent behavior of the ratio of anemometer-level wind speeds (V) to geostrophic wind speeds (G). Values for V/G have been normalized to neutral conditions assuming a value of V/G for land of 0.45

PART III: APPLICATION OF WAVE MODELS

21. Theoretical treatments of wave growth due to the action of the wind date back to Helmholtz.[22] Since then, a proliferation of theories has been offered to explain this phenomenon. It was not until the 1940's, however, that practical wave hindcasting and forecasting began. Sverdrup and Munk[11,12] presented semi-empirical methods for calculating wave growth due to winds. These methods used a single measure of wave height, "significant wave height," and a single measure of wave period, "significant period," to characterize waves on the ocean surface. The significant wave height was defined as the average of the one-third highest waves in an observation period and was intended to correspond to that wave height estimated visually by an observer. The significant period was meant to correspond to the period of the "significant" waves. Johnson[23] applied the Buckingham Pi theorem to obtain nondimensional relationships between wave heights, wave periods, wind speed, fetch, and duration of winds. The form of these relationships has remained essentially unchanged. The only real modifications have been based on changing the values of some of the empirical coefficients when warranted by additional data (Bretschneider[8,24]).

22. A different type of representation of the ocean surface also began during the late 1940's when investigators of random noise in circuits (Rice,[25] Tukey and Hamming[26]) began formulating spectral relationships for stationary time series. Pierson[27] took these concepts and applied them to ocean waves. In this characterization, waves are visualized as being a sum of an infinite number of wave trains composed of varying frequencies and directions of travel. Longuet-Higgins[28] showed that, under certain constraints, the distribution of wave heights in a spectrum was specified by a Rayleigh distribution and formally equated the concept of "significant wave height" with the energy spectrum by the relationship

$$H_{1/3} = 2.83 \sqrt{E} \qquad (3)$$

where $H_{1/3}$ is the significant wave height and E is twice the total variance in the wave spectrum. Several theories have since been advanced on the growth of wave spectra under the action of the wind (Appendix B). These provide the framework for several different spectral hindcast models that exist today.

23. A definite choice had to be made in this study whether to use a significant wave method (sometimes referred to as an SMB method) or a spectral model, and if a spectral model were to be used, which one would be selected.

24. To choose an optimal model for the Great Lakes requires an examination of the accuracy required by users of the wave information and the accuracy available from the various models. The high cost of dike construction for dredged material retention and the high cost of coastal zone construction certainly justify selection of the most accurate model.

25. The major disadvantages in applying the SMB technique are linked to its use of a single parameter to represent sometimes complex phenomena. If the wind field were a known constant over a uniform fetch and if the waves were truly monochromatic, the SMB technique should be an excellent method for estimating wave heights. The reduction in usefulness and accuracy of the SMB technique for the Great Lakes is related to deviations from these assumptions. Variability in the shoreline geometry of the Great Lakes and in wind velocities and directions during the passage of a storm can introduce considerable error in the attempt to simplify the winds and fetches to a form commensurate with assumptions inherent in SMB hindcasts.

26. In a wave spectrum specified at a given time, the energy density may be fetch-limited for some frequencies and duration-limited for others. With the SMB technique, however, waves can be treated only as fetch-limited or duration-limited.

27. Recent field studies into the growth of waves tend to point out this problem of fetch and duration equivalence. According to the most recent deepwater curves published for the significant wave method (SPM[5]) for a 30-knot wind, a 50-mile fetch is equivalent to about

a 7-hr duration. In other words, waves for a 50-mile fetch will be duration-limited as long as the wind has blown less than 7 hr. A field study by Barnett and Wilkerson[29] demonstrated that waves with periods as high as 8.5 sec were fully developed within 50 miles of a coast for winds of 30 knots blowing straight offshore (Figure 14). The group

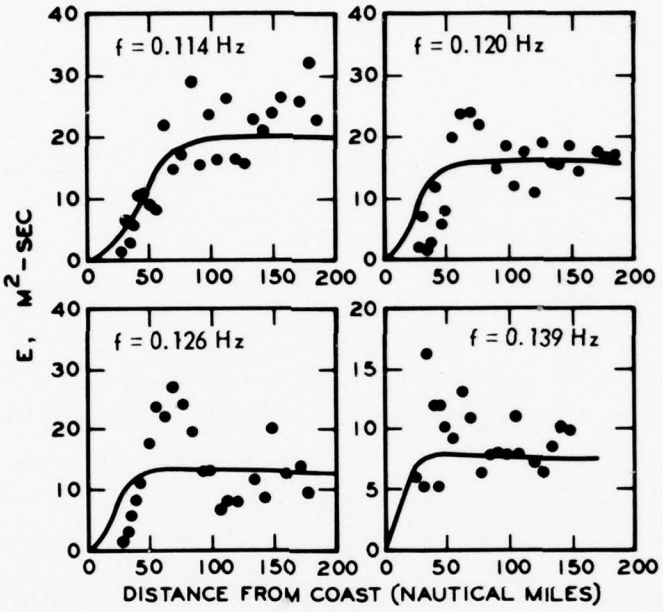

Figure 14. Growth of frequency components of waves for an offshore wind of 30 knots (after Barnett[30])

velocity of these waves is around 15 mph, so the total possible time under the action of the wind is only about 3.3 hr. Thus, the waves would become fetch-limited* after only 3.3 hr, not 7 hr as given by the SMB method.

28. Because of these apparent inadequacies in the SMB method for conditions typical of the Great Lakes, an investigation into the potential of numerical models was initiated. Such models have been in use since the early 1960's (Baer[31]) and, at various stages of development,

* This assumption that higher frequencies are fully developed before lower frequencies also was validated in the same field study.

have been proven capable of providing good estimates of wave heights. These models differ from the significant wave model in that they use a system of grid points on the water surface for calculations of energy transfer into and out of the wave spectrum. In this way, they can achieve a much more detailed representation of the shoreline and wind-field geometries. Also, since the model calculates energy transfers for small increments of time, the wind field in a numerical model can be specified more exactly in time than the wind field in a significant wave calculation.

29. Several numerical models are presently available. Basically, all of these using theoretical representations of energy transfer mechanisms compute energy spectra at each grid point. The ability to retain information from each grid point is certainly an advantage of these models. Thus, what might require several separate hindcasts with an SMB approach can often be done in one step with a numerical model.

30. Only two numerical models of wind-generated waves have been used extensively in the United States--one developed at New York University by Pierson and Moskowitz,[13] Inoue,[32] and Cardone,[19] and another developed at Scripps Institute of Oceanography, primarily by Barnett.[30] These two models are discussed in more detail in Appendix B. A third model, the French spectro-angulaire model, also has been used in the United States, but will not be examined here since it is similar in many respects to the model developed at Scripps.

31. The primary difference between these models is the form of the energy transfer into the waves attributed to different theoretical mechanisms. The "NYU" model essentially considers: (a) a linear source due to the interaction of the water surface with turbulent pressure fluctuations in the atmosphere (Eckart,[33] Phillips[34]); (b) a nonlinear mechanism due to a resonant interaction between waves and the mean wind profile (Miles[35]); and (c) a wave-breaking term related to the fully developed spectral form proposed by Pierson and Moskowitz.[13] The model developed by Barnett,[30] in addition to the Miles' and Phillips' mechanisms and wave breaking, considers the effect of wave-wave interactions on the development of a spectrum (Hasselmann[36-38]).

32. Even though the basic research needed to clarify the energy transfer mechanisms is far from complete, both models have been tested successfully in previous studies. Lazonoff et al.[39] documents comparisons between hindcast wave heights using the "NYU" model and observed waves on the Mediterranean Sea. For this set of comparisons, 80 percent of the observed and hindcast wave heights were within 3 ft of each other. The Barnett model has not been as widely tested in deep water.* Figure 15 shows a single time series comparison made by Barnett[30] for an area in the Atlantic.

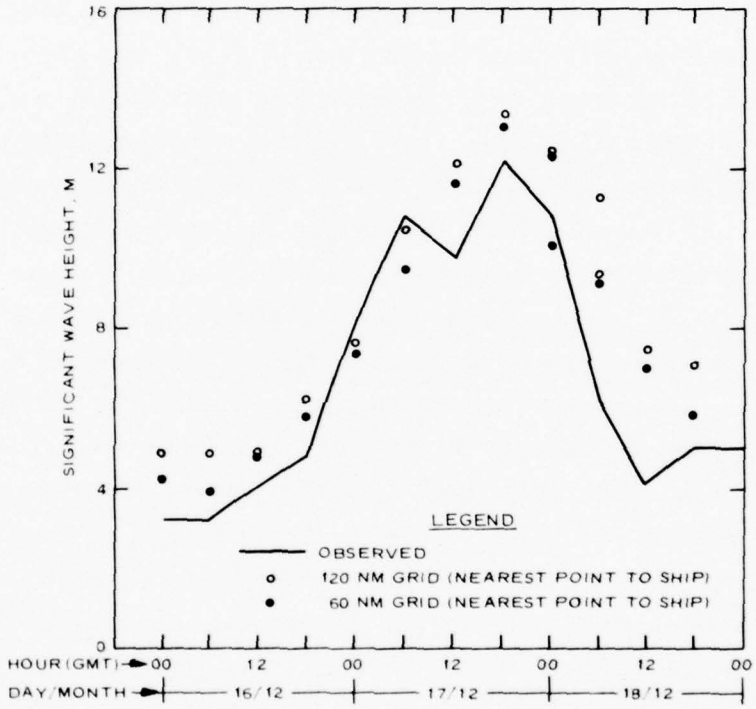

Figure 15. Hindcasted significant wave heights for 16-18 Dec 1959, using Barnett model with 60-nautical-mile grid "0" and 120-nautical-mile grid "0" as compared with observed wave heights from the OWS "Weather Reporter"

* Fleet Numerical Weather Central in Monterey, California, has now completed adapting a version of the wave-wave interaction model to their computer systems. Preliminary results from hindcasts in the Gulf of Alaska region have compared extremely well with wave observations (personal communication from Professor Warren Thompson of the Naval Postgraduate School, Monterey, California).

33. In previous tests on Lakes Erie and Ontario, several sequences of wave spectra were selected for comparison with hindcasts by the "NYU" and Barnett models. The corresponding significant wave heights for the periods from which these spectra were taken started at some low level (about 1 to 2 ft), progressed to some maximum or maxima (greater than 5 ft), and then returned to near the initial level. With these time series, the two important aspects in the model were (a) the comparison with the complete hydrograph and (b) the comparison between observed maxima and hindcast maxima. In this study, the behavior of both the time series and individual maxima hindcast with the "NYU" model was found to be more erratic than the hindcast with the wave-wave interaction model. Also, the nondimensional wave heights predicted by the "NYU" model were not consistent with recent field observations such as those of Hasselmann et al.[40] Figures 16 and 17 present two comparisons between sequences of wave heights hindcast by the latter model. Figure 18 gives the distribution of observed maxima relative to hindcast maxima. Additional results from model calibrations are given in Appendix B.

34. The wind input to these test runs on the computer consisted of 3-hr winds taken from wind data on magnetic tapes for Buffalo and Rochester on Lake Ontario and Toledo, Cleveland, Erie, and Buffalo on Lake Erie. These winds were input into the program directly, and all conversions and interpolations of the wind field are performed within the computer program. This means that subjectivity in the wind input used in this calibration was held to an absolute minimum.

35. At the time of the calibration tests for Lake Huron, there were no deepwater wave gage data available to this study. Consequently, no additional calibrations are included in this report.

36. The rms error for the hindcasts shown in Figure 18 is about 1.5 ft. The tendency of the model to overpredict in short-fetch conditions, as noted in Reports 1 and 2, is not as pronounced as indicated by the smaller number of hindcasts considered in those earlier reports. The underprediction during the summer period appears to remain, however, and is most likely due to the lack of resolution of the small-scale summer circulation features.

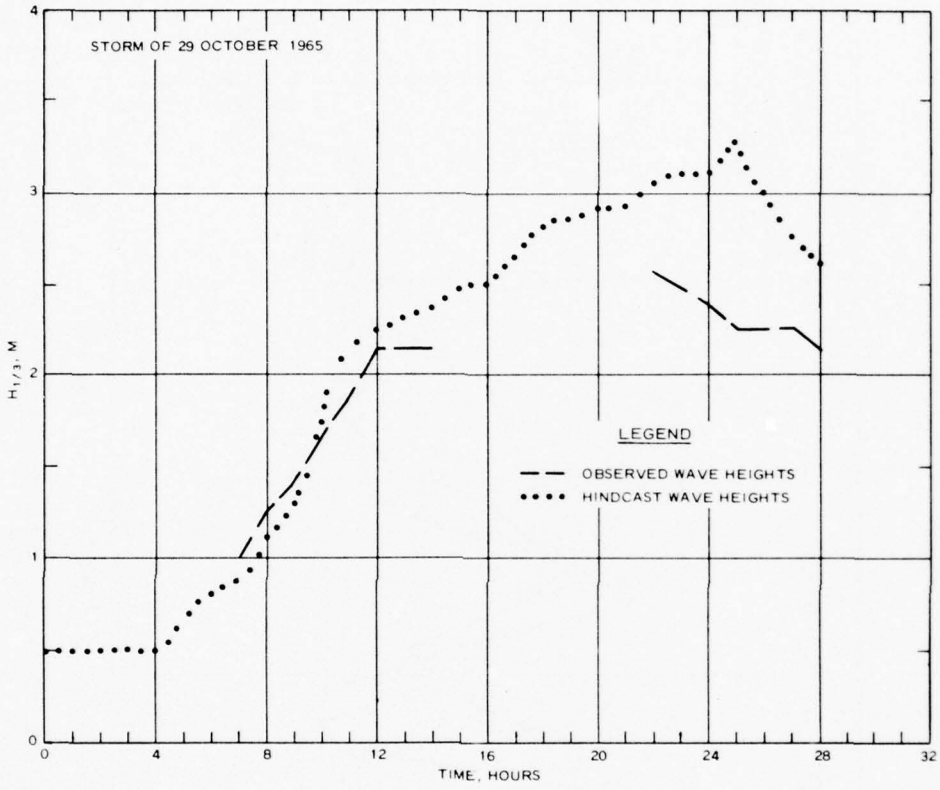

Figure 16. Comparison of time series of significant wave heights observed at Muskegon for storm of 29 October 1965 and wave heights hindcast by numerical model for same storm

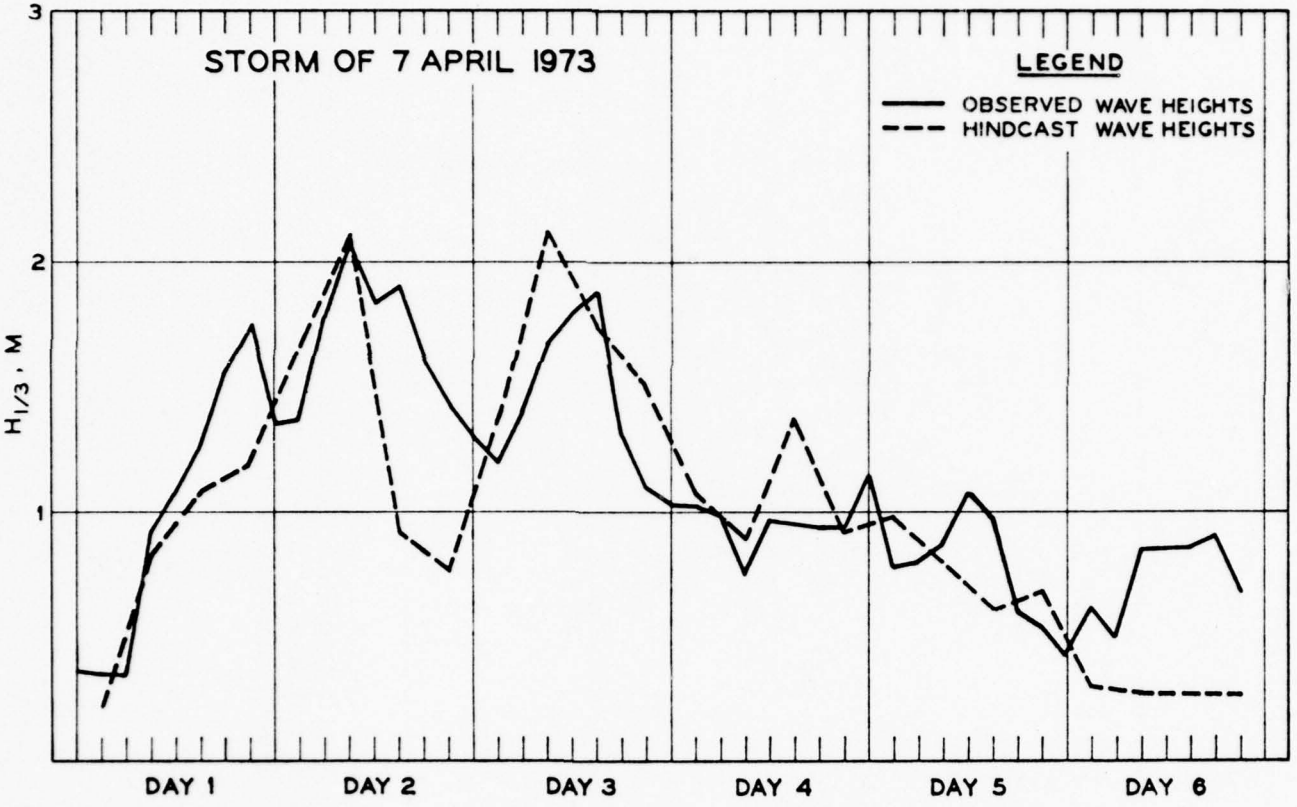

Figure 17. Comparison of time series of significant wave heights observed at Point Pelee for storm of 7 April 1973 and wave heights handcast by numerical model for same storm

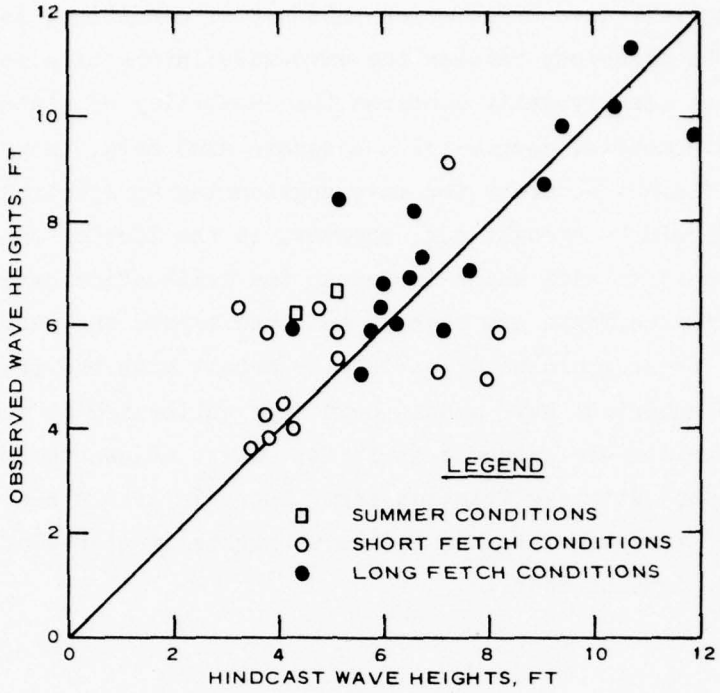

Figure 18. Comparison of maximum significant wave heights for individual storms as recorded by gages (Point Pelee, Lake Erie; and Toronto, Cobourg, and Main Duck, Lake Ontario) and significant wave heights hindcast by the numerical model using Barnett's parameterizations

37. Another possible contributor to the error in short fetch conditions is the relative importance of mesoscale inhomogeneities in the wind field for these cases. In the short fetch situation, the waves are propagating in an offshore direction; in the summer storms, actual maxima are only about 5 to 6 ft. Neither of these cases are critical to the practical problem of forecasting extreme wave heights along the coastlines of the Great Lakes. The agreement between hindcast wave maxima and observed wave maxima for cases involving fetches over 20 miles and for waves propagating toward shore was extremely good. All of the hindcast maxima* were within 1.5 ft of observed maxima. The rms error

* In some cases, the wave gages did not function part of the time during the high-wave conditions. For these instances, comparisons were made between wave heights at the time of the highest gage record.

in estimating peak wave heights for this set of conditions is about 1 ft.

38. The agreement between the wave-wave interaction model and observed waves unequivocally confirms the capability of state-of-the-art numerical wave models, coupled with adequate wind data, to produce results of sufficient accuracy for most engineering applications. One point that should be brought out, however, is the lack of observed wave heights above 15 ft with which to extend the calibration curve. If strong nonlinear effects are present in waves beyond the range of the calibration, these would be impossible to detect with the present data. However, the numerical wave models have been calibrated at ocean sites for waves considerably larger than 15 ft. Thus, unless there is a large error associated with the friction term, there is little reason to expect a marked increase in error for wave heights in excess of 15 ft hindcast with the present model.

PART IV: THE ANALYSIS OF EXTREME WAVE HEIGHTS

39. In Part III, a capability to reproduce wave heights from individual storms was demonstrated. This information is valuable, but it is the statistical synthesis of this information into the estimation of probabilities of extremes that is most important in design and planning applications. The analytical treatment of extremes is well developed (Jenkinson,[41] Gumbel,[42] and Gringorten[43]) and can be used very effectively for values not extrapolated too far beyond the total length of record.

40. A major facet of this study has been to obtain long records of reliable wind data. For this purpose, several problems had to be addressed. First, only about 26 yr of the wind data were available on magnetic tape; the remainder were handcopied from autograph forms available at the National Climatic Center, Asheville, North Carolina. Second, wind data are not available at a consistent height or a consistent location for the entire period of record; thus a detailed analysis of the wind profile, as discussed in Appendix A, is necessary. Results of these analyses are transformations of the wind from one height to another. For the simple case in which the wind to be transformed can be considered totally within a boundary layer characteristic of land, the one-seventh power law can be invoked. These winds are reduced to a common anemometer height (20 ft) and transformed, using the empirical results obtained in Part II, into winds over the lake. For stations located within a mile or so of the lakeshore, winds blowing off the lake still retain characteristics of the marine boundary layer (particularly for anemometer heights typical of older Great Lakes weather stations, 200-300 ft). These winds are transformed directly to winds over the lake using a theoretical treatment of meteorological boundary layers. In this way, a single, quasi-homogeneous population of winds estimated over the lake is obtained. Appendix A details the techniques used to formulate these transformations.

41. In order to obtain design information for all directions of wave approach for coastal structures, the wind data were stratified by

a 45-deg direction class (i.e., N, NW, W, etc.). They were further subdivided by separating the winds into seasonal categories (January-March, April-June, July-September, October-December). This was accomplished to facilitate treatment of seasonal variations in water level and icing conditions on the Great Lakes. Seasonal wind-speed maxima (in each direction) for each wind station were determined; the storms during which these wind speeds occurred were keypunched.* To reduce computer time, only the larger half of these storms (in terms of the wind-speed criteria) was input into the numerical model. For each storm (at 1-hr intervals), two-dimensional spectra for all grid points adjacent to shore were written onto magnetic tapes and saved. Maximum wave heights** by direction are output in the form of punched cards. It is the latter information that is used in the calculation of wave height recurrence intervals.

42. Since only seasonal maxima were computed for wave heights, the appropriate method to use in estimating recurrence intervals is taken from the asymptotic theory of extremes. In their texts, Gumbel[42] gives an excellent discussion of these techniques, and Gringorten[43] presents a good demonstration of the application of these techniques. Basically, the asymptotic forms are solutions to the equation

$$F^n(x) = F(a_n x + b_n) \tag{4}$$

---

* A minimum of 6 hr before the maximum and 3 hr after the maximum were included in the storm to ensure that the peak wave conditions were calculated.

** Significant wave heights for nearshore conditions are estimated from the two-dimensional spectra at the grid points by the relationship

$$H_{1/3} = 4.01\left[\int_{f_1}^{f_2}\int_{\theta_1}^{\theta_2} F(f,\theta)\, df\, d\theta\right]^{1/2}$$

where f_1 and f_2 are the lowest and highest frequencies considered in the numerical model, θ_1 and θ_2 are limiting angles for waves propagating toward the shore, and $F(f,\theta)$ is the two-dimensional spectrum.

where a_n and b_n are constants, which are functions of sample size n, and F is the cumulative probability function of x. This theory is based on the premise called the Stability Postulate, which states that the distribution of the largest value in Nn observations will approach the same asymptotic expression as the distribution of the largest value in N samples of size n. The only three solutions possible for Equation 4 are termed the Fisher-Tippett Types I, II, and III distributions. Each solution is derived from different constraints on a_n and b_n; however, Jenkinson[41] showed that all three of these distributions could be written in a common form as

$$x = x_o + \alpha \left(\frac{1 - e^{-ky}}{k} \right) \tag{5}$$

where

x_o = parameter of extremal distribution

α = parameter of extremal distribution

e = Napierian base (2.71828...)

k = parameter denoting curvature in extremal distribution

y = reduced variate in distribution of extremes

Figure 19 shows the form of Fisher-Tippett Types I, II, and III distributions when $k = 0$, $k < 0$, and $k > 0$, respectively. It is also important to note in this figure the bounds on the different types: (a) Type I is unbounded; (b) Type II has a lower limit; and (c) Type III has an upper limit. Unfortunately, there is no reliable, objective method for determining which distribution one is dealing with when given only a single set of sample characteristics. Arguments based on the stability of extrapolations and the ease of application usually favor the Fisher-Tippett Type I distribution when curvatures are relatively low.

43. In the analysis of wave height extremes, the first step was to plot the wave heights computed in the wave model against the logarithm of recurrence intervals* estimated from the formula

---

* The terms "recurrence interval" and "return period" are used interchangeably in this report.

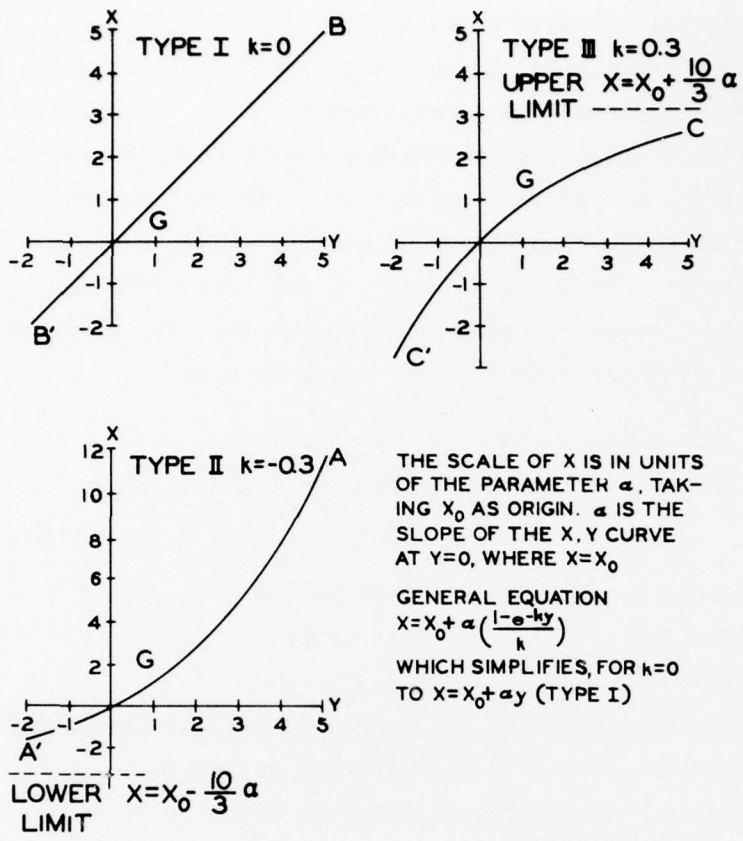

Figure 19. Schematic representation of the three Fisher-Tippett asymptotic distributions on x-y diagrams (after Jenkinson[44])

$$T(H) = \frac{1}{1 - F(H)} \tag{6}$$

where

T = return period

H = wave height

F(H) = cumulative probability function of H

A typical result of such plots is shown in Figure 20. The curvature at the bottom of these graphs is due to the inclusion of samples from storms other than the seasonal maxima for each direction and the inclusion of only the larger half of the annual maxima in the numerical hindcasts.

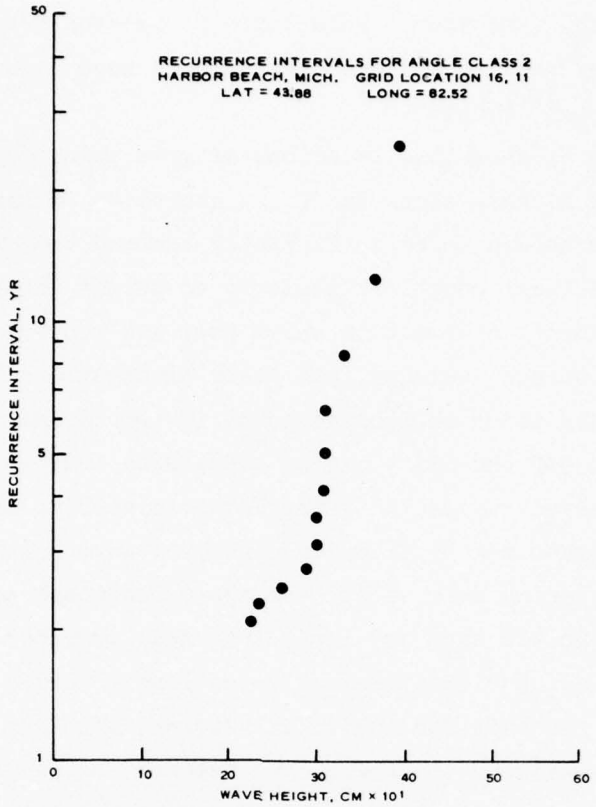

Figure 20. Sample plot of log T versus significant wave height as calculated from Equation 6

44. The upper portion of these graphs represents a region identical to that which would be calculated from an analysis of all of the annual maxima. As discussed in Appendix D, this section of the curve can be used to reconstruct estimates of parameters for the entire curve. These results are based on calculations designed to optimize the estimation of large return periods and hence should not be used to estimate return periods of less than a year. Another factor to consider in applying asymptotic methods to small recurrence intervals is emphasized by Dalrymple.[45] In a series of annual maxima, the recurrence interval is defined as the average interval in which a wave height greater than or equal to a given size will recur as an annual maximum. A partial-duration series must be used to define the average interval between wave heights of a given size regardless of their relationship to

other storms of the same year. Relationships between recurrence intervals defined by the two different techniques have been derived by Langbein[46] and Chow[47] (Table 5).

45. Figure 21 shows the locations of grid points used to define "deepwater"* wave heights along the U. S. shoreline of Lake Michigan. These points were chosen to be sufficiently removed from the effects of shallow water and local coastline geometry to permit them to be representative of the segments of coast in which they are centered. Also, the effects of storm surges, seiches, and other fluctuations in water level become increasingly important as the coast is approached. Whereas statistics specified off the coast can be considered independent of small changes in lake level, waves and water levels closer to shore must be superimposed in order to obtain calculations of wave heights. For storm waves calculated during this study, the two-dimensional spectra can be retrieved from magnetic tape and input into shallow-water wave routines along with detailed specifications of water levels during the storm. Although this is adequate for individual storms, it might be more advantageous to investigate the covariance between the wave spectra and short-term fluctuations of the lake level. Thus, a statistical model could be derived that could provide nearshore wave information at minimal cost.

46. Ice cover significantly influences winter wave climates on all of the Great Lakes with the possible exception of Lake Ontario. Two factors must be considered in examining the effect of ice cover on reducing wave heights incident on shores or structures: (a) reduction of fetch lengths for wave generation, and (b) protection from waves afforded by ice cover near the shore. Since ice typically forms around the periphery of a lake before extending toward the center, the second of these two factors is more important for most nearshore sites. As a reasonable first approximation, meteorological conditions that generate

---

* These depths are not greater than one-half the wavelength of some of the waves on the Great Lakes, but they are in locations where refraction and frictional effects would be minimally affected by changes in the water level of up to several feet.

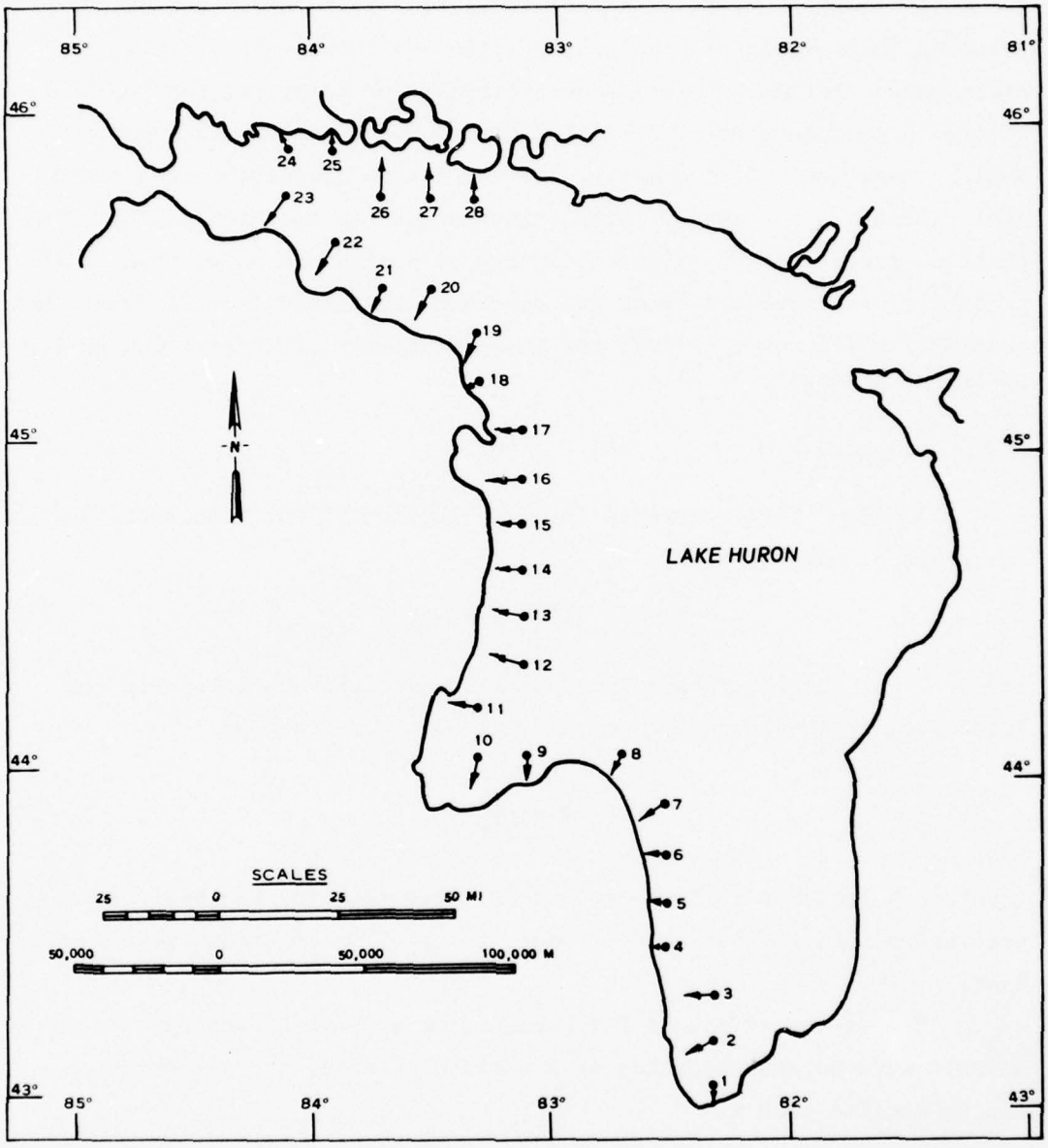

Figure 21. Locations of grid points for which two-dimensional spectra are retained on magnetic tape and for which design wave information is listed in Appendix E

large waves in the winter (individual extratropical cyclones) can be considered independent of meteorological conditions responsible for ice formation (long-term, large-scale circulation patterns). A much more detailed study would be required to establish relationships between storm probabilities and large-scale circulation patterns, and the increase in the accuracy of estimates of recurrence intervals could very well be marginal. Consequently, the assumption of independence seems justifiable in this study. With this assumption, the probability of a particular wave height (p(H)) occurring at a site can be written as the product of the probability of its occurence estimated from hindcasts not considering ice cover (p'(H)) and the probability of there being no ice at the site ($p(\varepsilon)$)

$$p(H) = p'(H)\, p(\varepsilon) \tag{7}$$

47. Thus the recurrence interval for conditions with possible ice cover can be expressed as

$$T' = T\, \Phi \tag{8}$$

where T is the recurrence interval for waves with no ice cover (as determined by the computer program) and Φ is defined as

$$\Phi = \frac{1}{p(\varepsilon)} \tag{9}$$

Equation 9 provides a simple method of converting the generalized wave statistics into statistics applicable to specific locations around a lake.

48. If the effect of fetch reduction appears necessary for reasonable wave height estimates at a particular site, a transformation can be applied such as

$$H_L = g(H, F, F_L) \tag{10}$$

where

H_L = actual wave height as affected by fetch reduction due to ice cover

g = function of H, F, and F_L

F = land-bounded fetch

F_L = fetch during partial ice cover

Since the original wave height is calculated with the complete numerical program, a simple relationship based on dimensional considerations can be applied to reproduce the approximate variation of wave height with fetch without introducing too much error. Hence, the curves given in SPM[4] for wave growth with fetch (ignoring the duration of winds) can be used to scale wave heights predicted with no ice cover into wave heights with reduced fetches. Figure 22 presents these curves for

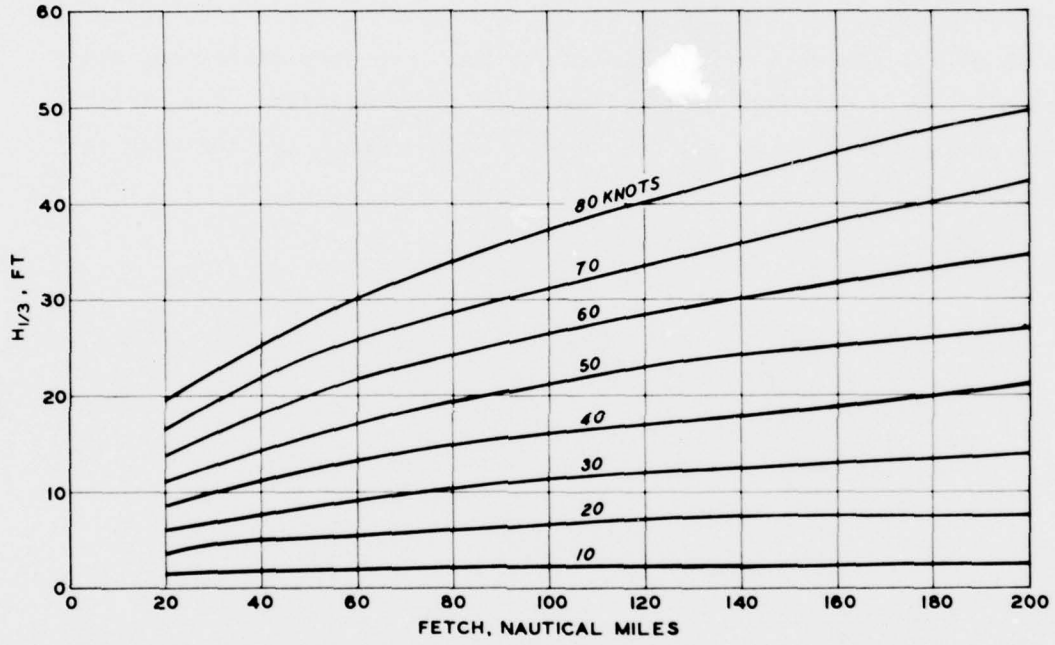

Figure 22. Growth of significant wave height as a function of wind speed and fetch (after SPM[5])

fetches from 20 to 200 miles. For example, if the original fetch were 100 miles, these curves indicate that a wind velocity of approximately 28 knots would be required to generate a significant wave height of 10 ft. If ice cover reduced the fetch to 50 miles, the significant wave height for this velocity is expected to be about 7 ft. Hence, the probability of exceeding a 10-ft wave height becomes the probability of

exceeding a 7-ft wave height. By using such a technique, the recurrence interval can be written as

$$T'(H) = T(H')\Phi \tag{11}$$

where H is the wave height into which H' is transformed by fetch reduction.

49. In Appendix E, results of numerical computations of wave heights with recurrence intervals of 5, 10, 20, 50, and 100 yr are given along with the control bands for each point in Figure 21. These are tabulated as (a) a function of season and approach direction, (b) a total of all seasonal probabilities for each approach direction, and (c) a total of all direction and seasonal probabilities. The significant periods associated with these wave heights also are included in Appendix E.

PART V: DISCUSSION OF RESULTS

50. This study represents a synthesis of three phases of wave hindcasting:

a. Estimation of winds over the water.

b. Operationalization of a wave model.

c. Calculation of return period information from program outputs.

Each phase of the study was treated in detail, since errors in any phase could alter the results dramatically. As discussed in Appendix D, the total error in wave hindcasts relative to the variability of annual maxima is sufficiently small that the distribution of waves from the hindcasts should not be affected by it; and as seen in the calibration results (Part III), the waves estimated from the wave model do not appear to contain any determinable bias. Thus, the primary source of error in the estimates of return periods is due to expected sampling variability and is inversely proportional to the square root of the number of years in the sample.

51. It is important for any user of information reported herein to bear in mind that the wave heights presented in Appendix E refer to deepwater conditions. The accuracy of the results appears to be quite good for these conditions, and they can be applied as a general approximation to wave heights along the coast. However, when detailed information for design and planning purposes is required, it is imperative that the two-dimensional spectra be retrieved from magnetic tapes and used in conjunction with the proper shallow-water transformations. Although significant wave techniques can provide some idea of the actual transformations, shallow-water wave heights estimated from these methods tend to be biased toward higher waves (Freeman et al.[48]). A better, less biased estimate of shallow-water wave heights probably could be obtained from numerical shallow-water routines such as developed by Collins.[49] Substantial evidence is now becoming available that indicates a marked energy loss in moving from deep to shallow water. This loss of energy,

if substantiated, could provide a significant reduction in the wave heights listed in Appendix E.

52. As a final point, it should be emphasized that the information presented in this report constitutes only a small portion of that available from the complete set of hindcast data stored on magnetic tapes.* For many purposes, a natural choice for design considerations formed by navigation constraints does not always coincide with seasons chosen for use in this study. However, the basic data set can be reprocessed within any arbitrary seasonal divisions. Other information, such as characteristic durations of wave heights, estimates of nearshore currents, and estimates of individual wave height probabilities, can all be obtained from analyses of the hindcast data.

---

* These two-dimensional spectra are stored at 1-hr intervals during each hindcast storm for all shoreline points and selected offshore points.

REFERENCES

1. Cole, A. L. and Hilfiker, R. C., "Wave Statistics for Lakes Michigan, Huron, and Superior," Final Report 01498-1-F, Aug 1970, University of Michigan, Ann Arbor, Mich.

2. U. S. Army Engineer Waterways Experiment Station, CE, "Wind, Wave, Water Level, and Ice Conditions Affecting Design and Construction of the Proposed Lake Erie Jetport, Cleveland, Ohio," Contract Report H-74-1, Mar 1974, Vicksburg, Miss.; prepared by A. H. Glenn and Associates under Contract No. DACW39-73-C-0063.

3. Saville, T., Jr., "Wave and Lake Level Statistics for Lake Erie," Technical Memorandum No. 37, 1953, U. S. Beach Erosion Board, CE, Washington, D. C.

4. Lee, C. E., "Additional Wave Statistics for Stations on Lake Michigan and Lake Erie," Beach Erosion Board Bulletin, Vol 12, Jul 1958, pp 1-8.

5. U. S. Army Coastal Engineering Research Center, "Shore Protection Manual," Vol I, 1973, Fort Belvoir, Va.

6. Resio, D. T. and Vincent, C. L., "Estimation of Winds Over the Great Lakes," Miscellaneous Paper H-76-12, Jun 1976, U. S. Army Engineer Waterways Experiment Station, CE, Vicksburg, Miss.

7. Cole, A. L., "An Evaluation of Wind Analysis and Wave Hindcasting Methods as Applied to the Great Lakes," Proceedings, Tenth Conference on Great Lakes Research, 1967, pp 186-196.

8. Bretschneider, C. L., "Revised Wave Forecasting Curves and Procedures," Technical Report No. HE-155047, 1951, Institute of Engineering Research, University of California, Berkeley, Calif.

9. Jacobs, S. J., "Wave Hindcasts vs. Recorded Waves," Final Report 06768, 1965, University of Michigan, Ann Arbor, Mich.

10. Richards, T. L., Dragert, H., and McIntyre, D. R., "Influence of Atmospheric Stability and Over-Water Fetch on Winds over the Lower Great Lakes," Monthly Weather Review, Vol 94, No. 1, 1966, pp 448-453.

11. Sverdrup, H. V. and Munk, W. H., "Wind, Sea and Swell: Theory of Relations for Forecasting," Publication No. 601, 1947, Hydrographic Office, U. S. Department of the Navy, Washington, D. C.

12. _____, "Techniques for Forecasting Wind, Waves, and Swell," Publication No. 604, 1951, Hydrographic Office, U. S. Department of the Navy, Washington, D. C.

13. Pierson, W. J., Jr., and Moskowitz, L., "A Proposed Spectral Form for Fully Developed Wind Seas Based on the Similarity Theory of S. A. Kitaigorodskii," Journal, Geophysical Research, Vol 69, No. 24, 1964, pp 5180-5190.

14. Pierson, W. J., Neumann, G., and James, R. W., "Observing and Forecasting Ocean Waves by Means of Wave Spectra and Statistics," Publication No. 603, 1955, Hydrographic Office, U. S. Department of the Navy, Washington, D. C.

15. Hunt, I. A., "Winds, Wind Set-Ups and Seiches on Lake Erie," paper presented to Second National Conference in Applied Meteorology, 1958.

16. Lemire, F., "Winds on the Great Lakes," CIR-3560, TEC-380, 1961, Meteorological Branch, Canadian Department of Transport, Toronto, Canada.

17. Richards, T. L., "Recent Developments in the Field of Great Lakes Evaporation," Verhandlungen, International Verin. Limnologie, Stuttgart, Vol 15, 1964, pp 247-256.

18. Richards, T. L. and Phillips, D. W., "Synthesized Winds and Wave Heights of the Great Lakes," Climatological Studies No. 17, 1970, Meteorological Branch, Canadian Department of Transport, Toronto, Canada.

19. Cardone, V. J., "Specification of the Wind Distribution in the Marine Boundary Layer for Wave Forecasting," Technical Report 69-1, 1969, Geophysical Sciences Laboratory, New York University, New York, N. Y.

20. Bijvoet, H. C., "A New Overlay for the Determination of the Surface Wind over the Sea from Surface Weather Charts," Mededelingen en Verhandelingen, 1957, Koninklijk Netherlands Meteorologisch Institut.

21. Johnson, P. W., "The Ratio of the Sea-Surface Wind to the Gradient Wind," Proceedings, First Conference on Ships and Waves, Chapter 9, 1955, pp 104-110.

22. Helmholtz, H., "Uber Discontinuirliche Flussigkeitsbewegungen," Mber. Preuss. Akad. Wiss., 1868, pp 215-228.

23. Johnson, J. W., "Relationships Between Wind and Waves, Abbotts Lagoon, California," Transactions, American Geophysical Union, Vol 31, No. 3, 1950, pp 386-392.

24. Bretschneider, C. L., "Deep-Water Forecasting Waves as a Function of Wind Speed, Fetch, and Duration," Shore Protection Manual, Vol 1, pp 3-36 - 3-37, 1973, U. S. Army Coastal Engineering Research Center, Fort Belvoir, Va.

25. Rice, S. O., "The Mathematical Analysis of Random Noise," Bell System Technical Journal, Vol 23, 1945, pp 283-332.

26. Tukey, J. W. and Hamming, R. W., "Measuring Noise Color," Internal Memorandum MM49, 1949, Bell Telephone Laboratories, Murray Hill, N. J.

27. Pierson, W. J., "A Unified Mathematical Theory for the Analysis, Propagation, and Refraction of Storm Generated Ocean Surface Waves," Part 1, 1952, Department of Meteorology, New York University, N. Y.

28. Longuet-Higgins, M. S., "On the Statistical Distribution of the Heights of Sea Waves," Journal, Marine Research, Vol 11, No. 3, 1952, pp 245-266.

29. Barnett, T. P. and Wilkerson, J. C., "On the Generation of Ocean Wind Waves as Inferred from Airborne Radar Measurements of Fetch-Limited Spectra," Journal, Marine Research, Vol 25, No. 3, 1967, pp 292-321.

30. Barnett, T. P., On the Generation, Dissipation, and Prediction of Ocean Wind Waves, Ph. D. Dissertation, 1966, University of California, San Diego, Calif.

31. Baer, L., "An Experiment in Numerical Forecasting of Deep Water Ocean Waves," LMSC-801296, 1962, Lockheed Missile and Space Company, Inc., Sunnyvale, Calif.

32. Inoue, T., "On the Growth of the Spectrum of a Wind-Generated Sea According to a Modified Miles-Phillips Mechanism and Its Application to Wave Forecasting," Technical Report 67-5, 1967, Geophysical Sciences Laboratory, New York University, New York, N. Y.

33. Eckart, C., "The Generation of Wind Waves over a Water Surface," Journal, Applied Physics, Vol 24, 1953, pp 1485-1494.

34. Phillips, O. M., "On the Generation of Waves by Turbulent Wind," Journal, Fluid Mechanics, Vol 2, 1957, pp 417-445.

35. Miles, J. W., "On the Generation of Surface Waves by Shear Flows," Journal, Fluid Mechanics, Vol 3, 1957, pp 185-204.

36. Hasselmann, K., "On the Non-Linear Energy Transfer in a Gravity-Wave Spectrum; General Theory," Journal, Fluid Mechanics, Vol 12, Part 1, 1962, pp 481-500.

37. _____, "On the Non-Linear Energy Transfer in a Gravity-Wave Spectrum; Conservation Theorems; Wave-Particle Analogy; Irreversibility," Journal, Fluid Mechanics, Vol 15, Part 2, 1963, pp 273-281.

38. _____, "On the Non-Linear Energy Transfer in a Gravity-Wave Spectrum; Evaluation of the Energy Flux and Swell-Sea Interaction for a Neumann Spectrum," Journal, Fluid Mechanics, Vol 15, Part 3, 1963, pp 385-398.

39. Lazonoff, S. M., Stevenson, N. M., and Cardone, V. J., "A Mediterranean Sea Wave Spectral Model," Technical Note No. 73-1, 1973, Fleet Numerical Weather Central, Monterey, Calif.

40. Hasselmann, K. et al., "Measurements of Wind-Wave Growth and Swell Decay During the Joint North Sea Wave Project JONSWAP," 1973, Deutsches Hydrographisches Institut, Hamburg, Germany.

41. Jenkinson, A. F., "The Frequency Distribution of the Annual Maximum (or Minimum) Values of Meteorological Elements," Quarterly Journal, Royal Meteorological Society, Vol 81, 1955, pp 158-171.

42. Gumbel, E. J., Statistics of Extremes, Columbia University Press, New York, 1959.

43. Gringorten, I. I., "Extreme-Value Statistics in Meteorology--A Method of Application," Air Force Surveys in Geophysics No. 125, 1963, Air Force Cambridge Research Center, Bedford, Mass.

44. Jenkinson, A. F., "Statistics of Extremes," Estimation of Maximum Floods, Technical Note No. 98 (WMO-No. 223, TP. 126), Chapter 5, pp 183-227, 1969, World Meteorological Organization, Geneva, Switzerland.

45. Dalrymple, T., "Flood-Frequency Analyses," Manual of Hydrology: Part 3. Flow-Flow Techniques, Water Supply Paper 1543, Chapter A, pp 1-79, 1960, U. S. Geological Survey, Washington, D. C.

46. Langbein, W. B., "Annual Floods and the Partial-Duration Flood Series," Transactions, American Geophysical Union, Vol 30, No. 6, 1949, pp 879-881.

47. Chow, V. T., Discussion of "Annual Floods and the Partial Duration Flood Series," by W. B. Langbein, Transactions, American Geophysical Union, Vol 31, 1950, pp 939-941.

48. Freeman, J. C., Jr., Zeis, J. R., and Ross, S., "Effects of Directionality on Wave Statistics and Wave Spectra," 1972 Offshore Technology Conference Preprints, Paper No. OTC-1689, Vol II, 1972, pp II-645 - II-656.

49. Collins, J. I. and Wier, T. W., "Prediction of Shallow Water Spectra," Final Technical Report TETRAT P-71-164-2, Aug 1971, Tetra Tech, Inc., Pasadena, Calif.

50. Kitaigorodskii, S. A., "The Physics of Air-Sea Interaction," translated by A. Baruch, Israel Program for Scientific Translations, Ltd. (available from National Technical and Information Services, U. S. Department of Commerce, Springfield, Va.), 1970.

51. Shames, I. H., Mechanics of Fluids, McGraw-Hill, New York, 1962.

52. Panofsky, H. A., "Determinations of Stress from Wind and Temperature Measurements," Quarterly Journal, Royal Meteorological Society, Vol 89, 1963, pp 85-94.

53. Gelci, R. and Cazalé, H., "Une équation synthétique de l'évolution de l'état de la mer," J. Méchan. Phys. Atmosphere, Series 2, Vol 4, 1962, pp 15-41.

54. Hasselmann, K., "Feynman Diagrams and Interaction Rules of Wave-Wave Scattering Processes," Reviews of Geophysics, Vol 4, No. 1, Feb 1966, pp 1-32.

55. Hasselmann, K., "Nonlinear Interactions Treated by the Methods of Theoretical Physics," Proceedings, Royal Society of London, Series A, Vol 299, 1967, pp 77-100.

56. _____, "Grundgleichungen der Seegangsvoraussage," Schiff-stechnik, Vol 7, 1960, pp 191-195.

57. Hasselmann, K. and Collins, J. I., "Spectral Dissipation of Finite-Depth Gravity Waves Due to Turbulent Bottom Friction," Journal, Marine Research, Vol 26, No. 1, 1968, pp 1-12.

58. Barnett, T. P., "On the Generation, Dissipation, and Prediction of Wind Waves," Journal, Geophysical Research, Vol 73, No. 2, 1968, pp 513-529.

59. Snyder, R. L. and Cox, C. S., "A Field Study of the Wind Generation of Ocean Waves," Journal, Marine Research, Vol 24, No. 2, 1966, pp 141-178.

60. Tyler, G. L. et al., "Wave Directional Spectra from Synthetic Aperture Observations of Radio Scatter," Deep-Sea Research, Vol 21, No. 12, 1974, pp 989-1016.

61. Sell, W. and Hasselmann, K., "Computations of Nonlinear Energy Transfer for JONSWAP and Empirical Wind Wave Spectra," 1972, Inst. Geophys., Univ. Hamburg, Hamburg, Germany.

62. Phillips, O. M., "The Equilibrium Range in The Spectrum of Wind-Generated Waves," Journal, Fluid Mechanics, Vol 4, 1958, pp 426-434.

63. Mitsuyasu, H., "On the Growth of the Spectrum of Wind-Generated Waves (I)," Reports of Research Institute for Applied Mechanics, Kyushu University, Fukuoka, Japan, Vol 16, No. 55, 1968, pp 459-482.

64. Platzman, G. W., "The Dynamic Prediction of Wind Tides on Lake Erie," Meteorological Monographs, Vol 4, No. 26, 1963.

65. Gringorten, I. I., "A Simplified Method of Estimating Extreme Values from Data Samples," Journal, Applied Meteorology, Vol 2, 1962, pp 82-89.

Table 1

Wind Analyses*

Comparisons with Observed Winds	Number of Data Pairs	Correlation Coefficient
Bretschneider winds versus 10-m winds	36	0.63
Jacobs 7.5-m winds versus 7.5-m winds	43	0.55
Jacobs 19.5-m winds versus 16-m winds	49	0.37
Richards winds versus 16-m winds	44	0.36
Richards winds versus 10-m winds	36	0.24

* From Reference 7.

Table 2

Estimates of Wind Ratios "R" for the Great Lakes*

Hunt[15]		Lemire[16]			Richards[17] Extension	Richards, Dragert, and McIntyre[10]
			Jan		1.96	--
			Feb		1.94	--
			Mar	1.88	1.88	--
			Apr	1.81	1.81	--
Spring	1.35	1.38	May	1.71	1.71	--
			Jun	1.31	1.31	--
			Jul	1.16	1.16	--
			Aug	1.39	1.39	--
Fall	1.82	1.87	Sep	1.78	1.78	--
			Oct	1.99	1.99	--
			Nov		2.09	--
			Dec		1.98	--
Average	1.56**	1.63**			1.66†	1.56†

* From Reference 18.
** Navigation season.
† Annual.

Table 3

Correlation Between Winds Over Land and Wind Observations by Ship Stratified by Stability Class and Number of Observations per Three Hours

Stability Class	Number of Observations per 3 hr			
	1	2	3	4
1	0.780(38)	0.825(17)	0.809(9)	--
2	0.528(119)	0.695(50)	0.717(30)	0.707(13)
3	0.480(207)	0.590(92)	0.610(39)	0.715(11)
4	0.589(227)	0.698(83)	0.898(34)	0.920(11)
5	0.370(97)	0.631(36)	0.672(15)	0.825(3)
6	0.358(31)	0.426(15)	0.594(6)	--
7	0.730(10)	0.097(4)	--	--

Note: Number in parentheses represents number of samples on which correlation is based.

Table 4

RMS Error in Wind Estimates Over the Great Lakes

Land Wind Speed knots	RMS Error knots
0-3	5.2
3-6	5.9
6-9	5.3
9-12	4.6
12-15	4.0
15-18	3.9
18-21	3.9
21-24	3.6
24-27	3.5

Table 5

Relationship Between Recurrence Intervals as Calculated from Partial-Duration Series and from Annual Maxima

Partial-Duration Series	Annual Floods
0.50	1.16
1.00	1.58
1.45	2.00
2.00	2.54
5.00	5.52
10.00	10.50
20.00	20.50
50.00	50.50
100.00	100.50

APPENDIX A: METHODOLOGY OF OVERLAKE WIND ESTIMATION

1. In deep water, the generation of waves by the wind can be given in functional forms as (Kitaigorodskii[50†]):

$$F(\omega) = G(\omega, T, X) \tag{A1}$$

where

$F(\omega)$ = one-dimensional spectral energy and a function of angular frequency ω

G = function

T = nondimensional time factor

X = nondimensional fetch factor

Both T and X are in turn functions of the friction velocity

$$X = \frac{xg}{u_*^2} \tag{A2}$$

$$T = \frac{tg}{u_*} \tag{A3}$$

where

x = actual fetch

g = gravitational acceleration

u_* = friction velocity

t = wind duration

The dependence of wave growth on the friction velocity necessitates a knowledge of the wind profile rather than the wind at only one level.

2. Prior to the mid-1960's, the height of wind instruments above ground varied considerably from station to station (20 to > 300 ft). Instrument heights and station locations at most cities were changed several times.

3. The methods for transforming the raw wind-speed data into inputs to the wave hindcasting program will be considered in two parts: (a) data taken prior to 1948, and (b) data taken after 1948. This date is chosen as a separator because the National Weather Service began

---

† Raised numbers refer to similarly numbered items in "References" on pp 45-49 at end of main text.

consistently recording data at all first-order airport weather stations in 1948.

Post-1948 Wind Transformations

4. If the assumption is made that the wind profile at an instrument site is logarithmic in shape, the following relationship can be used to relate two wind speeds (u_1 , u_2) taken at different elevations (Z_1 , Z_2):

$$\frac{u_1}{u_2} = \frac{u(Z_1)}{u(Z_2)} = \left(\frac{Z_1}{Z_2}\right)^{1/7} \tag{A4}$$

Over land where a neutral profile can usually be assumed for hourly average conditions, Equation A4 gives a good estimate of the wind, if only the instrument height varies and not location of the instrument tower.

5. Changes in the location of the wind instruments generally result in changes in roughness for the local boundary layer unless the distances are small and the environmental characteristics homogeneous over a large area. Hence, the one-seventh power law may produce errors. To test the effect of movement of stations, the subsequent approach was used.

6. For every season and station, the wind-speed distribution function was estimated for each period where instrument location and height were constant. Recurrence intervals were calculated and plotted (Figure A1) and the linear least-square estimate of the relationship between the logarithm of the recurrence interval and wind speed was determined for winds in the 15- to 30-knot velocity range.*

7. To calculate the transformation to the standard station height since 1965 (20 ft), the equations between recurrence interval and wind

---

* This range was selected on the basis of there being a sufficient frequency of occurrence of these wind speeds to provide a large sample for the regression calculations. The nonlinear effect of deviations due to sampling in higher velocities was thus avoided.

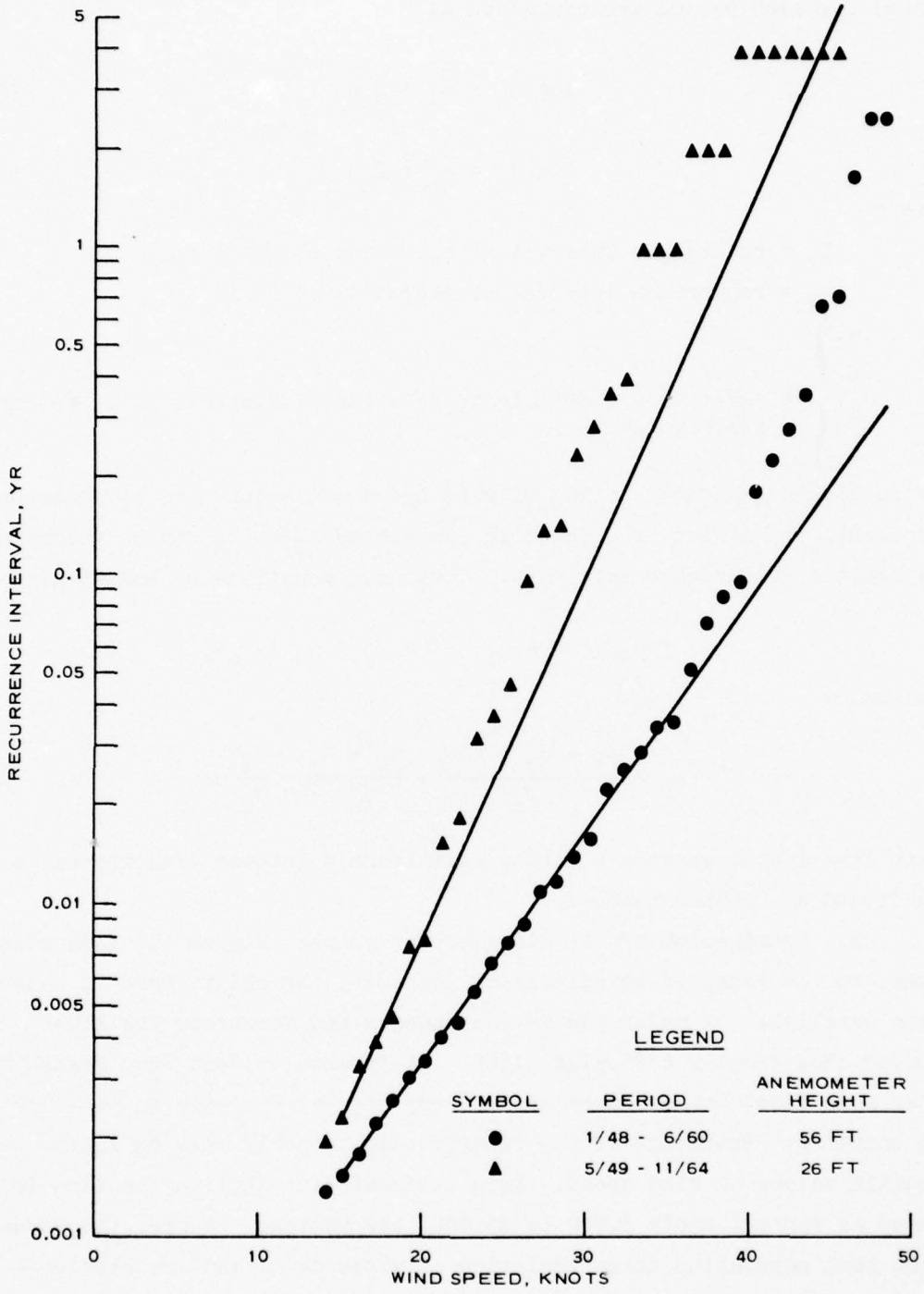

Figure A1. Shifts in distribution function of winds for different anemometer levels at Watertown (Winter)

speed for each period are expressed as

$$\log T_\ell = a_\ell + B_\ell u \tag{A5}$$

$$\log T_s = a_s + B_s u_s \tag{A6}$$

where

T_ℓ = recurrence interval at elevation above 20 ft

T_s = recurrence interval at elevation of 20 ft

a_ℓ, B_ℓ, a_s, B_s = regression coefficients relating wind speeds at different elevations

If population characteristics of wind speed are assumed to be reasonably constant, the effect of changes in anemometer location can be estimated by equating recurrence intervals. Combining Equations A5 and A6 gives

$$a_\ell + B_\ell u = \log T_\ell = \log T_s = a_s + B_s u_s \tag{A7}$$

and hence

$$u_s = \frac{a_\ell - a_s + B_\ell u}{B_s} = \frac{a_\ell - a_s}{B_s} + \frac{B_\ell}{B_s} u \tag{A8}$$

with Equation A5 showing a linear relationship between wind speeds at 20 ft and at another height.

8. Examination of the distribution graphs (Figure A1) indicates that, in the range of velocities of interest, the shifts have in general been parallel. If major population changes had occurred, the lines should show greatly differing tilts. It is also evident from Figure A1 that some fluctuations do occur for very high wind speeds in part due to sampling. Estimates of the relationship properly rely on intermediate values of wind speed. Each seasonal distribution function is based on approximately 5,000 to 25,000 observations. Hence, the assumption that population characteristics of winds over land are statistically stable appears to be reasonable.

9. For changes in instrument height or small spatial movements

of site, the values predicted from Equation A5 agree well with the one-seventh power law. If the spatial change is several miles, however, the results differ greatly.

10. In summary, transformation following the method of Equations A4 and A8 can be derived to adjust wind speeds. The primary assumption that must be met, however, is that the wind profile is neutral on the time scale of average hourly winds. If the site is a land site away from immediate lake influence, this assumption is usually assured and is also probably good for post-1948 wind stations, as shown in the next section.

Pre-1948 Winds

11. Prior to 1948, most available weather data were taken at sites located in the downtown areas of the cities and not at the airports. Among the problems that had to be resolved before transformation of these winds were (a) the proximity of these stations to the lake, (b) the shifting of station heights and locations, and (c) the unavailability of the data on magnetic tape or computer cards.

12. The pre-1948 data are only available in autograph form. Hence, the cost of applying the distribution function arguments of the previous section was prohibitive. However, the shifts in station location were small spatially and the variations in height were large; thus, the one-seventh power law could be reasonably applied. The effect of large buildings, typical of downtown areas, upon the wind climate must be regarded as unknown at this time. However, the extreme height of the site locations (100-300 ft) atop these buildings somewhat alleviates the problems associated with funneling between buildings.

13. A major problem that must be confronted for these stations involves their proximity to the lake. For winds blowing offshore, the assumption of a neutral land profile is probably justified; the winds can be transformed to 20 ft using Equation A8. After this adjustment in height, the land and lake transformation formulae of Part II are used to estimate the lake winds.

14. For winds blowing onshore, the boundary layer associated with land roughness elements grows in height with distance inland. Hence, if the instrument site is sufficiently high and near the lake, it is in the marine boundary layer; therefore, stability effects must be considered.

15. If flow from the lake-wind regime onto land is regarded as an analogue to the classical problem of incompressible, turbulent flow over the leading edge of a flat plate, the depth of the land boundary layer (δ_*) can be expressed as (Shames[51])

$$\delta_* = \left(\frac{\nu}{V_o}\right)^{1/5} X_\ell^{4/5}(0.376) \tag{A9}$$

where

ν = dynamic viscosity of air

V_o = wind velocity†

X_ℓ = distance inland from the lake-land interface

When this analogue is used for a velocity of 50 mph and temperatures typical of the Great Lakes environment, the thickness of the land boundary layer is calculated to be 25 ft at 1 mile from shore, 42 ft at 2 miles, 58 ft at 3 miles, and 88 ft at 5 miles.

16. Many stations prior to 1948 were located within 2 miles of the lake. Thus, although the calculated boundary-layer thickness is only a crude estimate, it appears that such stations were in the marine boundary layer. Likewise, all of the post-1948 land sites were located more than 5 miles inland and have anemometers at heights well within the land boundary layer as predicted by Equation A9.

17. For cases in which stations appeared to fall within the marine boundary layer, a theoretical form of the wind profile was applied to transform winds from one level to another. In this transformtion, the similarity form of a wind profile in the presence of vertical temperature gradients is given by

$$u(Z) = \frac{u_*}{K} \ln\left(\frac{Z}{Z_o}\right) - \phi\left(\frac{Z}{L'}\right) \tag{A10}$$

---

† In the classical problem, the velocity V is constant with height up to the edge of the plate; however, in this case, V must be replaced by a velocity averaged over height.

where

K = Von Karman constant

Z_o = roughness height

ϕ = modification function for wind profile due to thermal effects

L' = stability length

For stable conditions, ϕ has been found to be representable as a linear function of Z/L'

$$\phi = \frac{BZ}{L'} \tag{A11}$$

where B , the linear constant for log-linear wind profile, equals -7 . In unstable conditions, ϕ is given by

$$\phi = \int_1^{\varepsilon} \left(-1 + \frac{2}{1+\delta} + \frac{2}{1+\delta^2} + \frac{2\delta}{1+\delta^2} - \frac{3}{\delta} \right) d\delta \tag{A12}$$

where ε is nondimensional wind shear and δ is the integration variable. The relationship between ε and Z/L' is specified by the KEYPS function constant k (Panofsky[52])

$$\varepsilon^4 - \frac{kZ}{L'} \varepsilon^3 - 1 = 0 \tag{A13}$$

with $k = 18$.

18. These equations can be solved to yield u_* , Z_o , and L' as a function of wind speed, anemometer height, air-sea temperature difference, and height of air thermometer above water surface. A numerical solution and computer routine developed by Cardone[19] are incorporated into the wave-hindcast model. Once u_* , Z_o , and L' are computed, the wind speed at another level can be obtained by the use of Equation A10; hence, wind velocities at the desired anemometer elevation (19.5 m) can be calculated.

Transformation to Winds Over the Lake

19. After winds have been transformed to a standard elevation

of 20 ft* (by the one-seventh power law for pre-1948 winds and by the regression relationships for post-1947 winds), the transformation to winds over the lake is given by

$$U_w = RU_\ell \tag{A14}$$

where U_w is the wind velocity over water, R is a function of wind velocity and air-sea temperature difference $(T_a - T_s)$, and U_ℓ is the wind velocity over land

$$R = R(U_\ell, T_a - T_s) \tag{A15}$$

20. Figure A2 gives the relationship between R and U_ℓ. The dependence of R on air-sea temperature difference is given in Figure 11 of the main text.

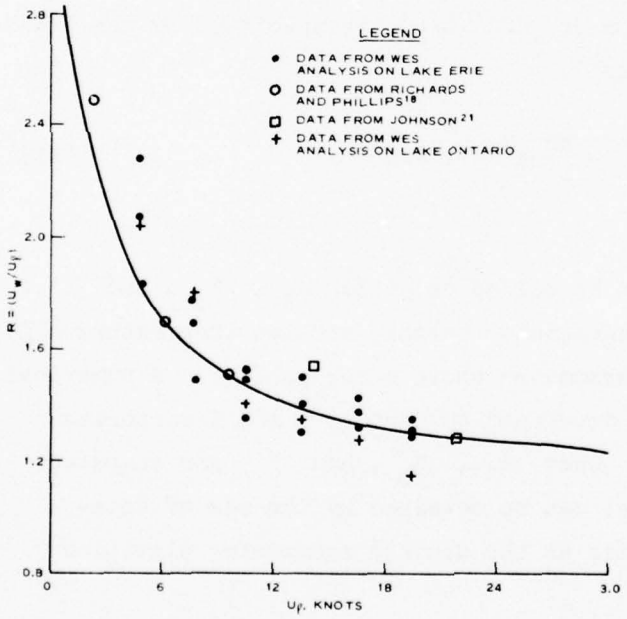

Figure A2. Velocity ratios as a function of wind speed over land

* This does not refer to winds which lie in the marine boundary layer, as given by Equation A9.

APPENDIX B: TREATMENT OF GENERAL ASPECTS OF NUMERICAL WAVE MODEL

1. The spectral energy density in a wave spectrum is treated as a five-dimensional variable. It is a function of surface location $\vec{x}(x,y)$, wave number vector $\vec{k}(k_1,k_2)$, and time (t), i.e., $F(\vec{x},\vec{k},t)$. The wave number vector can alternately be viewed in terms of frequency (f) and propagation direction (θ). The total energy* at point (x_o,y_o,t_o) can be obtained by integrating it over wave number space

$$\sigma^2 = \int_{k_1}\int_{k_2} F(x_o,y_o,t_o,k_1,k_2)\, dk_1\, dk_2 \qquad \text{(B1)}$$

or in frequency and direction space

$$\sigma^2 = \int_{f}\int_{\theta} F(x_o,y_o,t_o,f,\theta)\, df\, d\theta \qquad \text{(B2)}$$

2. Ocean waves are a statistical phenomenon. The complex manner in which they interact with other media at boundaries along internal boundaries, or even within a spectrum, can be described only in terms of statistical averages over space and time. When $\vec{k}$ and $\vec{x}$ are given as the wave number vector and location vector, respectively, the transfer of energy into and out of a wave component can be written in the form of an energy balance or radiative transfer equation (Gelci and Cazalé,[53]** Hasselmann[54])

$$\frac{DF}{Dt} = \frac{\partial F}{\partial t} + \dot{x}_i \frac{\partial F}{\partial x_i} + \dot{k}_i \frac{\partial F}{\partial k_i} = S \qquad \text{(B3)}$$

where

$\partial F/\partial t$ = local (in space) rate of change of F

$\dot{x}_i(\partial F/\partial x_1)$ = effect of advection of energy into F

---

* In actual application, the term F does not have the units of energy but rather of length squared. It also represents that portion of the variance of the surface elevation in a particular frequency band and direction band at location $\vec{x}$.

** Raised numbers refer to similarly numbered items in "References" on pp 45-49 at end of main text.

$\dot{k}_i(\partial F/\partial k_i)$ = effect of changes in the wave number on F

S = any process that transfers energy into and out of wave component $F(\vec{x},\vec{k},t)$

The dot over x_i and k_i denotes differentiation with respect to time, and the subscript i represents the conventional summation over all dimensions. In a Lagrangian context, DF/Dt represents the rate of change of F as it propagates through $\vec{x}$ to $\vec{k}$ space along the path determined by the Hamiltonian equations.

$$\dot{x}_i = \frac{\partial}{\partial k_i} \sigma(\vec{x},\vec{k}) \tag{B4}$$

$$\dot{k}_i = \frac{\partial}{\partial x_i} \sigma(\vec{x},\vec{k}) \tag{B5}$$

where σ is the circular frequency associated with F. In deep water or in water of constant depth d, the refraction term $(\dot{k}_i \partial F/\partial k_i)$ vanishes. In this case, Equation B4 becomes

$$\dot{x}_i = \frac{\partial}{\partial k_i} \sigma = \text{constant} \tag{B6}$$

where the constant is the group velocity of waves with circular frequency in water of depth d.

3. Hasselmann[55] demonstrated that the source term S can be represented in a general form by

$$S(\vec{k}) = S_1 + S_2 + S_3 + S_4 + S_1' + S_2' + S_3' + S_4' + S_5 + S_6 + S_7 \tag{B7}$$

where

$S_1 = \alpha$

$S_2 = BF(\vec{k})$ in which B is the coefficient of coupling between surface waves and mean wind profile

$S_3 = F(\vec{k}) \int \gamma(\vec{k},\vec{k}')F(\vec{k}')\, d\vec{k}'$

$S_4 = -SF(\vec{k}) + \int \varepsilon(\vec{k},\vec{k}')F(\vec{k}')\, d\vec{k}'$

$S_1' \ldots S_4'$ = same functional form as $S_1 \ldots S_4$

$S_5 = \iiiint T_1 F(\vec{k}')F(\vec{k}'')F(\vec{k} - \vec{k}' - \vec{k}'') - T_2 F(\vec{k})F(\vec{k}')F(\vec{k}'')\, d\vec{k}'\, d\vec{k}''$ in which T_1 and T_2 are transfer functions and are dependent on the coupling coefficients between spectral components involved in the interactions

$S_6 = -\nu_{ij} k_i k_j F(\vec{k})$ with ν_{ij} as the viscosity sensor

S_7 = an undetermined dissipation function due to wave breaking

The processes embodied in these terms are as follows:

a. $S_1(\alpha)$ - energy transfer to the wave field through turbulent pressure fluctuations in the atmosphere (Eckart,[33] Phillips[34]).

b. S_2 - energy transfer due to Miles[35] instability mechanism.

c. S_3 - energy transfer in a nonlinear correction to Miles' theory.

d. S_4 - energy transfer due to wave-turbulence interactions (Hasselmann[56]).

e. S_1', S_2', S_3', S_4' - energy transfers due to analogous processes to S_1, S_2, S_3, and S_4, except the interaction is between waves and other ocean phenomena rather than waves and atmospheric phenomena.

f. S_5 - energy transfer due to nonlinear wave-wave interactions (Hasselmann[36,37,38,56]).

g. S_6 - loss of energy from waves due to turbulent bottom friction (Hasselmann and Collins[57]).

4. When the processes are presented in this way, the multitude of theoretical treatments of the wind generation of waves can be put in some context and thus compared. However, the theory presented by Hasselmann covers only weak interactions. Any processes that violate the assumption of a slowly varying spectrum and some nonexpansible processes are not included in Equation B7. It is still a definite improvement over the unorganized development of empirical and theoretical mechanisms for wave growth and provides a means of comparing and evaluating source functions proposed by different investigations.

5. Source functions for the two models used in the study can be written as follows:

a. For the Inoue model[32] using modified Miles-Phillips mechanism,†

$$S_I = S_1(1 - q^2)^{1/2} + S_2^*(1 - q^2)^2 \tag{B8}$$

where

S_I = sum of sources

q = ratio of energy density in one-dimensional spectrum $E(f)$ to that in fully developed spectrum $E_\infty(f)$

As given by Pierson and Moskowitz,[13]

$$E_\infty(f) = \frac{2\pi a g^2}{\sigma^5} \exp\left[-\beta\left(\frac{\omega_o}{\omega}\right)^4\right] \tag{B9}$$

where

a = Phillips equilibrium constant (0.0081)

g = gravity

β = energy transfer due to interaction between mean wind profile and waves (as a constant = 0.74)

ω_o = wind frequency (ratio of g to wind speed u)

b. For the Barnett model[30] using parameterized wave-wave interactions,

$$S_B = (S_1 + S_2)(1 - \phi) + S_5 \tag{B10}$$

where S_B represents the sum of sources. The limiting function ϕ for wind input equals $d_1 \exp[-d_2(R' - F)/F]$ with d_1 and d_2 constants and R, the angular spreading function, defined by Phillips equilibrium spectrum as

$$R(f,\theta) = \frac{ag^2}{\sigma^5} h(\theta) \tag{B11}$$

---

† The actual form of S_2 in the Inoue model was a one-dimensional spectrum in place of a two-dimensional spectrum. S_2^* is given by $BE(f)'$ as opposed to $BF(f,\theta)$ where $F(f,\theta)$ is the two-dimensional spectrum.

6. For numerical processing, Barnett[58] chose a *normalized* $\cos^4 \theta$ distribution of energy as a function of direction for $h(\theta)$, the spreading factor; that is,

$$h(\theta) = \frac{3\pi}{8} \cos^4 \theta \tag{B12}$$

7. With two such different source functions, one might expect vastly different results from the application of these two models; however, this is not the case. The inability of experimental procedure to adequately separate the different source terms has led to a situation in which source terms in hindcast models are most likely an empirical mixture of more than one theoretical source term. As an example of this, the same data from the limited-fetch study by Snyder and Cox[59] have been used by both Barnett[30] and Inoue[32] to justify totally different functional forms for source terms. Yet, in most cases the two models appear to coincide rather well, at least in terms of gross-scale parameters such as significant wave height and frequency of the maximum spectral energy density. It is easier to compare the functional forms of the two models if the limiting terms are temporarily discarded. The full radiative transfer Equation B3 is solved by Barnett, whereas Inoue reduces the equation to its linear form

$$\frac{dF}{dt} = S_1 + S_2^* \tag{B13}$$

In the linear form of this model, energy is "jumped" from one grid point to another in a somewhat erratic manner.

8. During the preparation of some preliminary results for sites on Lake Erie and Lake Ontario, it was determined that the one-dimensional nature of the Inoue source function could not adequately treat variations in shoreline geometry typical of the Great Lakes. The asymmetry of the spectrum with respect to propagation direction could not be accounted for near the coast. Winds blowing parallel to a coast thus tend to generate large waves in proximity to the coastline. Other areas of weakness were the difficulty of treating a rapidly changing

wind direction and the lack of consideration given to the variation of fetch in cases with highly irregular shorelines. For most wave generation sequences on the Great Lakes, the one-dimensional treatment still gave very reasonable results; however, under some conditions wave heights appeared to grow improbably fast and at other times improbably slow.

9. The success of the Inoue model in deep water (where the spatial gradients are usually somewhat small) makes it very difficult to dismiss the validity of the source function, at least in terms of reproducing significant wave heights and periods. This prompted a modification of the Inoue source function to the form

$$S_I = \alpha + \beta F \phi(\theta,\theta_w) \tag{B14}$$

where $\phi(\theta,\theta_w)$ represents an attempt to account for the effect of the angle between the propagation direction θ and wind direction θ_w. A simple form of $\phi(\theta,\theta_w)$ equal to $\cos |\theta - \theta_w|$ was found to perform reasonably well in generating a spectrum with a spreading factor proportional to $\cos^2 \theta$ around the mean propagation direction. Recent field studies (Hasselmann et al.[40]) have shown that such a spreading factor gives the best fit to observations. Deviations from this form and detailed fine structure in the directional distribution of wave energy have been found to be irreproducible (Tyler et al.[60]).

10. By using Equation B13, the Inoue model can be compared with the Barnett model. Barnett[30] parameterized the net transfer of energy due to wave-wave interactions and expressed the general form of this nonlinear ($n\ell$) energy transfer as

$$\left(\frac{\partial F}{\partial t}\right)_{n\ell} = \Gamma - \tau F \tag{B15}$$

where Γ represents the gain of energy of wave component F from all interactions in which it plays a passive role and $-\tau F$ represents the loss of energy due to all the interactions in which it plays an active role. For a slowly varying spectrum (as necessary for the theory of

weak interactions to be valid), the form of the radiative transfer equation at time t_o for the two different source functions is (again neglecting the limiting terms in each model) written as

Inoue Model

$$\frac{\partial F}{\partial t} = \alpha_I + \beta_I F - \vec{C}_G \cdot \vec{\nabla} F \tag{B16}$$

and

Barnett Model

$$\frac{\partial F}{\partial t} = \alpha_B + \Gamma + (\beta_B - \tau) F - \vec{C}_G \cdot \vec{\nabla} F \tag{B17}$$

where C_G represents group velocity and the subscripts I and B refer to the specific, empirically determined source terms used by Inoue and Barnett, respectively. The superficial similarity is striking. It would seem that, if $\alpha_I = \alpha_B + \Gamma$ and $\beta_I = \beta_B - \tau$, the two source functions would be equivalent. However, whereas α_I, α_B, β_I, and β_B are functions only of wind speed, gravity, wave direction, and wave frequency, the functional forms of τ and Γ, wave-wave interaction parameters, are

$$\tau = \tau(g, E, f, f_o, \theta, \theta_o) \tag{B18}$$

and

$$\Gamma = \Gamma(g, E, f, f_o, \theta, \theta_o) \tag{B19}$$

Thus the following three new parameters E, f_o, and θ_o are introduced:

$$E = \iint F(f,\theta)\, df\, d\theta \tag{B20}$$

$$f_o = \left[\frac{1}{E} \iint F(f,\theta) f^2\, df\, d\theta\right]^{1/2} \tag{B21}$$

and

$$\theta_o = \tan^{-1} \frac{\iint F(f,\theta) \sin\theta\, df\, d\theta}{\iint F(f,\theta) \cos\theta\, df\, d\theta} \tag{B22}$$

* These terms are given as

$$f_o = \frac{1}{E} \iint F(f,\theta) f\, df\, d\theta \quad \text{and} \quad \theta_o = \frac{1}{E} \iint F(f,\theta) \theta\, df\, d\theta$$

in the original work by Barnett[30] but cannot be correctly computed from these forms.

11. These new parameters couple the source function to the local spectrum, something not done in the Inoue model. This change is very important at least in terms of evaluating the physical interpretation of the energy transfers. In the Barnett model, the source function produces an eventual quasi-equilibrium, whereas the source function must be artificially cut off once the spectral energy has reached a velocity-dependent form. Since the wave-wave model does not require such an unrealistic cutoff, it should be interpreted as being a better representation of the actual physics of wave growth.

12. The dependence of the wave spectra on wave-wave interactions has received additional support in recent years by the documentation of an "overshoot" effect (Barnett,[30] Hasselmann et al.[40]). Figure B1 shows

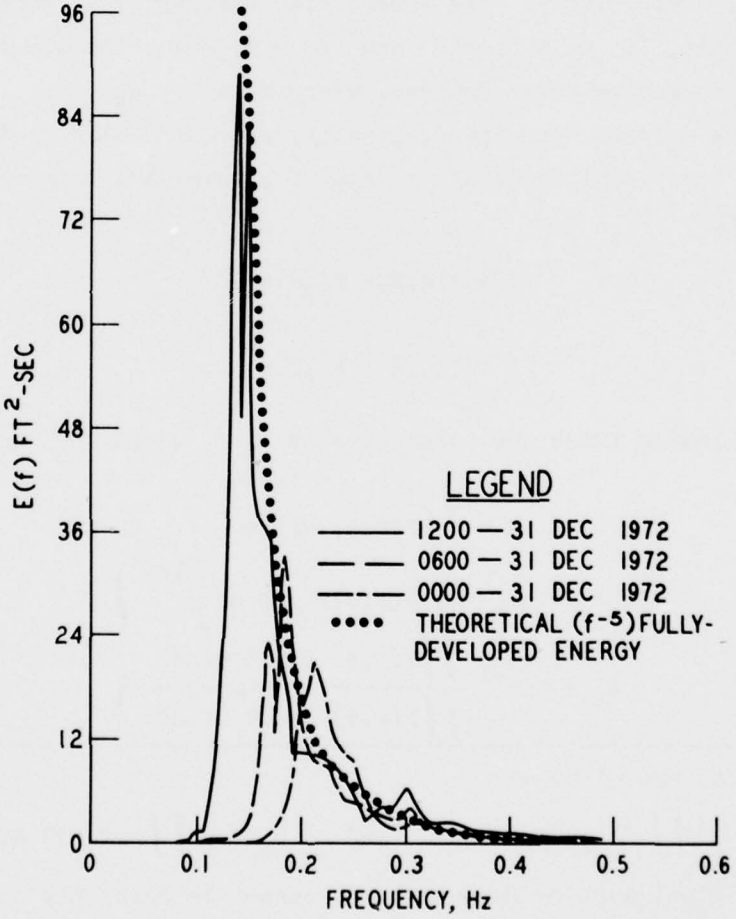

Figure B1. Sequence of spectra from Toronto

a typical time sequence of wave spectra from Toronto. The presence of energy in the spectral peak above that predicted on a strict similarity basis ($\sim f^{-5}$) is evidence that the spectrum is also affected by a self-similarity criterion $\left[\sim\left(F^5 \ , \ f/f_{max}\right)\right]$, suggesting a relationship between wave breaking and spectral peak.

13. The parameterizations used by Barnett to represent the effect of wave-wave interactions are

$$\tau = \frac{7.5 \times 10^{7} E^{2} f_o^{7}}{g^{4} f} \left[1 + 16 \left|\cos\left(\theta - \theta_o\right)\right|\right] \left(f - 0.53\, f_o\right)^{3} \qquad \text{(B23)}$$

for $f > 0.53\, f_o$; otherwise, $\tau = 0$

$$\Gamma = \frac{4.4 \times 10^{8} E^{3} f_o^{8}}{g^{4}} \cos^{4}\left(\theta - \theta_o\right)\left(1 - 0.42\, \frac{f_o}{f}\right)^{3} \times \exp -4\left(1 - \frac{f_o}{f}\right)^{2} + 0.1\left(\frac{f_o}{f}\right)^{5} \qquad \text{(B24)}$$

for $f > 0.42\, f_o$ and $\left|\theta - \theta_o\right| < \pi/2$; in all other conditions $\Gamma = 0$. Comparisons between calculations of energy transfer rates based on these parameterizations have shown good agreement for an empirical Neumann spectrum (Barnett[30]). Barnett contends that differences in spectral shape do not alter the wave-wave transfer rates excessively since they are dependent on integral expressions of spectral energy. However, results from the JONSWAP (Joint North Sea Wave Project) study indicate that spectral shape may significantly alter rates of energy transfer under some conditions. Even so, the time necessary to evaluate the theoretical form of the wave-wave interactions (30 min on a CDC 6600 per spectrum; Sell and Hasselmann[61]) makes their practical application to hindcasting infeasible at present.

14. Up to this point only source terms S_1 , S_2 , and S_5 have been considered. Terms S_3 and S_4 are possibly included in the empirical forms of S_1 and S_2 ; terms S_1' , S_2' , S_3' , and S_4' are neglected on the Great Lakes. The interaction between the spectrum and the bottom (S_6) in general cannot be neglected. Hasselmann and Collins[57] proposed the following spectral dissipation function

calculated from a quadratic stress law using a perturbation technique on the equations of motion:

$$\left(\frac{\partial F}{\partial t}\right)_{\text{friction}} = \Phi = -\nu_{ij} k_i k_j F(\vec{k}) \tag{B25}$$

with

$$\nu_{ij} = \frac{gC_f}{\sigma^2 \cosh^2 kh} \delta_{ij} \langle u \rangle + \left\langle \frac{u_i u_j}{u} \right\rangle \tag{B26}$$

where

C_f = coefficient of bottom friction

δ_{ij} = Kronecker delta

u = fluid velocity relative to the bottom

The brackets $\langle\rangle$ indicate averages taken over the entire ensemble of all possible wave fields having the specified spectrum. Collins[49] uses a decoupled form of Equation B25 for numerical purposes. In this approximation, the frictional dissipation function is defined as

$$\Phi(f,\theta) = \frac{-C_f g k C_G}{2\pi\sigma^2 \cosh^2 kd} \times F(f,\theta) \times \langle u \rangle \tag{B27}$$

with

$$\langle u \rangle = \sum \frac{g^2 k^2}{\sigma^2 \cosh^2 kd} E(f) \Delta f^{1/2} \tag{B28}$$

The multiplication of $E(f)$ by $g^2k^2/(\sigma^2 \cosh^2 kd)$ in Equation B28 converts the surface spectrum to a bottom velocity spectrum.

15. The only term now unaccounted for is S_7, energy loss due to breaking. Phillips[62] hypothesized on a similarity basis that the equilibrium form of the spectrum should be independent of wind speed. Although the rate of energy transfer through a fully developed spectral component would increase with an increase in wind speed, the net gain would still be zero. The Inoue and Barnett models both have limiting factors in their original presentation. For the Inoue model, it is given by $\left(1 - E_o^2/E_\infty^2\right)^{1/2}$; and for the Barnett model, it is given by

$1 - \phi$ (at least for the wind input). In light of recent evidence for the tendency of an "overshoot" effect, the need for such limiting terms as a spectral component approaches the spectral energy E_∞ is dubious. Thus, the source terms are given instead by Equations B16 and B17 in which there are no limiting terms. This facilitates the expansion of Equations B16 and B17 and the numerical evaluation by a Taylor series resulting in

$$F + \Delta F = F + \frac{(S_\ell + S_{n\ell}F)}{1!}\Delta t + \frac{(S_\ell + S_{n\ell}F)}{2!}\Delta t^2 S_{n\ell}$$

$$+ \frac{(S_\ell + S_{n\ell}F)}{3!}\Delta t^3 S_{n\ell}^2 + \ldots + \frac{(S_\ell + S_{n\ell}F)}{n!}\Delta t^n S_{n\ell}^{n-1} \qquad \text{(B29)}$$

for $F + \Delta F < E_\infty$; otherwise, $F + \Delta F = E_\infty$. Terms S_ℓ and $S_{n\ell}$ represent the sum of linear source terms and the sum of nonlinear source terms, respectively. It should be noted that both one-dimensional and two-dimensional forms are involved in this calculation. Details of these numerical methods will be given in the sixth report of this series.

16. Experimental research is continuing in attempts to improve the source terms. However, the forms of the source function used in this report have performed well in previous comparisons between hindcasts and observed waves (Part III). Such success supports the contention that, if other processes are imported besides S_1 , S_2 , and S_5 , they are effectively included in the empirical evaluations of the coefficients of S_1 , S_2 , and S_5 . Thus, even though Hasselmann[55] points out that term S_3 should be larger than S_2 , the actual form of β used in hindcast models is probably the sum of effects from both S_2 and S_3 . Whether numerical models treat each source term in Equation B7 separately or, in fact, compound several terms is beyond the scope of this study. The critical question is the overall accuracy of the models relative to the needs of users of wave information on the Great Lakes. In the end, this is assessed only by comparisons with actual data and the needs of the user.

17. In Part III, some results from the wave model used in this

study were compared with wave gage records at Point Pelee on Lake Erie and Toronto, Cobourg, and Main Duck on Lake Ontario. These comparisons showed the relationship between maximum observed significant wave heights, a single time series, and a single spectrum. Additional comparisons are given in Figures B2-B10.

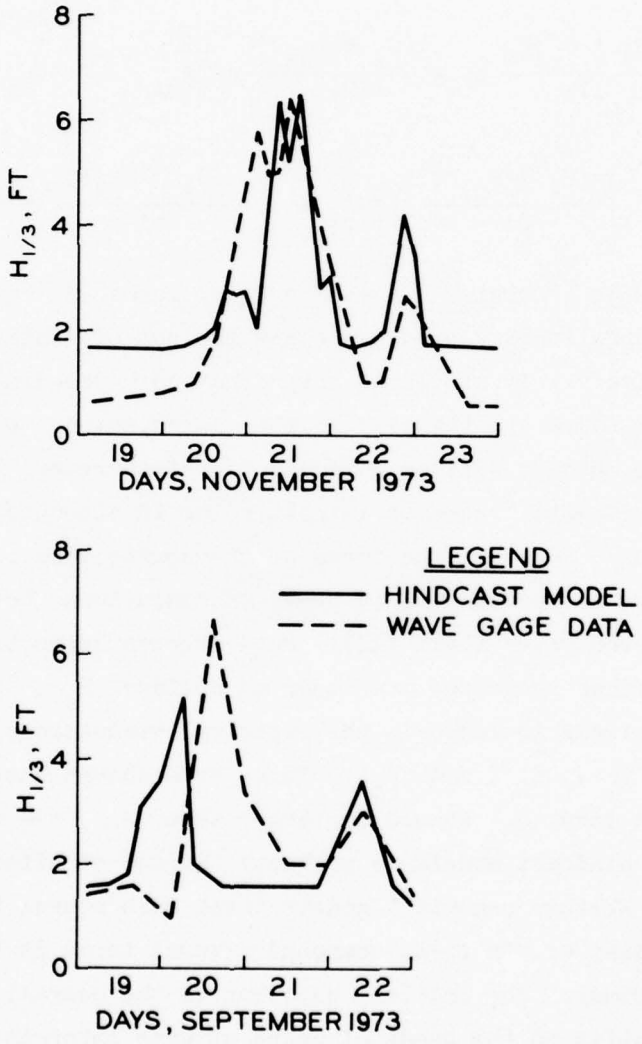

Figure B2. Comparisons of hindcast and observed sequences of significant wave height at Point Pelee, with the best agreement shown at the top and the worst at the bottom

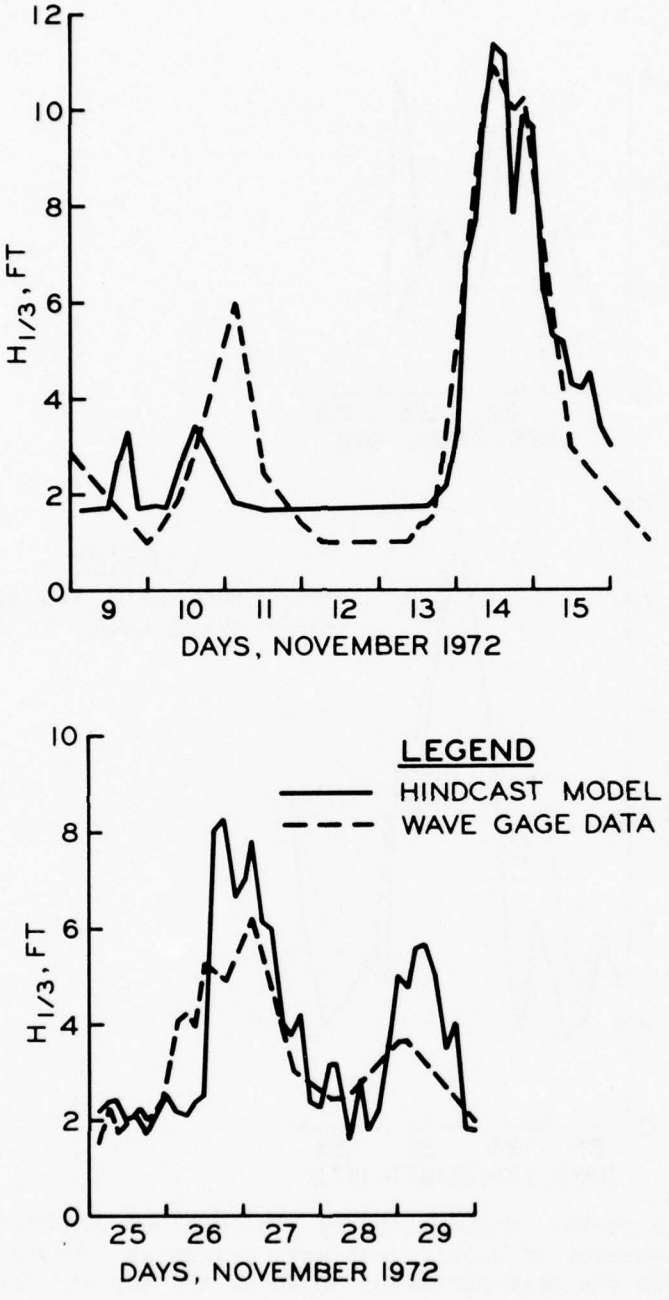

Figure B3. Comparisons of hindcast and observed sequences of significant wave height at Toronto, with the best agreement shown at the top and the worst at the bottom

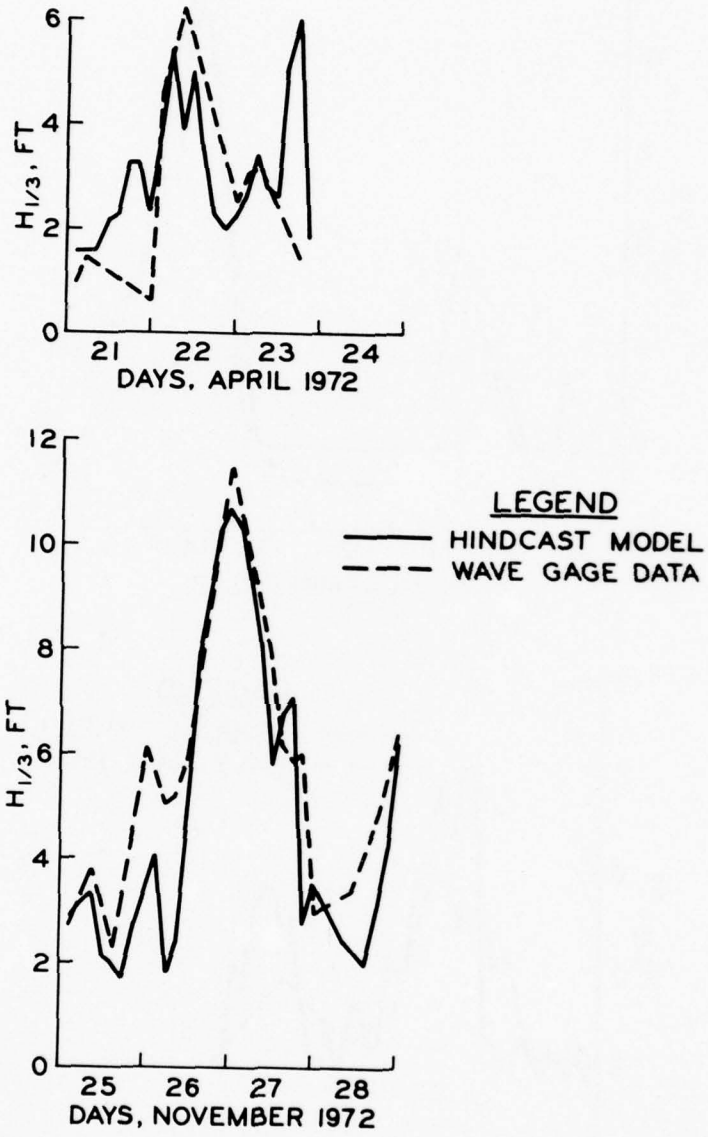

Figure B4. Comparisons of hindcast and observed sequences of significant wave height at Cobourg, with the best agreement shown at the top and the worst at the bottom

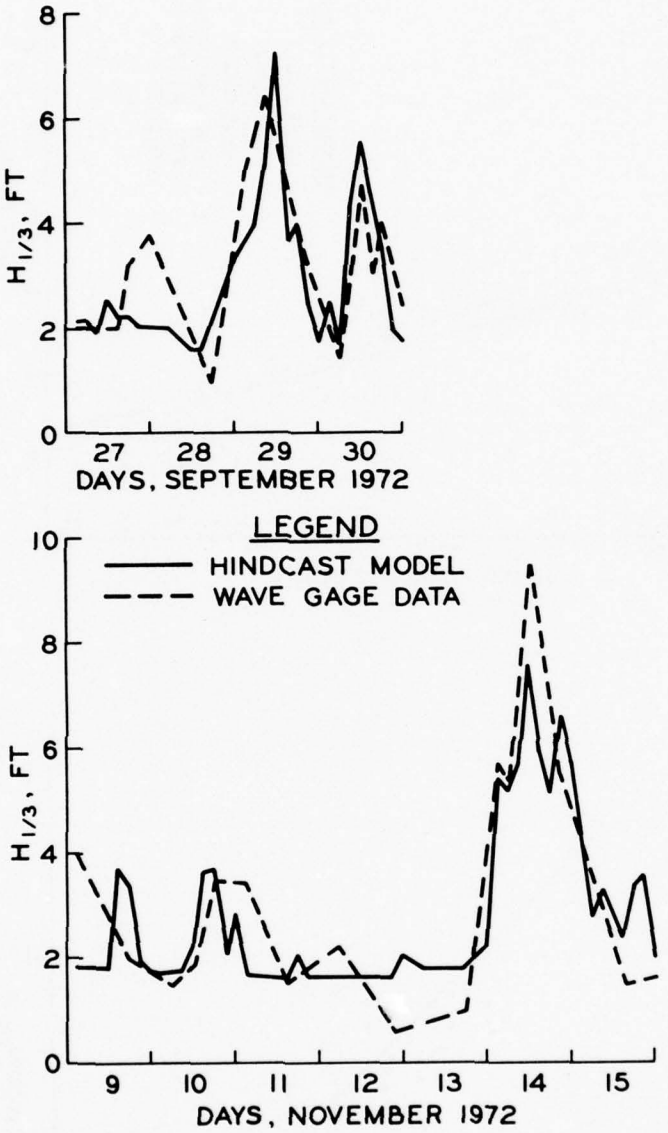

Figure B5. Comparisons of hindcast and observed sequences of significant wave height at Main Duck, with the best agreement shown at the top and the worst at the bottom

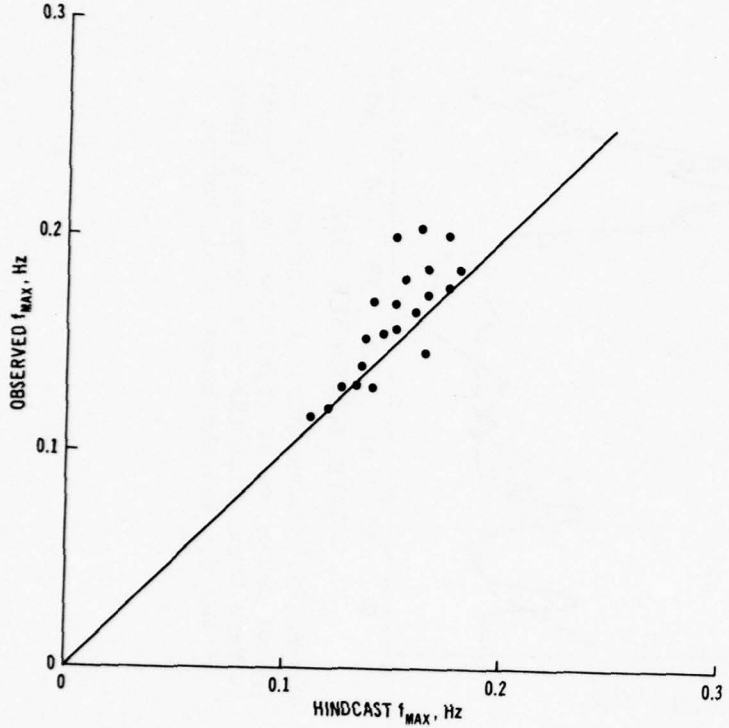

Figure B6. Comparison of observed frequencies of spectral maxima with hindcast frequencies of spectral maxima

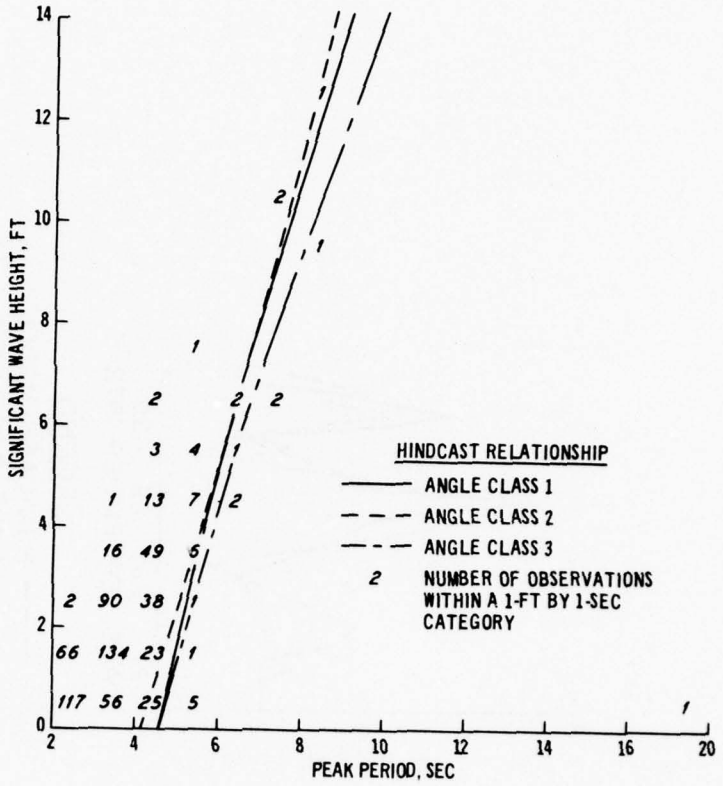

Figure B7. Comparison of hindcast significant wave periods at Cleveland with the number of occurrences of significant periods at Point Pelee, both as a function of significant wave height

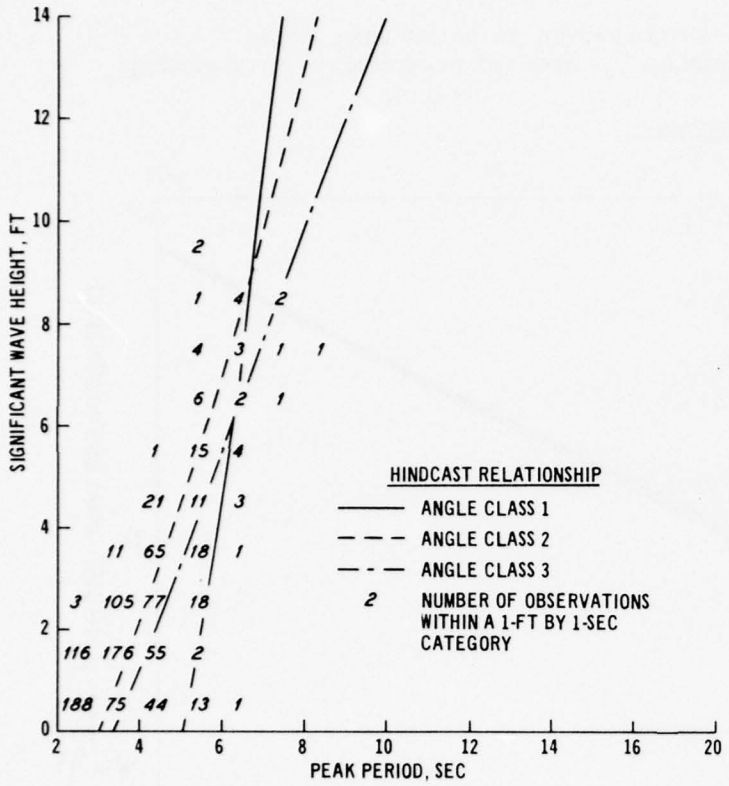

Figure B8. Comparison of hindcast significant wave periods at Point Breeze with the number of occurrences of significant periods at Cobourg, both as a function of significant wave height

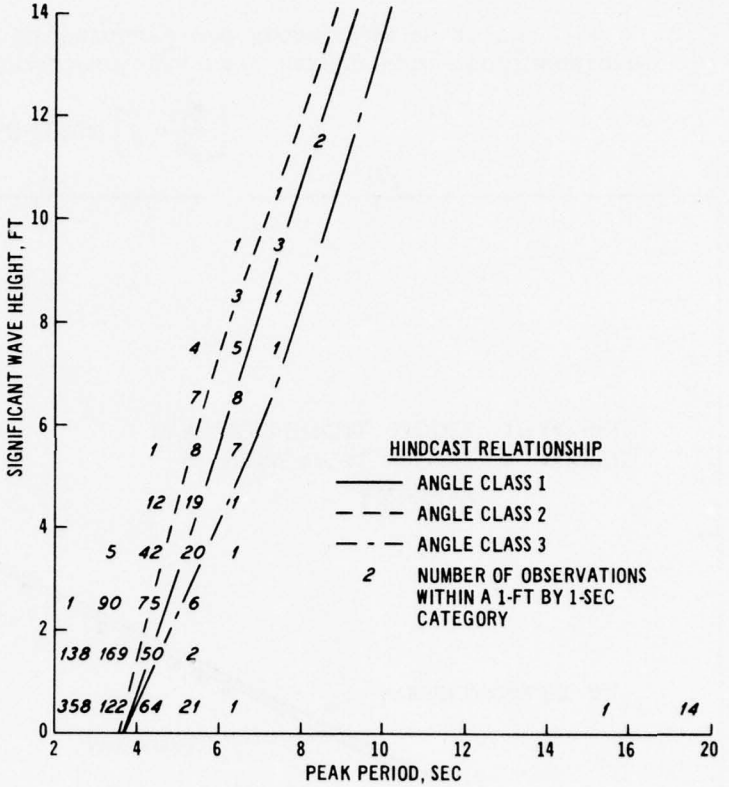

Figure B9. Comparison of hindcast significant wave periods at Oswego with the number of occurrences of significant periods at Main Duck, both as a function of significant wave height

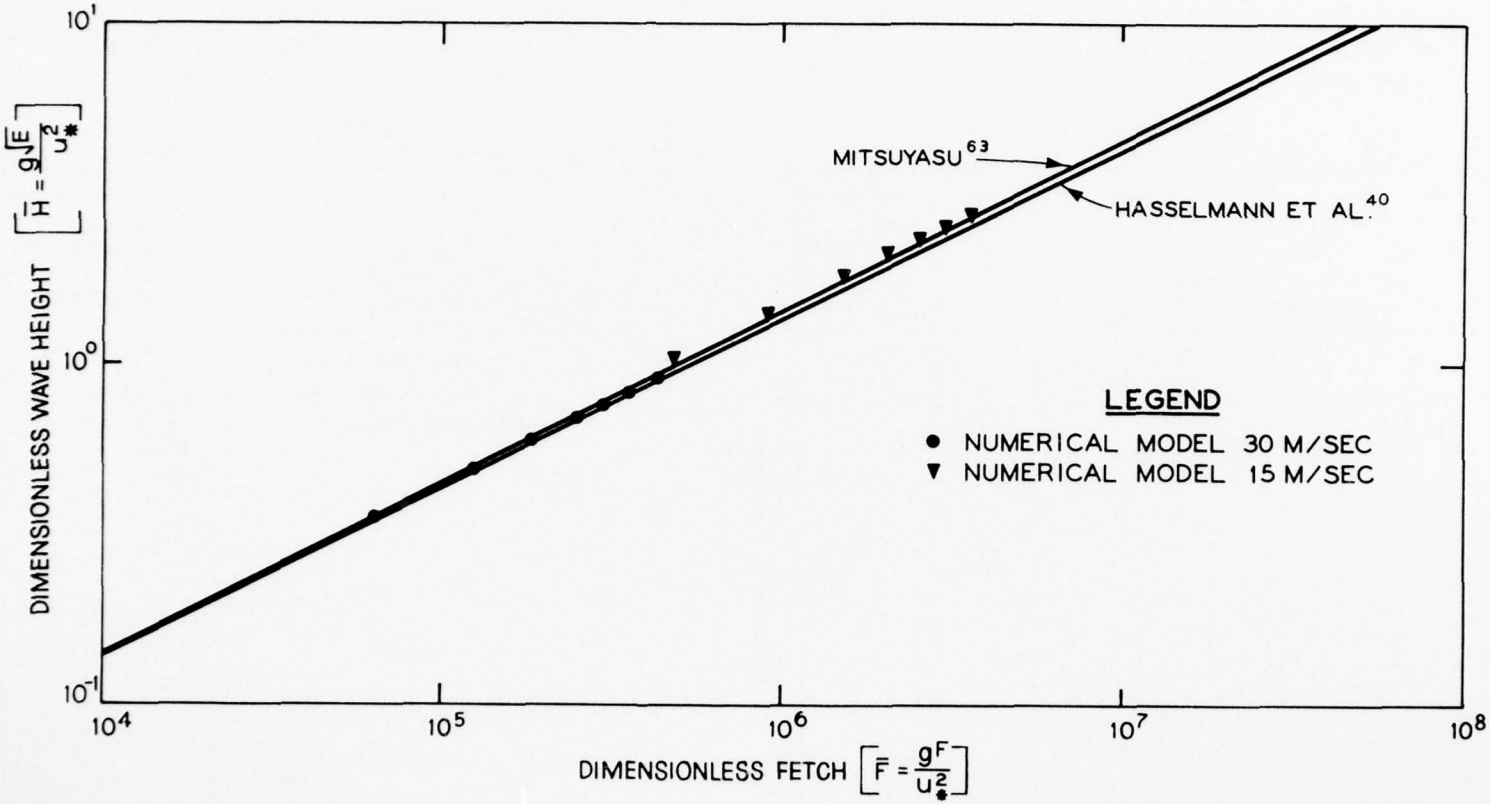

Figure B10. Comparison of rate of change of nondimensional wave height with nondimensional fetch with rates of change observed by Mitsuyasu[63] and Hasselmann et al.[40]

18. In Figures B2-B5, hydrographs of significant wave heights for selected periods of time are shown for each of the four sites previously specified. For each site, the hydrograph with best agreement and that with worst agreement between observed and hindcast waves are given. In general, the phasing and magnitude of the two series agree rather well, with larger wave heights tending to show a somewhat higher correlation.

19. In Figure B6, observed frequencies of spectral maxima are compared with hindcast frequencies of spectral maxima for the same peak storm conditions included in Figure 18. This graph indicates a tendency to underestimate f_{max} at high frequencies but shows good agreement at frequencies less than 0.15 Hz. This effect is due in part to some of the numerical assumptions included in the wave model in order to reduce computation time at the high-frequency end of the spectrum.

20. For all grid points shown in Figure 21, the relationship between significant period and significant wave height was obtained from model outputs. Since both significant period and significant height are functions of nondimensional fetch, they must also be highly related to each other in situations where little swell is present. Consequently, sites in similar geometric situations should have similar relationships between significant height and significant period. To test this, regression lines were constructed for significant period as a function of significant height for the three angle classes of wave approach (Appendix E). These lines are drawn over tables of peak wave period versus significant wave height taken from the Canadian gage data (Figures B7-B9). In each case, the sites compared are across the lake from each other and should have similar fetch geometries. The numbers in Figures B7-B9 represent the number of occurrences of waves in each 1-ft by 1-sec category. These figures indicate that significant periods hindcast by the numerical model are in close agreement with periods observed on the Great Lakes.

21. In addition to the comparisons between gage data and hindcast data, the rate of growth of nondimensional wave height ($\overline{H} = g\sqrt{E}/u_*^2$) with nondimensional fetch ($\overline{F} = gF/u_*^2$) computed with the wave model was

compared with field evidence from Mitsuyasu[63] and Hasselmann et al.[40] As seen in Figure B10, the agreement between the wave model and these data is excellent.

APPENDIX C: WIND INTERPOLATION OVER THE LAKE

1. When wind speed and direction are given at a series of stations either along the lake periphery or on the lake itself, it is necessary to interpolate corresponding wind speed and direction data at every grid point used in the calculation of the wave spectra. The method of interpolation generally follows that of Platzman.[64*]

2. For a grid point, the distance to each location for which input data are available is calculated and is denoted by d_i , i enumerating the data input points and ranging from 1 to N. The following N products are formed:

$$\ell_i = \Pi_{j \neq i} d_j \ , \ (i = 1, N), \ (j = 1, N)$$

where as an example,

$$\ell_1 = d_2 \times d_3 \ldots d_N$$

A normalizing factor is calculated

$$\text{NORM} = \sum_{i=1}^{N} \ell_i$$

and a series of N weights is formed

$$W_i = \frac{\ell_i}{\text{NORM}}$$

where NORM is the sum of the multiple products ℓ_i and W_i represents the weighting of the interpolation function on the i^{th} wind station.

3. To interpolate wind speed at the grid point the following weighted sum is used:

$$U = W_1 U_1 + W_2 U_2 + \ldots + W_n U_n$$

where the U_i is input wind data at the i^{th} station.

---

* Raised numbers refer to similarly numbered items in "References" on pp 45-49 at end of main text.

4. The vectorial wind velocity was decomposed into U (east-west) and V (north-south) components. Each component was interpolated over the lake and recombined to give a wind speed and direction. As a further modification, if adjacent input data stations had wind directions within 90 deg of each other, directions were produced using the Platzman scheme, but wind speeds were assigned the average. This modification is to allow for the rotation of the winds without divergence and a lowering of the wind speed.

APPENDIX D: ANALYSIS OF EXTREMES

1. Since curvatures in the upper portions of the graphs of wave height H versus return period T^* were small, only the problem of estimation of parameters for the Fisher-Tippett Type I distribution need be considered here. For this distribution, the asymptotic distribution function is given by

$$F(H) = \exp\ -\exp\left[-\alpha(H - u)\right] \tag{D1}$$

where α and u are parameters** of the distribution and must be estimated from the sample characteristics. From Equation D1, the reduced variate y can be defined as

$$y = \alpha(H - u) \tag{D2}$$

and, as shown by Gumbel,[42†] the reduced variate and the return period are related by

$$y = -\ln \ln \frac{T}{T - 1} \tag{D3}$$

For increasing values of T, Equation D3 converges to

$$y = \ln T - \frac{1}{2} T \tag{D4}$$

which holds with an error of less than 0.7 percent from $T = 7$ onward. Solving for T, one obtains

$$T = e^y + \frac{1}{2} \tag{D5}$$

where, for large T, combining Equations D2 and D5 results in

---

* Calculated by the relationship, $T = 1/1 - F(H)$.

** The units of α and u are 1/length and length, respectively.

† Raised numbers refer to similarly numbered items in "References" on pp 45-49 at end of main text.

$$T = e^{\alpha(H-u)} \tag{D6}$$

where e represents the Napierian base (2.71828...) or

$$H = u + \frac{\ell n\ T}{\alpha} \tag{D7}$$

Equation D7 clearly demonstrates the expected increase in extreme wave heights as the logarithm of the return periods. Empirical results supporting this conclusion can be found in many early studies of flooding on rivers. It is this relationship that allows plots of large values of a variate (wave heights, water levels, river discharges, etc.) against return periods to be fit by a straight line on semilogarithmic paper. Hence, the parameters u and α can be calculated by fitting a straight line to the upper region of the semilogarithmic plots of wave height versus return period. The slope of these lines is an estimate of $1/\alpha$, and the extrapolated value of H, for T equal to 1, can be used as an estimate of u. This method is somewhat equivalent to the method of moments for estimating α and u. The method of moments is simple, straightforward, and reasonably efficient (Gringorten[43,65]); and although several other methods for calculating α and u are available, the method of moments was used in this report.

2. The problem of constructing control bands for estimates of return periods is relatively simple in the method of moments. For a Fisher-Tippett Type I distribution, the expected rms error of an estimated return period is given by

$$S_x = S\sqrt{\frac{1.1000y^2 + 1.1396y + 1}{N}} \tag{D8}$$

where S is the standard deviation of the annual wave height maxima and N is the number of years in the sample. It is the term S_x that is presented along with all return intervals given in Appendix E. In the following discussion, it is important to bear in mind that predictions of extremes are based on characteristics of the distribution of a variate, not on individual values of the variate. Hence, errors that result

in hindcasts sometimes too low and sometimes too high may, in fact, be tolerable if the range of errors is sufficiently small. This range is determined by the sum of all the components of error inherent in hindcasting: (a) misrepresentation of wind fields, (b) inadequate specification of boundary conditions, (c) simplification of assumptions in numerical calculations, and (d) lack of properly formulated source terms in the radiative transfer equation. The total error must be separated into two parts, bias and random error. The bias is assumed to be negligible after proper calibration of the wave model. What remains, possibly nonnegligible, is the random error; and it is random error and the relationship between this error and errors in estimates of return periods that are addressed in this appendix.

3. In previous investigations of properties of extremes, the variate was assumed to be a known, measured quantity and, hence, contained zero random error. In wave hindcasts, the computed probability of wave heights depends on the combined effects of the actual wave height probability in nature and errors present in wave hindcasts. This can be considered as the probability statement

$$p(H') = \int p(H'|H)p(H)\, dH \tag{D9}$$

where H' represents hindcast wave heights and H represents actual wave heights. If the actual wave heights follow a double exponential distribution, the result is written as (Gumbel[42])

$$p(H) = \frac{\alpha e^{-\alpha(H-u)}}{n} \tag{D10}$$

where n is the number of independent observations in each annual or seasonal set of observations.

4. If it is assumed that there is negligible bias and that many independent factors create random errors in wave heights hindcast by numerical techniques, a loose application of the central limit theorem may be invoked to support a Gaussian distribution of these errors. Thus, we obtain

$$p(H'|H) = \int \frac{1}{\sigma\sqrt{2\pi}} \exp\left[\frac{-1}{2}\left(\frac{H - H'}{\sigma}\right)^2\right] \qquad (D11)$$

where σ is the standard deviation of the errors in hindcast wave heights. Substituting Equations D9 and D10 into D8 yields

$$p(H') = \frac{\alpha}{n\sigma\sqrt{2\pi}}\int \exp\left[-\frac{1}{2}\left(\frac{H - H'}{\sigma}\right)^2 - \sigma(H - u)\, dH\right] \qquad (D12)$$

Rearranging Equation D12 shows that the probability of H' can be written as a product of a double exponential probability density and an integral function of the parameters α and σ

$$p(H') = \frac{\alpha e^{-\alpha(H-u)}}{n} \int \frac{1}{\sqrt{2\pi}} e^{-H^{*2}/2 - ZH}\, dH \qquad (D13)$$

where the reduced wave height variate H is expressed as

$$H^* = \frac{H - H'}{\sigma} \qquad (D14)$$

and parameter Z of the combined exponential and Gaussian distribution is defined as

$$Z = \alpha\sigma \qquad (D15)$$

Integrating Equation D12 yields

$$p(H') = \frac{\alpha e^{-\alpha(H-u)}}{n} e^{Z^2/\sqrt{2}} \left[1 - \Phi\left(\frac{Z}{\sqrt{2}}\right)\right] \qquad (D16)$$

where $\Phi(x)$ is the probability integral

$$\Phi(x) = \frac{2}{\sqrt{\pi}} \int_0^x e^{-x^2}\, dx \qquad (D17)$$

Thus, the distribution function can be calculated from the relationship

$$F(H') = 1 - \frac{1}{n} e^{-\alpha(H-u)}\Psi(Z) \qquad (D18)$$

where $\Psi(Z)$ is defined as

$$\Psi(Z) = e^{Z^2/\sqrt{2}} \left[1 - \Phi\left(\frac{Z}{\sqrt{2}}\right)\right] \tag{D19}$$

Figure D1 shows the relationship between $\Psi(Z)$ and Z.

5. At this point, it is necessary to recall the definition of the term, $Z = \alpha\sigma$, in order to return to the original point of this discussion, the effects of random error in hindcasts on estimates of return periods. In this definition, the parameter σ represents the standard deviation of the errors in hindcasts, and α represents an inverse function of the variation of the annual maxima. If we choose a new parameter β to be proportional to the variation in annual maxima, Equation D15 becomes

$$Z = \frac{\sigma}{\beta} \tag{D20}$$

In this form, the meaning of Z becomes more intuitive. Its value represents the ratio of the coefficients of variation of the Gaussian and double exponential distributions contributing to $p(H)$. If the asymptotic variation is much larger than the random error present in hindcasts, the effect of the random error is very small. On the other hand, if the random error is larger than the variation of annual maxima, the distribution $p(H')$ is significantly different from $p(H)$.

6. In Part III, the rms error in the hindcasts was given as 0.5 ft. When the distributions of extremes hindcast by the wave model were examined, values of β were found to lie between 1 and 10. If the rms error is not dependent on fetch, the values predict up to a 50 percent factor of conservatism for small waves. For large variations in annual maxima, the effect of the random error in hindcasts can clearly be neglected.

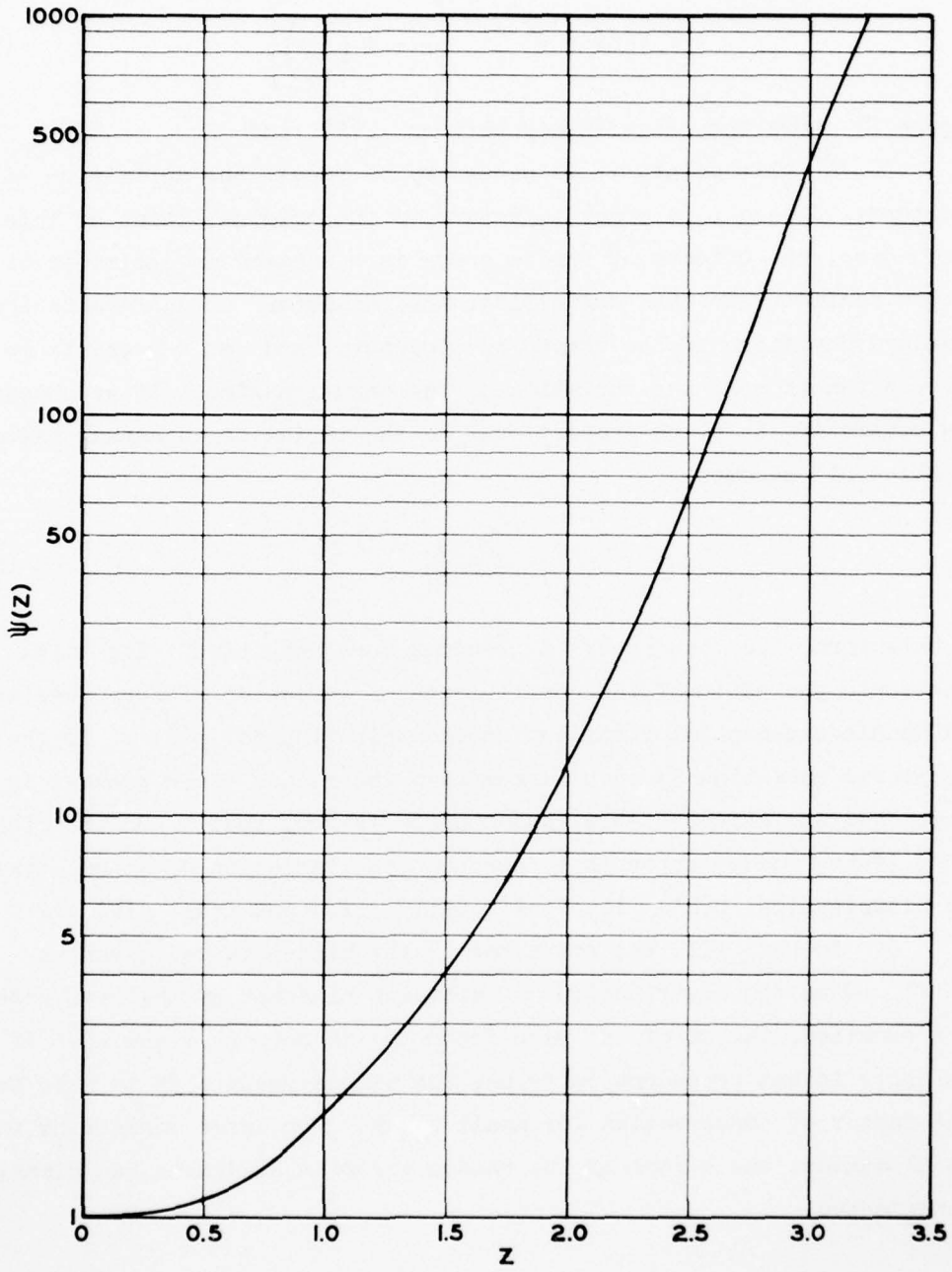

Figure D1. Relationship between $\Psi(Z)$ and Z

APPENDIX E: TABLES OF DESIGN WAVE INFORMATION

1. Tables in this appendix contain calculated estimates of return periods from techniques discussed in Part IV and Appendix D. Raw data input into the calculations are wave height maxima from individual storms. These storms were selected with objective criteria as discussed in Part IV; and a numerical model, based on the wave-wave interaction parameterizations by Barnett, was used to calculate waves from each storm.

2. Figure 21 in Part IV shows the locations of all the deepwater sites for which tables are listed. The wave information is separated into two sets: (a) Tables E1 and E2 with wave height information, and (b) Table E3 with wave period information.

3. The format for Table E1 is as follows:

   a. A separate page is given for each point shown in Figure 21.

   b. With each site, 5-, 10-, 20-, 50-, and 100-yr significant wave heights are listed for each season.

   c. Control band (one standard deviation) estimates for each wave height are included inside parentheses.

   d. The three angle classes are defined as viewed by an observer standing on shore (Figure E1):

      (1) Angle Class 1 - Mean wave approach angle greater than 30 deg to right of normal to shore.

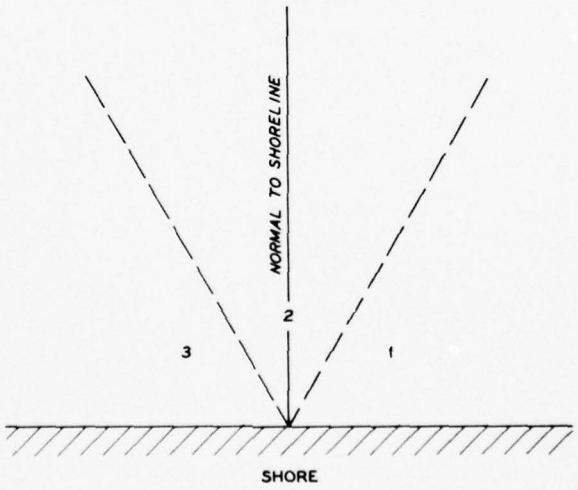

Figure E1. Definition sketch of the angle classes

(2) Angle Class 2 - Mean wave approach angle within 30 deg to either side of normal to shore.

(3) Angle Class 3 - Mean wave approach angle greater than 30 deg to left of normal to shore.

Originally, a finer stratification of wave angles was attempted; however, it was determined that even though the wind might be blowing parallel to shore, the mean angle of approach shoreward almost always fell within 60 deg of normal to shore. Thus, additional angle classes were not necessary.

4. Table E2 gives the significant wave heights for all approach angles and seasons combined for return periods of 5, 10, 20, 50, and 100 yr.

5. Table E3 wave period information presents the data as a function of location (one per page), wave height (rows), and angle of wave approach (columns).

6. Table E4 presents the azimuths of the normal to shore vectors shown in Figure 21.

Table E1

TABLE OF EXTREMES ESTIMATES
GRID LOCATION 22,12 LAT=43.02 LON=82.33 PORT HURON MI

SHORELINE GRID POINT 1

WINTER

	ANGLE CLASSES 1	2	3	ALL
5	8.9(1.6)	19.7(1.6)	9.5(1.6)	19.7(0.4)
10	10.8(2.1)	20.3(2.1)	10.2(2.1)	20.3(0.5)
20	12.1(2.7)	21.0(2.7)	10.8(2.7)	21.0(0.6)
50	13.4(3.3)	21.6(3.3)	11.8(3.3)	21.6(0.7)
100	14.1(3.8)	22.0(3.8)	12.1(3.8)	22.0(0.9)

SPRING

	ANGLE CLASSES 1	2	3	ALL
5	2.0(1.5)	9.8(1.5)	5.1(1.5)	9.9(0.6)
10	2.8(2.0)	11.4(2.0)	6.3(2.0)	11.5(0.7)
20	3.1(2.5)	12.2(2.5)	7.5(2.5)	12.3(0.9)
50	3.5(3.0)	13.4(3.0)	8.7(3.0)	13.5(1.1)
100	3.9(3.5)	14.2(3.5)	9.1(3.5)	14.3(1.3)

SUMMER

	ANGLE CLASSES 1	2	3	ALL
5	1.3(1.6)	9.8(1.6)	6.9(1.6)	9.8(0.4)
10	2.6(2.1)	10.8(2.1)	7.9(2.1)	10.8(0.6)
20	3.6(2.7)	11.5(2.7)	8.9(2.7)	11.5(0.7)
50	4.6(3.3)	12.1(3.3)	9.8(3.3)	12.2(0.9)
100	5.2(3.8)	12.5(3.8)	10.2(3.8)	12.6(1.0)

FALL

	ANGLE CLASSES 1	2	3	ALL
5	6.9(1.5)	17.7(1.5)	8.9(1.5)	17.8(0.4)
10	9.8(2.0)	19.0(2.0)	9.8(2.0)	19.1(0.6)
20	11.8(2.5)	19.7(2.5)	10.8(2.5)	19.7(0.7)
50	14.1(3.0)	20.3(3.0)	11.5(3.0)	20.3(0.9)
100	15.4(3.5)	21.0(3.5)	11.8(3.5)	21.0(1.1)

(Continued)

Table E1 (Continued)

TABLE OF EXTREMES ESTIMATES
GRID LOCATION 21,12 LAT=43.16 LON=82.33 LAKE HURON

SHORELINE GRID POINT 2

WINTER
ANGLE CLASSES

	1	2	3	ALL
5	6.2(1.6)	14.8(1.6)	18.4(1.6)	18.5(0.4)
10	6.9(2.1)	16.4(2.1)	19.0(2.1)	19.1(0.5)
20	7.5(2.7)	17.7(2.7)	19.7(2.7)	19.7(0.6)
50	8.2(3.3)	18.7(3.3)	20.3(3.3)	20.3(0.7)
100	8.5(3.8)	19.4(3.8)	20.7(3.8)	20.7(0.9)

SPRING
ANGLE CLASSES

	1	2	3	ALL
5	1.6(1.5)	4.7(1.5)	8.7(1.5)	8.8(0.6)
10	1.6(2.0)	6.7(2.0)	10.6(2.0)	10.7(0.8)
20	2.0(2.5)	8.3(2.5)	11.8(2.5)	11.9(1.0)
50	2.0(3.0)	9.8(3.0)	13.0(3.0)	13.1(1.2)
100	2.0(3.5)	11.0(3.5)	13.8(3.5)	13.9(1.4)

SUMMER
ANGLE CLASSES

	1	2	3	ALL
5	1.0(1.6)	3.3(1.6)	9.2(1.6)	9.3(0.4)
10	1.0(2.1)	6.6(2.1)	9.8(2.1)	10.2(0.5)
20	1.0(2.7)	8.9(2.7)	10.2(2.7)	10.5(0.7)
50	1.0(3.3)	11.5(3.3)	10.8(3.3)	11.6(0.8)
100	1.0(3.8)	13.1(3.8)	11.2(3.8)	13.2(1.0)

FALL
ANGLE CLASSES

	1	2	3	ALL
5	4.9(1.5)	13.4(1.5)	16.7(1.5)	17.1(0.6)
10	6.2(2.0)	16.4(2.0)	17.7(2.0)	18.4(0.8)
20	6.9(2.5)	18.7(2.5)	18.4(2.5)	19.4(1.0)
50	7.9(3.0)	21.0(3.0)	19.0(3.0)	21.1(1.2)
100	8.5(3.5)	22.3(3.5)	19.4(3.5)	22.4(1.4)

(Continued)

AD-A046 414 ARMY ENGINEER WATERWAYS EXPERIMENT STATION VICKSBURG MISS F/G 8/8
DESIGN WAVE INFORMATION FOR THE GREAT LAKES: REPORT 4. LAKE HUR--ETC(U)
SEP 77 D T RESIO, C L VINCENT

UNCLASSIFIED WES-TR-H-76-1-4 NL

2 OF 2
ADA
046414

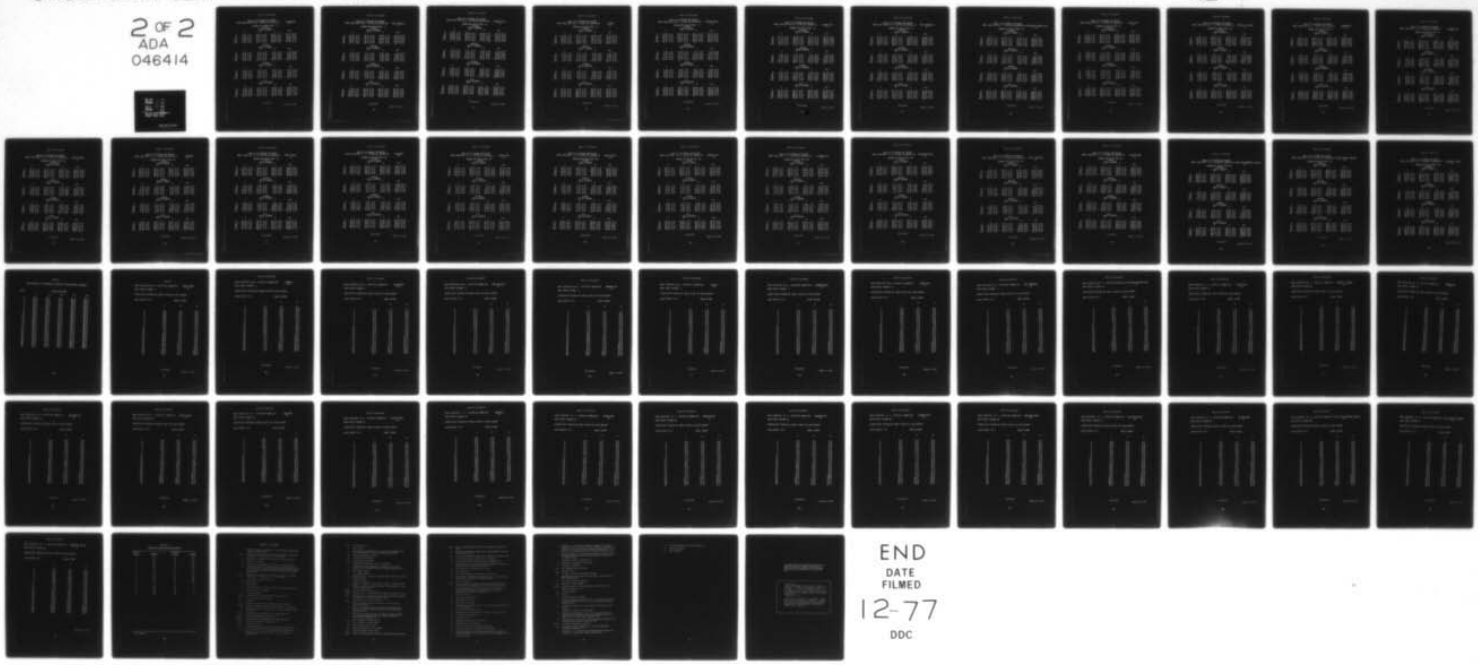

END
DATE
FILMED
12-77
DDC

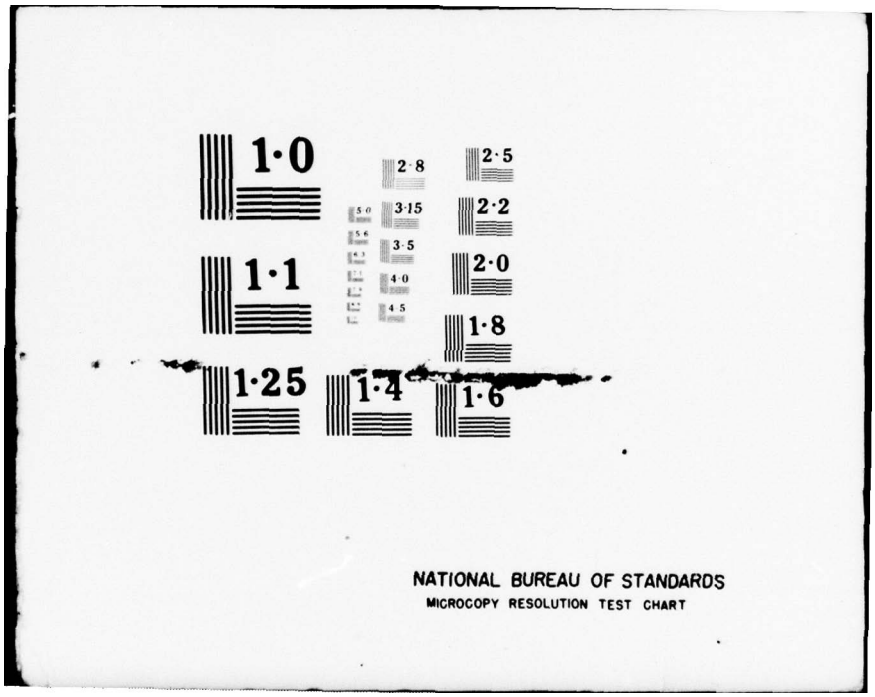
1·0
1·1
1·25
1·4
1·6
1·8
2·0
2·2
2·5
2·8
3·15
3·5
4·0
4·5
5·0
5·6
NATIONAL BUREAU OF STANDARDS
MICROCOPY RESOLUTION TEST CHART

TABLE OF EXTREMES ESTIMATES
GRID LOCATION 20,12 LAT=43.31 LON=82.33 LEXINGTON MI

SHORELINE GRID POINT 3

WINTER

	ANGLE CLASSES 1	2	3	ALL
5	6.9(1.6)	13.8(1.6)	13.1(1.6)	14.1(0.5)
10	7.9(2.1)	15.1(2.1)	13.8(2.1)	15.1(0.6)
20	8.5(2.7)	16.1(2.7)	14.1(2.7)	16.2(0.8)
50	8.9(3.3)	17.1(3.3)	14.4(3.3)	17.2(1.0)
100	9.5(3.8)	17.7(3.8)	14.8(3.8)	17.8(1.1)

SPRING

	ANGLE CLASSES 1	2	3	ALL
5	2.4(1.5)	5.9(1.5)	6.3(1.5)	6.4(0.6)
10	2.8(2.0)	7.5(2.0)	7.5(2.0)	7.6(0.8)
20	3.1(2.5)	8.7(2.5)	8.7(2.5)	8.8(1.0)
50	3.5(3.0)	9.8(3.0)	9.8(3.0)	9.9(1.2)
100	3.5(3.5)	10.2(3.5)	10.2(3.5)	10.3(1.4)

SUMMER

	ANGLE CLASSES 1	2	3	ALL
5	2.3(1.6)	1.6(1.6)	6.2(1.6)	6.3(0.7)
10	3.3(2.1)	3.0(2.1)	7.9(2.1)	7.9(0.9)
20	3.9(2.7)	3.9(2.7)	8.9(2.7)	9.0(1.1)
50	4.6(3.3)	4.6(3.3)	9.8(3.3)	9.8(1.4)
100	5.2(3.8)	5.2(3.8)	10.5(3.8)	10.5(1.6)

FALL

	ANGLE CLASSES 1	2	3	ALL
5	7.2(1.5)	13.1(1.5)	12.8(1.5)	13.8(0.8)
10	8.5(2.0)	14.4(2.0)	14.8(2.0)	15.4(1.0)
20	9.8(2.5)	15.4(2.5)	16.1(2.5)	16.7(1.3)
50	10.8(3.0)	16.4(3.0)	17.4(3.0)	18.0(1.6)
100	11.5(3.5)	16.7(3.5)	18.4(3.5)	19.0(1.8)

(Continued)

Table E1 (Continued)

TABLE OF EXTREMES ESTIMATES
GRID LOCATION 19,11 LAT=43.45 LON=82.52 PORT SANILAC MI

SHORELINE GRID POINT 4

WINTER

	ANGLE CLASSES 1	2	3	ALL
5	10.5(1.6)	14.4(1.6)	13.8(1.6)	14.8(0.3)
10	11.5(2.1)	15.4(2.1)	14.4(2.1)	15.4(0.4)
20	12.1(2.7)	15.7(2.7)	14.8(2.7)	15.7(0.5)
50	12.8(3.3)	16.4(3.3)	15.1(3.3)	16.4(0.7)
100	13.1(3.8)	16.7(3.8)	15.1(3.8)	16.7(0.8)

SPRING

	ANGLE CLASSES 1	2	3	ALL
5	3.5(1.5)	7.1(1.5)	5.9(1.5)	7.2(0.5)
10	5.1(2.0)	8.7(2.0)	7.5(2.0)	8.8(0.7)
20	5.9(2.5)	9.4(2.5)	8.3(2.5)	9.5(0.9)
50	7.1(3.0)	10.6(3.0)	9.4(3.0)	10.7(1.1)
100	7.9(3.5)	11.4(3.5)	9.8(3.5)	11.5(1.2)

SUMMER

	ANGLE CLASSES 1	2	3	ALL
5	2.6(1.6)	2.3(1.6)	6.9(1.6)	6.9(0.6)
10	4.3(2.1)	4.3(2.1)	8.2(2.1)	8.2(0.9)
20	5.2(2.7)	5.6(2.7)	9.2(2.7)	9.3(1.1)
50	6.2(3.3)	6.9(3.3)	10.2(3.3)	10.2(1.3)
100	7.2(3.8)	7.5(3.8)	10.8(3.8)	10.8(1.5)

FALL

	ANGLE CLASSES 1	2	3	ALL
5	9.8(1.5)	13.8(1.5)	13.4(1.5)	14.8(0.9)
10	11.2(2.0)	15.4(2.0)	15.7(2.0)	16.7(1.2)
20	12.5(2.5)	16.7(2.5)	17.4(2.5)	18.4(1.5)
50	13.4(3.0)	18.0(3.0)	19.4(3.0)	20.0(1.8)
100	14.1(3.5)	18.7(3.5)	20.3(3.5)	21.0(2.1)

(Continued)

Table E1 (Continued)

TABLE OF EXTREMES ESTIMATES
GRID LOCATION 18,11 LAT=43.59 LON=82.52 FORESTVILLE MI

SHORELINE GRID POINT 5

WINTER

	ANGLE CLASSES 1	2	3	ALL
5	10.8(1.6)	14.8(1.6)	14.4(1.6)	15.4(0.3)
10	12.1(2.1)	15.7(2.1)	15.4(2.1)	16.1(0.4)
20	12.8(2.7)	16.4(2.7)	16.1(2.7)	16.4(0.5)
50	13.8(3.3)	17.1(3.3)	17.1(3.3)	17.1(0.7)
100	14.1(3.8)	17.4(3.8)	17.4(3.8)	17.4(0.8)

SPRING

	ANGLE CLASSES 1	2	3	ALL
5	5.1(1.5)	7.1(1.5)	6.3(1.5)	7.2(0.6)
10	5.9(2.0)	8.7(2.0)	7.9(2.0)	8.8(0.8)
20	6.7(2.5)	9.8(2.5)	9.1(2.5)	9.9(1.0)
50	7.5(3.0)	11.0(3.0)	10.2(3.0)	11.1(1.2)
100	7.9(3.5)	11.8(3.5)	11.0(3.5)	11.9(1.4)

SUMMER

	ANGLE CLASSES 1	2	3	ALL
5	2.6(1.6)	3.9(1.6)	6.6(1.6)	6.6(0.7)
10	3.9(2.1)	5.2(2.1)	8.2(2.1)	8.2(1.0)
20	4.9(2.7)	6.2(2.7)	9.5(2.7)	9.6(1.2)
50	5.9(3.3)	7.2(3.3)	10.5(3.3)	10.5(1.5)
100	6.6(3.8)	7.9(3.8)	11.2(3.8)	11.2(1.7)

FALL

	ANGLE CLASSES 1	2	3	ALL
5	10.2(1.5)	14.8(1.5)	14.1(1.5)	15.7(1.0)
10	11.8(2.0)	16.7(2.0)	16.7(2.0)	18.0(1.3)
20	13.1(2.5)	18.0(2.5)	18.7(2.5)	19.7(1.7)
50	14.1(3.0)	19.4(3.0)	20.7(3.0)	21.3(2.1)
100	15.1(3.5)	20.3(3.5)	21.6(3.5)	22.3(2.4)

(Continued)

Table E1 (Continued)

TABLE OF EXTREMES ESTIMATES
GRID LOCATION 17,11 LAT=43.74 LON=82.52 HELENA MI

SHORELINE GRID POINT 6

WINTER
ANGLE CLASSES

	1	2	3	ALL
5	11.8(1.6)	15.4(1.6)	14.8(1.6)	15.4(0.4)
10	12.1(2.1)	16.4(2.1)	15.7(2.1)	16.4(0.6)
20	12.8(2.7)	17.1(2.7)	16.4(2.7)	17.1(0.7)
50	13.1(3.3)	18.0(3.3)	17.1(3.3)	18.1(0.9)
100	13.4(3.8)	18.4(3.8)	17.4(3.8)	18.5(1.0)

SPRING
ANGLE CLASSES

	1	2	3	ALL
5	5.1(1.5)	7.1(1.5)	5.9(1.5)	7.2(0.5)
10	6.3(2.0)	8.7(2.0)	7.5(2.0)	8.8(0.7)
20	7.1(2.5)	9.8(2.5)	8.7(2.5)	9.9(0.9)
50	7.9(3.0)	11.0(3.0)	9.8(3.0)	11.1(1.1)
100	8.7(3.5)	11.8(3.5)	10.6(3.5)	11.9(1.2)

SUMMER
ANGLE CLASSES

	1	2	3	ALL
5	3.6(1.6)	3.9(1.6)	6.6(1.6)	6.6(0.8)
10	4.3(2.1)	5.2(2.1)	8.2(2.1)	8.2(1.1)
20	5.2(2.7)	5.9(2.7)	9.5(2.7)	9.6(1.3)
50	5.9(3.3)	6.6(3.3)	10.8(3.3)	10.8(1.7)
100	6.2(3.8)	7.2(3.8)	11.5(3.8)	11.5(1.9)

FALL
ANGLE CLASSES

	1	2	3	ALL
5	10.2(1.5)	14.8(1.5)	13.8(1.5)	16.1(0.9)
10	12.1(2.0)	16.7(2.0)	16.7(2.0)	18.0(1.2)
20	13.8(2.5)	18.0(2.5)	18.7(2.5)	19.7(1.5)
50	15.1(3.0)	19.7(3.0)	20.7(3.0)	21.3(1.9)
100	16.1(3.5)	20.3(3.5)	22.0(3.5)	22.3(2.2)

(Continued)

Table E1 (Continued)

TABLE OF EXTREMES ESTIMATES
GRID LOCATION 16,11 LAT=43.88 LON=82.52 HARBOR BEACH MI

SHORELINE GRID POINT 7

WINTER
ANGLE CLASSES

	1	2	3	ALL
5	10.2(1.6)	16.1(1.6)	16.1(1.6)	16.7(0.4)
10	11.8(2.1)	17.1(2.1)	16.7(2.1)	17.7(0.5)
20	13.1(2.7)	18.0(2.7)	17.4(2.7)	18.4(0.7)
50	14.4(3.3)	19.0(3.3)	18.0(3.3)	19.1(0.8)
100	15.1(3.8)	19.4(3.8)	18.4(3.8)	19.4(1.0)

SPRING
ANGLE CLASSES

	1	2	3	ALL
5	5.9(1.5)	6.3(1.5)	7.1(1.5)	7.2(0.6)
10	7.9(2.0)	8.7(2.0)	9.1(2.0)	9.2(0.8)
20	9.1(2.5)	10.2(2.5)	10.6(2.5)	10.7(1.0)
50	10.6(3.0)	11.8(3.0)	11.8(3.0)	11.9(1.3)
100	11.4(3.5)	13.0(3.5)	12.6(3.5)	13.1(1.5)

SUMMER
ANGLE CLASSES

	1	2	3	ALL
5	1.6(1.6)	3.6(1.6)	8.2(1.6)	8.9(0.6)
10	2.3(2.1)	6.2(2.1)	9.5(2.1)	10.2(0.9)
20	3.0(2.7)	8.2(2.7)	10.5(2.7)	11.2(1.1)
50	3.6(3.3)	10.2(3.3)	11.5(3.3)	12.1(1.3)
100	3.9(3.8)	11.5(3.8)	12.1(3.8)	12.8(1.5)

FALL
ANGLE CLASSES

	1	2	3	ALL
5	8.2(1.6)	16.7(1.5)	14.8(1.5)	17.1(0.9)
10	11.8(2.2)	19.0(2.0)	16.1(2.0)	19.1(1.2)
20	14.8(2.7)	20.7(2.5)	17.1(2.5)	20.8(1.5)
50	17.4(3.3)	22.3(3.0)	18.0(3.0)	22.4(1.8)
100	19.0(3.9)	23.3(3.5)	18.7(3.5)	23.4(2.1)

(Continued)

Table E1 (Continued)

TABLE OF EXTREMES ESTIMATES
GRID LOCATION 15,10 LAT=44.03 LON=82.71 HURON CITY MI

SHORELINE GRID POINT 8

WINTER

	ANGLE CLASSES 1	2	3	ALL
5	15.7(1.6)	18.0(1.6)	16.1(1.6)	18.1(0.5)
10	17.1(2.1)	19.0(2.1)	17.7(2.1)	19.1(0.6)
20	17.7(2.7)	20.0(2.7)	19.4(2.7)	20.0(0.8)
50	18.4(3.3)	20.7(3.3)	20.7(3.3)	20.7(1.0)
100	19.0(3.8)	21.3(3.8)	21.6(3.8)	21.7(1.1)

SPRING

	ANGLE CLASSES 1	2	3	ALL
5	5.5(1.5)	8.3(1.5)	7.5(1.5)	8.4(0.5)
10	7.5(2.0)	9.4(2.0)	9.1(2.0)	9.5(0.6)
20	9.1(2.5)	10.6(2.5)	10.2(2.5)	10.7(0.8)
50	10.2(3.0)	11.4(3.0)	11.4(3.0)	11.5(1.0)
100	11.0(3.5)	12.2(3.5)	12.2(3.5)	12.3(1.1)

SUMMER

	ANGLE CLASSES 1	2	3	ALL
5	2.3(1.6)	9.5(1.6)	9.8(1.6)	10.5(0.8)
10	4.3(2.1)	11.2(2.1)	11.8(2.1)	12.1(1.0)
20	5.9(2.7)	12.5(2.7)	13.1(2.7)	13.4(1.3)
50	7.5(3.3)	13.4(3.3)	14.4(3.3)	14.4(1.6)
100	8.5(3.8)	14.1(3.8)	15.1(3.8)	15.4(1.8)

FALL

	ANGLE CLASSES 1	2	3	ALL
5	14.4(1.5)	16.7(1.5)	15.4(1.5)	17.4(0.7)
10	16.7(2.0)	18.7(2.0)	16.7(2.0)	19.4(1.0)
20	18.4(2.5)	20.3(2.5)	17.7(2.5)	20.3(1.2)
50	20.0(3.0)	22.0(3.0)	19.0(3.0)	22.1(1.5)
100	21.0(3.5)	23.0(3.5)	19.7(3.5)	23.1(1.8)

(Continued)

Table E1 (Continued)

TABLE OF EXTREMES ESTIMATES
GRID LOCATION 15, 8 LAT=44.03 LON=83.11 PORT CRESCENT MI

SHORELINE GRID POINT 9

WINTER

	ANGLE CLASSES 1	2	3	ALL
5	16.4(1.6)	18.0(1.6)	11.5(1.6)	18.1(0.6)
10	17.4(2.1)	19.4(2.1)	12.8(2.1)	19.4(0.7)
20	18.0(2.7)	20.3(2.7)	14.1(2.7)	20.3(0.9)
50	18.7(3.3)	21.3(3.3)	15.1(3.3)	21.3(1.2)
100	19.0(3.8)	22.0(3.8)	15.7(3.8)	22.1(1.3)

SPRING

	ANGLE CLASSES 1	2	3	ALL
5	6.3(1.5)	9.1(1.5)	7.5(1.5)	9.2(0.4)
10	8.3(2.0)	10.2(2.0)	8.3(2.0)	10.3(0.5)
20	9.4(2.5)	11.0(2.5)	9.1(2.5)	11.1(0.7)
50	11.0(3.0)	11.8(3.0)	9.8(3.0)	11.9(0.8)
100	11.8(3.5)	12.6(3.5)	10.2(3.5)	12.7(1.0)

SUMMER

	ANGLE CLASSES 1	2	3	ALL
5	5.2(1.6)	9.8(1.6)	8.9(1.6)	10.8(0.4)
10	7.9(2.1)	11.5(2.1)	9.5(2.1)	11.8(0.6)
20	9.8(2.7)	12.5(2.7)	10.2(2.7)	12.6(0.7)
50	12.1(3.3)	13.8(3.3)	10.8(3.3)	13.9(0.9)
100	13.1(3.8)	14.4(3.8)	11.2(3.8)	14.5(1.0)

FALL

	ANGLE CLASSES 1	2	3	ALL
5	15.4(1.5)	17.1(1.5)	10.2(1.5)	17.1(0.7)
10	17.7(2.0)	17.7(2.0)	11.8(2.0)	18.7(0.9)
20	19.4(2.5)	18.4(2.5)	13.1(2.5)	19.7(1.1)
50	21.0(3.0)	19.0(3.0)	14.4(3.0)	21.0(1.4)
100	22.3(3.5)	19.4(3.5)	15.1(3.5)	22.4(1.6)

(Continued)

TABLE OF EXTREMES ESTIMATES
GRID LOCATION 15, 7 LAT=44.03 LON=83.30 ENTRANCE SAGINAW BAY

SHORELINE GRID POINT 10

WINTER

	ANGLE CLASSES 1	2	3	ALL
5	18.0(1.6)	18.0(1.6)	10.2(1.6)	18.7(0.6)
10	19.0(2.1)	19.7(2.1)	11.2(2.1)	20.0(0.8)
20	19.7(2.7)	21.0(2.7)	12.1(2.7)	21.0(1.0)
50	20.3(3.3)	22.6(3.3)	12.8(3.3)	22.7(1.2)
100	20.7(3.8)	23.3(3.8)	13.1(3.8)	23.4(1.4)

SPRING

	ANGLE CLASSES 1	2	3	ALL
5	6.7(1.5)	7.1(1.5)	5.1(1.5)	7.2(0.5)
10	8.7(2.0)	8.7(2.0)	6.7(2.0)	8.8(0.6)
20	9.8(2.5)	9.8(2.5)	7.9(2.5)	9.9(0.8)
50	11.0(3.0)	11.4(3.0)	9.1(3.0)	11.5(1.0)
100	11.8(3.5)	12.2(3.5)	9.8(3.5)	12.3(1.1)

SUMMER

	ANGLE CLASSES 1	2	3	ALL
5	4.6(1.6)	8.2(1.6)	6.6(1.6)	8.5(0.8)
10	6.9(2.1)	10.2(2.1)	8.2(2.1)	10.2(1.0)
20	8.5(2.7)	11.2(2.7)	9.2(2.7)	11.5(1.3)
50	10.2(3.3)	12.5(3.3)	10.2(3.3)	12.6(1.6)
100	11.2(3.8)	13.4(3.8)	10.8(3.8)	13.5(1.8)

FALL

	ANGLE CLASSES 1	2	3	ALL
5	17.1(1.5)	16.4(1.5)	11.8(1.5)	18.0(0.7)
10	18.4(2.0)	18.7(2.0)	13.4(2.0)	19.7(0.9)
20	19.7(2.5)	20.3(2.5)	14.8(2.5)	20.7(1.2)
50	20.7(3.0)	22.3(3.0)	15.7(3.0)	22.4(1.4)
100	21.3(3.5)	23.3(3.5)	16.7(3.5)	23.4(1.7)

(Continued)

TABLE OF EXTREMES ESTIMATES
GRID LOCATION 14, 7 LAT=44.17 LON=83.30 TAWAS CITY MI

SHORELINE GRID POINT 11

WINTER

	ANGLE CLASSES 1	2	3	ALL
5	9.2(1.6)	15.7(1.6)	19.4(1.6)	19.4(0.4)
10	10.2(2.1)	16.4(2.1)	20.3(2.1)	20.3(0.6)
20	10.8(2.7)	17.1(2.7)	21.0(2.7)	21.0(0.7)
50	11.5(3.3)	17.7(3.3)	21.6(3.3)	21.6(0.9)
100	11.8(3.8)	18.0(3.8)	22.0(3.8)	22.0(1.0)

SPRING

	ANGLE CLASSES 1	2	3	ALL
5	3.9(1.5)	7.5(1.5)	6.7(1.5)	7.6(0.7)
10	5.1(2.0)	9.4(2.0)	8.3(2.0)	9.5(1.0)
20	5.9(2.5)	11.4(2.5)	9.4(2.5)	11.5(1.2)
50	6.7(3.0)	13.0(3.0)	10.6(3.0)	13.1(1.5)
100	7.1(3.5)	14.2(3.5)	11.0(3.5)	14.3(1.8)

SUMMER

	ANGLE CLASSES 1	2	3	ALL
5	3.9(1.6)	4.3(1.6)	5.6(1.6)	6.2(0.7)
10	5.2(2.1)	5.9(2.1)	7.2(2.1)	7.5(0.9)
20	6.2(2.7)	6.9(2.7)	8.5(2.7)	8.5(1.1)
50	7.2(3.3)	7.9(3.3)	9.8(3.3)	9.8(1.4)
100	7.9(3.8)	8.5(3.8)	10.5(3.8)	10.5(1.6)

FALL

	ANGLE CLASSES 1	2	3	ALL
5	9.2(1.5)	14.1(1.6)	17.1(1.5)	17.1(0.9)
10	11.2(2.0)	17.7(2.1)	19.4(2.0)	19.4(1.2)
20	12.5(2.5)	20.3(2.6)	20.7(2.5)	21.0(1.5)
50	14.1(3.0)	23.3(3.3)	22.3(3.0)	23.4(1.9)
100	14.8(3.5)	24.9(3.8)	23.3(3.5)	25.0(2.2)

(Continued)

Table E1 (Continued)

TABLE OF EXTREMES ESTIMATES
GRID LOCATION 13, 8 LAT=44.31 LON=83.11 OSCGDA AU SABLE MI

SHORELINE GRID POINT 12

WINTER

	ANGLE CLASSES 1	2	3	ALL
5	11.5(1.6)	16.4(1.6)	18.0(1.6)	18.1(0.6)
10	12.5(2.1)	17.1(2.1)	19.4(2.1)	19.4(0.7)
20	13.1(2.7)	17.7(2.7)	20.3(2.7)	20.3(0.9)
50	13.8(3.3)	18.0(3.3)	21.3(3.3)	21.4(1.2)
100	14.1(3.8)	18.4(3.8)	21.6(3.8)	21.6(1.3)

SPRING

	ANGLE CLASSES 1	2	3	ALL
5	5.1(1.5)	7.9(1.5)	5.1(1.5)	8.0(0.6)
10	6.7(2.0)	9.8(2.0)	7.5(2.0)	9.9(0.8)
20	7.5(2.5)	11.0(2.5)	9.4(2.5)	11.1(1.0)
50	8.7(3.0)	12.6(3.0)	11.4(3.0)	12.7(1.2)
100	9.1(3.5)	13.8(3.5)	12.2(3.5)	13.9(1.4)

SUMMER

	ANGLE CLASSES 1	2	3	ALL
5	5.6(1.6)	4.9(1.6)	4.3(1.6)	5.9(0.6)
10	6.6(2.1)	5.9(2.1)	6.2(2.1)	7.2(0.9)
20	7.2(2.7)	6.6(2.7)	7.5(2.7)	8.2(1.1)
50	7.9(3.3)	7.5(3.3)	8.9(3.3)	9.5(1.3)
100	8.2(3.8)	7.9(3.8)	9.8(3.8)	10.2(1.5)

FALL

	ANGLE CLASSES 1	2	3	ALL
5	11.8(1.5)	15.1(1.5)	16.4(1.5)	16.7(0.9)
10	13.8(2.0)	18.0(2.0)	18.0(2.0)	19.0(1.2)
20	15.1(2.5)	20.3(2.5)	19.4(2.5)	20.3(1.5)
50	16.4(3.0)	22.6(3.0)	20.7(3.0)	22.7(1.8)
100	17.4(3.5)	24.3(3.5)	21.3(3.5)	24.4(2.1)

(Continued)

TABLE OF EXTREMES ESTIMATES
GRID LOCATION 12, 8 LAT=44.46 LON=85.11 GREENBUSH MI

SHORELINE GRID POINT 13

WINTER

	ANGLE CLASSES 1	2	3	ALL
5	12.8(1.6)	16.4(1.6)	18.0(1.6)	18.4(0.4)
10	13.4(2.1)	17.4(2.1)	19.4(2.1)	19.4(0.5)
20	14.1(2.7)	18.0(2.7)	20.0(2.7)	20.0(0.7)
50	14.8(3.3)	18.7(3.3)	21.0(3.3)	21.1(0.8)
100	15.4(3.8)	19.0(3.8)	21.3(3.8)	21.4(1.0)

SPRING

	ANGLE CLASSES 1	2	3	ALL
5	5.9(1.5)	7.5(1.5)	3.9(1.5)	7.6(0.6)
10	7.1(2.0)	9.4(2.0)	6.3(2.0)	9.5(0.8)
20	8.3(2.5)	11.0(2.5)	7.9(2.5)	11.1(1.0)
50	9.4(3.0)	12.6(3.0)	9.8(3.0)	12.7(1.2)
100	9.8(3.5)	13.8(3.5)	10.6(3.5)	13.9(1.4)

SUMMER

	ANGLE CLASSES 1	2	3	ALL
5	5.6(1.6)	5.2(1.6)	4.3(1.6)	6.2(0.8)
10	6.2(2.1)	6.9(2.1)	6.2(2.1)	7.9(1.0)
20	6.9(2.7)	8.2(2.7)	7.9(2.7)	9.2(1.3)
50	7.5(3.3)	9.2(3.3)	9.2(3.3)	10.5(1.6)
100	7.9(3.8)	10.2(3.8)	10.2(3.8)	11.2(1.8)

FALL

	ANGLE CLASSES 1	2	3	ALL
5	13.1(1.5)	14.4(1.5)	16.1(1.5)	16.7(0.9)
10	14.8(2.0)	18.0(2.0)	17.7(2.0)	18.7(1.2)
20	15.7(2.5)	20.3(2.5)	19.0(2.5)	20.3(1.5)
50	17.1(3.0)	23.0(3.1)	20.0(3.0)	23.1(1.9)
100	17.7(3.5)	24.6(3.6)	21.0(3.5)	24.7(2.2)

(Continued)

TABLE OF EXTREMES ESTIMATES
GRID LOCATION 11, 8 LAT=44.60 LON=83.11 HARRISVILLE MI

SHORELINE GRID POINT 14

WINTER

	ANGLE CLASSES 1	2	3	ALL
5	13.1(1.6)	19.0(1.6)	14.8(1.6)	19.1(0.6)
10	14.8(2.1)	20.0(2.1)	16.4(2.1)	20.0(0.7)
20	15.7(2.7)	21.0(2.7)	17.4(2.7)	21.0(0.9)
50	16.7(3.3)	22.0(3.3)	18.7(3.3)	22.0(1.2)
100	17.7(3.8)	22.3(3.8)	19.4(3.8)	22.3(1.3)

SPRING

	ANGLE CLASSES 1	2	3	ALL
5	6.7(1.5)	8.3(1.5)	5.1(1.5)	8.4(0.7)
10	7.5(2.0)	10.2(2.0)	7.1(2.0)	10.3(0.9)
20	7.9(2.5)	11.4(2.5)	8.7(2.5)	11.5(1.1)
50	8.7(3.0)	13.0(3.0)	10.2(3.0)	13.1(1.4)
100	8.7(3.5)	13.8(3.5)	11.0(3.5)	13.9(1.6)

SUMMER

	ANGLE CLASSES 1	2	3	ALL
5	3.9(1.6)	5.9(1.6)	6.2(1.6)	6.6(0.8)
10	5.2(2.1)	7.2(2.1)	8.2(2.1)	8.2(1.1)
20	6.6(2.7)	8.2(2.7)	9.8(2.7)	9.9(1.3)
50	7.5(3.3)	9.2(3.3)	11.2(3.3)	11.3(1.7)
100	8.2(3.8)	9.8(3.8)	12.1(3.8)	12.2(1.9)

FALL

	ANGLE CLASSES 1	2	3	ALL
5	11.2(1.5)	17.1(1.5)	14.1(1.5)	17.7(0.8)
10	13.1(2.0)	19.4(2.0)	17.1(2.0)	19.7(1.1)
20	14.4(2.5)	21.0(2.5)	19.0(2.5)	21.0(1.3)
50	16.1(3.0)	22.6(3.0)	21.0(3.0)	22.7(1.7)
100	17.1(3.5)	23.6(3.5)	22.3(3.5)	23.7(1.9)

(Continued)

Table E1 (Continued)

TABLE OF EXTREMES ESTIMATES
GRID LOCATION 10, 8 LAT=44.74 LON=83.11 BLACK RIVER MI

SHORELINE GRID POINT 15

WINTER

	ANGLE CLASSES 1	2	3	ALL
5	13.1(1.6)	18.7(1.6)	14.8(1.6)	18.8(0.5)
10	14.1(2.1)	19.7(2.1)	16.1(2.1)	19.7(0.6)
20	14.8(2.7)	20.7(2.7)	17.1(2.7)	20.7(0.8)
50	15.4(3.3)	21.3(3.3)	18.0(3.3)	21.3(1.0)
100	16.1(3.8)	22.0(3.8)	18.4(3.8)	22.0(1.1)

SPRING

	ANGLE CLASSES 1	2	3	ALL
5	7.1(1.5)	8.3(1.5)	4.7(1.5)	8.4(0.7)
10	7.9(2.0)	10.2(2.0)	6.7(2.0)	10.3(0.9)
20	8.3(2.5)	11.8(2.5)	7.9(2.5)	11.9(1.2)
50	9.1(3.0)	13.4(3.0)	9.4(3.0)	13.5(1.4)
100	9.4(3.5)	14.2(3.5)	10.2(3.5)	14.3(1.7)

SUMMER

	ANGLE CLASSES 1	2	3	ALL
5	3.9(1.6)	5.9(1.6)	5.9(1.6)	6.6(0.8)
10	5.2(2.1)	6.9(2.1)	7.9(2.1)	8.2(1.0)
20	5.9(2.7)	7.9(2.7)	9.5(2.7)	9.6(1.3)
50	6.9(3.3)	8.5(3.3)	11.2(3.3)	11.3(1.6)
100	7.5(3.8)	9.2(3.8)	12.1(3.8)	12.2(1.8)

FALL

	ANGLE CLASSES 1	2	3	ALL
5	12.1(1.5)	17.1(1.5)	12.8(1.6)	17.7(0.8)
10	13.8(2.0)	19.4(2.0)	16.4(2.2)	19.7(1.1)
20	15.1(2.5)	21.3(2.5)	19.4(2.7)	21.4(1.4)
50	16.4(3.0)	23.3(3.0)	22.0(3.3)	23.4(1.7)
100	17.4(3.5)	24.3(3.5)	23.6(3.9)	24.4(2.0)

(Continued)

Table E1 (Continued)

TABLE OF EXTREMES ESTIMATES
GRID LOCATION 9, 8 LAT=44.89 LON=83.11 OSSINEKE MI

SHORELINE GRID POINT 16

WINTER
ANGLE CLASSES

	1	2	3	ALL
5	13.4(1.6)	18.7(1.6)	14.4(1.6)	18.8(0.6)
10	14.4(2.1)	20.0(2.1)	15.4(2.1)	20.0(0.9)
20	15.1(2.7)	21.0(2.7)	16.4(2.7)	21.0(1.1)
50	15.4(3.3)	22.0(3.3)	17.1(3.3)	22.0(1.3)
100	16.1(3.8)	22.6(3.8)	17.7(3.8)	22.6(1.5)

SPRING
ANGLE CLASSES

	1	2	3	ALL
5	7.5(1.5)	7.9(1.5)	4.7(1.5)	8.0(0.7)
10	9.1(2.0)	10.2(2.0)	6.3(2.0)	10.3(1.0)
20	10.2(2.5)	11.8(2.5)	7.9(2.5)	11.9(1.2)
50	11.4(3.0)	13.0(3.0)	9.1(3.0)	13.1(1.5)
100	12.2(3.5)	14.2(3.5)	9.8(3.5)	14.3(1.8)

SUMMER
ANGLE CLASSES

	1	2	3	ALL
5	4.9(1.6)	5.2(1.6)	5.6(1.6)	6.2(0.8)
10	5.6(2.1)	6.6(2.1)	7.5(2.1)	7.9(1.1)
20	6.2(2.7)	7.2(2.7)	9.2(2.7)	9.3(1.3)
50	6.9(3.3)	8.2(3.3)	10.8(3.3)	10.9(1.7)
100	7.2(3.8)	8.5(3.8)	11.8(3.8)	11.9(1.9)

FALL
ANGLE CLASSES

	1	2	3	ALL
5	11.5(1.5)	16.4(1.5)	12.1(1.6)	17.1(1.0)
10	13.8(2.0)	19.4(2.0)	15.7(2.2)	19.7(1.4)
20	15.4(2.5)	21.3(2.5)	18.4(2.7)	21.3(1.7)
50	17.1(3.0)	23.3(3.0)	21.3(3.3)	23.4(2.1)
100	18.0(3.5)	24.6(3.5)	23.0(3.9)	24.7(2.5)

(Continued)

Table E1 (Continued)

TABLE OF EXTREMES ESTIMATES
GRID LOCATION 8, 8 LAT=45.04 LON=83.11 NORTH POINT

SHORELINE GRID POINT 17

WINTER
ANGLE CLASSES

	1	2	3	ALL
5	13.1(1.6)	18.4(1.6)	12.1(1.6)	18.5(0.6)
10	14.4(2.1)	19.7(2.1)	14.8(2.1)	19.7(0.9)
20	15.1(2.7)	20.7(2.7)	17.1(2.7)	20.7(1.1)
50	16.1(3.3)	21.6(3.3)	19.0(3.3)	21.6(1.3)
100	16.7(3.8)	22.3(3.8)	20.3(3.8)	22.3(1.5)

SPRING
ANGLE CLASSES

	1	2	3	ALL
5	7.5(1.5)	7.9(1.5)	4.3(1.5)	8.0(0.7)
10	9.4(2.0)	9.8(2.0)	5.9(2.0)	9.9(1.0)
20	10.6(2.5)	11.4(2.5)	7.5(2.5)	11.5(1.2)
50	11.8(3.0)	13.0(3.0)	9.1(3.0)	13.1(1.5)
100	12.6(3.5)	13.8(3.5)	9.8(3.5)	13.9(1.8)

SUMMER
ANGLE CLASSES

	1	2	3	ALL
5	4.6(1.6)	4.9(1.6)	4.6(1.6)	5.6(0.8)
10	4.9(2.1)	6.2(2.1)	6.9(2.1)	7.2(1.0)
20	5.2(2.7)	7.5(2.7)	8.9(2.7)	9.0(1.3)
50	5.6(3.3)	8.5(3.3)	10.5(3.3)	10.6(1.6)
100	5.9(3.8)	9.2(3.8)	11.8(3.8)	11.9(1.8)

FALL
ANGLE CLASSES

	1	2	3	ALL
5	11.5(1.5)	16.1(1.5)	11.5(1.6)	16.7(1.1)
10	13.8(2.0)	19.4(2.0)	15.1(2.2)	19.4(1.5)
20	15.4(2.5)	21.6(2.5)	17.7(2.7)	21.7(1.9)
50	17.4(3.0)	23.9(3.0)	20.7(3.3)	24.0(2.4)
100	18.4(3.5)	25.3(3.5)	22.3(3.9)	25.4(2.7)

(Continued)

TABLE OF EXTREMES ESTIMATES
GRID LOCATION 7, 7 LAT=45.18 LON=85.30 ROCKPORT MI

SHORELINE GRID POINT 18

WINTER

	ANGLE CLASSES 1	2	3	ALL
5	14.1(1.6)	18.0(1.6)	13.1(1.6)	18.1(0.8)
10	15.1(2.1)	19.7(2.1)	14.8(2.1)	19.7(1.0)
20	15.4(2.7)	21.0(2.7)	16.1(2.7)	21.0(1.3)
50	16.1(3.3)	22.3(3.3)	17.4(3.3)	22.4(1.6)
100	16.4(3.8)	23.0(3.8)	18.4(3.8)	23.0(1.8)

SPRING

	ANGLE CLASSES 1	2	3	ALL
5	6.7(1.5)	5.5(1.5)	5.1(1.5)	6.8(0.7)
10	9.1(2.0)	6.7(2.0)	7.1(2.0)	9.2(0.9)
20	10.6(2.5)	7.5(2.5)	8.7(2.5)	10.7(1.1)
50	12.2(3.0)	8.3(3.0)	9.8(3.0)	12.3(1.4)
100	13.0(3.5)	9.1(3.5)	11.0(3.5)	13.1(1.6)

SUMMER

	ANGLE CLASSES 1	2	3	ALL
5	3.6(1.6)	5.2(1.6)	6.6(1.6)	7.2(0.8)
10	4.6(2.1)	7.5(2.1)	7.9(2.1)	8.9(1.0)
20	5.2(2.7)	9.2(2.7)	8.9(2.7)	10.2(1.3)
50	5.9(3.3)	10.8(3.3)	9.8(3.3)	11.5(1.6)
100	6.2(3.8)	11.8(3.8)	10.5(3.8)	12.1(1.8)

FALL

	ANGLE CLASSES 1	2	3	ALL
5	12.5(1.8)	16.7(1.5)	11.2(1.5)	16.7(0.8)
10	16.4(2.4)	18.4(2.0)	11.8(2.0)	18.7(1.1)
20	19.7(2.9)	20.0(2.5)	12.5(2.5)	20.0(1.4)
50	22.6(3.7)	21.3(3.0)	13.1(3.0)	22.7(1.7)
100	24.3(4.2)	22.3(3.5)	13.4(3.5)	24.4(2.0)

(Continued)

TABLE OF EXTREMES ESTIMATES
GRID LOCATION 6, 7 LAT=45.32 LON=83.30 STONE PORT MI

SHORELINE GRID POINT 19

WINTER

	ANGLE CLASSES 1	2	3	ALL
5	15.1(1.6)	13.4(1.6)	15.1(1.6)	16.4(0.3)
10	17.1(2.1)	15.1(2.1)	16.1(2.1)	17.1(0.4)
20	18.4(2.7)	16.4(2.7)	17.1(2.7)	18.5(0.5)
50	19.7(3.3)	17.7(3.3)	17.7(3.3)	19.8(0.7)
100	20.3(3.8)	18.4(3.8)	18.0(3.8)	20.4(0.8)

SPRING

	ANGLE CLASSES 1	2	3	ALL
5	5.1(1.5)	3.5(1.5)	7.1(1.5)	7.2(0.7)
10	6.7(2.0)	6.3(2.0)	9.4(2.0)	9.5(0.9)
20	7.9(2.5)	7.9(2.5)	11.0(2.5)	11.1(1.2)
50	9.1(3.0)	9.4(3.0)	12.6(3.0)	12.7(1.4)
100	9.8(3.5)	10.6(3.5)	13.4(3.5)	13.5(1.7)

SUMMER

	ANGLE CLASSES 1	2	3	ALL
5	2.3(1.6)	3.3(1.6)	9.2(1.6)	9.5(0.6)
10	4.3(2.1)	6.2(2.1)	10.5(2.1)	10.5(0.7)
20	5.6(2.7)	8.2(2.7)	11.5(2.7)	11.5(0.9)
50	6.9(3.3)	10.2(3.3)	12.5(3.3)	12.6(1.2)
100	7.9(3.8)	11.5(3.8)	13.1(3.8)	13.2(1.3)

FALL

	ANGLE CLASSES 1	2	3	ALL
5	13.4(1.5)	12.5(1.5)	13.8(1.5)	15.1(0.5)
10	15.1(2.0)	15.1(2.0)	14.1(2.0)	16.1(0.6)
20	16.1(2.5)	17.1(2.5)	14.4(2.5)	17.1(0.8)
50	17.1(3.0)	19.4(3.0)	15.1(3.0)	19.5(1.0)
100	17.7(3.5)	20.7(3.5)	15.1(3.5)	20.8(1.1)

(Continued)

Table E1 (Continued)

TABLE OF EXTREMES ESTIMATES
GRID LOCATION 5, 6 LAT=45.46 LON=83.50 ADAMS POINT MI

SHORELINE GRID POINT 20

WINTER

	ANGLE CLASSES 1	2	3	ALL
5	13.1(1.6)	12.1(1.6)	13.8(1.6)	14.4(0.4)
10	15.1(2.1)	13.8(2.1)	15.1(2.1)	15.4(0.5)
20	16.4(2.7)	15.1(2.7)	16.1(2.7)	16.5(0.7)
50	17.7(3.3)	16.4(3.3)	16.7(3.3)	17.8(0.8)
100	18.4(3.8)	17.1(3.8)	17.4(3.8)	18.5(1.0)

SPRING

	ANGLE CLASSES 1	2	3	ALL
5	4.7(1.5)	3.9(1.5)	6.3(1.5)	6.4(0.6)
10	5.9(2.0)	5.9(2.0)	8.7(2.0)	8.8(0.8)
20	6.7(2.5)	7.5(2.5)	10.2(2.5)	10.3(1.0)
50	7.9(3.0)	8.7(3.0)	11.8(3.0)	11.9(1.2)
100	8.3(3.5)	9.4(3.5)	12.6(3.5)	12.7(1.4)

SUMMER

	ANGLE CLASSES 1	2	3	ALL
5	2.3(1.6)	2.0(1.6)	8.5(1.6)	8.5(0.5)
10	3.9(2.1)	4.3(2.1)	9.5(2.1)	9.6(0.7)
20	5.2(2.7)	6.2(2.7)	10.5(2.7)	10.5(0.9)
50	6.6(3.3)	7.9(3.3)	11.2(3.3)	11.2(1.1)
100	7.2(3.8)	8.9(3.8)	11.8(3.8)	11.9(1.2)

FALL

	ANGLE CLASSES 1	2	3	ALL
5	12.1(1.5)	11.5(1.5)	12.8(1.5)	13.8(0.3)
10	13.4(2.0)	13.8(2.0)	13.4(2.0)	14.8(0.4)
20	14.4(2.5)	15.4(2.5)	14.1(2.5)	15.4(0.6)
50	15.4(3.0)	17.4(3.0)	14.4(3.0)	17.5(0.7)
100	16.1(3.5)	18.4(3.5)	14.8(3.5)	18.5(0.8)

(Continued)

TABLE OF EXTREMES ESTIMATES
GRID LOCATION 5, 5 LAT=45.46 LON=83.70 ROGERS CITY MI

SHORELINE GRID POINT 21

WINTER

	ANGLE CLASSES 1	2	3	ALL
5	14.1(1.6)	13.4(1.6)	15.7(1.6)	16.1(0.4)
10	15.4(2.1)	15.1(2.1)	16.7(2.1)	16.7(0.5)
20	16.4(2.7)	16.7(2.7)	17.4(2.7)	17.5(0.6)
50	17.4(3.3)	18.0(3.3)	18.4(3.3)	18.5(0.7)
100	18.0(3.8)	19.0(3.8)	18.7(3.8)	19.1(0.9)

SPRING

	ANGLE CLASSES 1	2	3	ALL
5	5.1(1.5)	4.3(1.5)	6.7(1.5)	6.8(0.6)
10	6.7(2.0)	6.3(2.0)	9.1(2.0)	9.2(0.7)
20	8.3(2.5)	7.9(2.5)	10.2(2.5)	10.3(0.9)
50	9.4(3.0)	9.4(3.0)	11.8(3.0)	11.9(1.1)
100	10.2(3.5)	10.2(3.5)	13.0(3.5)	13.1(1.3)

SUMMER

	ANGLE CLASSES 1	2	3	ALL
5	3.0(1.6)	3.3(1.6)	9.8(1.6)	9.8(0.4)
10	4.9(2.1)	5.9(2.1)	10.8(2.1)	10.8(0.5)
20	6.2(2.7)	7.9(2.7)	11.5(2.7)	11.5(0.7)
50	7.5(3.3)	9.8(3.3)	12.1(3.3)	12.2(0.8)
100	8.2(3.8)	11.2(3.8)	12.5(3.8)	12.6(1.0)

FALL

	ANGLE CLASSES 1	2	3	ALL
5	12.8(1.5)	12.8(1.5)	14.4(1.5)	15.4(0.2)
10	14.8(2.0)	14.8(2.0)	15.1(2.0)	15.7(0.3)
20	16.4(2.5)	16.4(2.5)	15.4(2.5)	16.4(0.4)
50	18.0(3.0)	18.0(3.0)	15.7(3.0)	18.1(0.5)
100	19.0(3.5)	19.0(3.5)	16.1(3.5)	19.1(0.5)

(Continued)

Table E1 (Continued)

TABLE OF EXTREMES ESTIMATES
GRID LOCATION 4, 4 LAT=45.61 LON=83.90 HAMMOND BAY MI

SHORELINE GRID POINT 22

WINTER
ANGLE CLASSES

	1	2	3	ALL
5	12.5(1.6)	13.1(1.6)	14.1(1.6)	14.8(0.4)
10	13.8(2.1)	14.4(2.1)	15.4(2.1)	15.4(0.5)
20	14.8(2.7)	15.4(2.7)	16.4(2.7)	16.5(0.6)
50	15.7(3.3)	16.4(3.3)	17.4(3.3)	17.5(0.7)
100	16.1(3.8)	17.1(3.8)	18.0(3.8)	18.1(0.9)

SPRING
ANGLE CLASSES

	1	2	3	ALL
5	4.7(1.5)	3.5(1.5)	6.3(1.5)	6.4(0.5)
10	5.9(2.0)	5.5(2.0)	8.7(2.0)	8.8(0.6)
20	7.1(2.5)	6.7(2.5)	10.2(2.5)	10.3(0.8)
50	7.9(3.0)	8.3(3.0)	11.8(3.0)	11.9(1.0)
100	8.7(3.5)	9.1(3.5)	12.6(3.5)	12.7(1.1)

SUMMER
ANGLE CLASSES

	1	2	3	ALL
5	2.6(1.6)	3.3(1.6)	9.2(1.6)	9.3(0.3)
10	3.9(2.1)	5.6(2.1)	9.8(2.1)	9.8(0.4)
20	4.9(2.7)	7.2(2.7)	10.5(2.7)	10.5(0.5)
50	5.9(3.3)	8.9(3.3)	10.8(3.3)	10.8(0.7)
100	6.6(3.8)	10.2(3.8)	11.2(3.8)	11.2(0.8)

FALL
ANGLE CLASSES

	1	2	3	ALL
5	11.2(1.5)	12.1(1.5)	13.8(1.5)	14.4(0.2)
10	13.4(2.0)	13.8(2.0)	14.4(2.0)	14.8(0.2)
20	14.8(2.5)	14.8(2.5)	15.1(2.5)	15.1(0.3)
50	16.4(3.0)	15.7(3.0)	15.4(3.0)	16.5(0.4)
100	17.4(3.5)	16.4(3.5)	15.7(3.5)	17.5(0.4)

(Continued)

TABLE OF EXTREMES ESTIMATES
GRID LOCATION 3, 3 LAT=45.75 LON=84.09 CORDWOOD POINT
MI

SHORELINE GRID POINT 23

WINTER

	ANGLE CLASSES 1	2	3	ALL
5	11.2(1.6)	12.5(1.6)	11.8(1.6)	13.4(0.2)
10	11.8(2.1)	13.8(2.1)	13.1(2.1)	13.8(0.3)
20	12.5(2.7)	14.8(2.7)	14.1(2.7)	14.9(0.4)
50	13.1(3.3)	15.4(3.3)	15.1(3.3)	15.5(0.5)
100	13.4(3.8)	16.1(3.8)	15.7(3.8)	16.2(0.6)

SPRING

	ANGLE CLASSES 1	2	3	ALL
5	4.3(1.5)	3.1(1.5)	5.5(1.5)	5.6(0.5)
10	5.1(2.0)	4.7(2.0)	7.5(2.0)	7.6(0.7)
20	5.5(2.5)	5.9(2.5)	8.7(2.5)	8.8(0.9)
50	6.3(3.0)	7.1(3.0)	10.2(3.0)	10.3(1.1)
100	6.3(3.5)	7.5(3.5)	11.0(3.5)	11.1(1.2)

SUMMER

	ANGLE CLASSES 1	2	3	ALL
5	2.3(1.6)	4.6(1.6)	7.9(1.6)	8.2(0.3)
10	3.9(2.1)	6.9(2.1)	8.5(2.1)	8.9(0.4)
20	4.9(2.7)	8.5(2.7)	9.2(2.7)	9.3(0.5)
50	5.9(3.3)	10.5(3.3)	9.5(3.3)	10.6(0.6)
100	6.6(3.8)	11.5(3.8)	9.8(3.8)	11.6(0.7)

FALL

	ANGLE CLASSES 1	2	3	ALL
5	10.2(1.5)	11.5(1.5)	12.1(1.5)	12.8(0.3)
10	11.5(2.0)	12.5(2.0)	13.1(2.0)	13.4(0.3)
20	12.5(2.5)	13.1(2.5)	13.8(2.5)	13.8(0.4)
50	13.4(3.0)	13.8(3.0)	14.8(3.0)	14.9(0.5)
100	14.1(3.5)	14.1(3.5)	15.1(3.5)	15.2(0.6)

(Continued)

Table E1 (Continued)

TABLE OF EXTREMES ESTIMATES
GRID LOCATION 2, 3 LAT=45.89 LON=84.09 POINT DOLOMITE MI

SHORELINE GRID POINT 24

WINTER

	ANGLE CLASSES 1	2	3	ALL
5	9.5(1.6)	15.7(1.6)	10.5(1.6)	15.7(0.4)
10	12.5(2.1)	16.4(2.1)	11.2(2.1)	16.4(0.5)
20	14.4(2.7)	17.1(2.7)	11.8(2.7)	17.1(0.6)
50	16.7(3.3)	17.7(3.3)	12.5(3.3)	17.8(0.7)
100	18.0(3.8)	18.0(3.8)	12.8(3.8)	18.1(0.9)

SPRING

	ANGLE CLASSES 1	2	3	ALL
5	4.7(1.5)	9.4(1.5)	1.2(1.5)	9.5(0.7)
10	5.5(2.0)	11.4(2.0)	1.6(2.0)	11.5(0.9)
20	6.3(2.5)	13.0(2.5)	2.0(2.5)	13.1(1.2)
50	6.7(3.0)	14.2(3.0)	2.4(3.0)	14.3(1.4)
100	7.1(3.5)	15.0(3.5)	2.8(3.5)	15.1(1.7)

SUMMER

	ANGLE CLASSES 1	2	3	ALL
5	4.6(1.6)	6.2(1.6)	1.0(1.6)	6.9(0.4)
10	6.6(2.1)	7.5(2.1)	1.3(2.1)	7.5(0.6)
20	7.9(2.7)	8.5(2.7)	1.3(2.7)	8.5(0.7)
50	9.2(3.3)	9.2(3.3)	1.6(3.3)	9.3(0.9)
100	10.2(3.8)	9.8(3.8)	1.6(3.8)	10.3(1.0)

FALL

	ANGLE CLASSES 1	2	3	ALL
5	7.9(1.5)	15.7(1.5)	7.9(1.5)	15.7(1.0)
10	10.5(2.0)	18.0(2.0)	8.9(2.0)	18.1(1.3)
20	12.5(2.5)	19.7(2.5)	9.8(2.5)	19.7(1.7)
50	14.4(3.0)	21.3(3.0)	10.5(3.0)	21.3(2.1)
100	15.7(3.5)	22.3(3.5)	11.2(3.5)	22.3(2.4)

(Continued)

TABLE OF EXTREMES ESTIMATES
GRID LOCATION 2, 4 LAT=45.89 LON=83.90 DETOUR REEF MI

SHORELINE GRID POINT 25

WINTER

	ANGLE CLASSES 1	2	3	ALL
5	7.9(1.8)	15.7(1.6)	13.8(1.6)	15.7(0.2)
10	11.5(2.3)	16.4(2.1)	14.8(2.1)	16.4(0.3)
20	14.4(2.9)	16.7(2.7)	15.7(2.7)	16.7(0.4)
50	17.1(3.6)	17.1(3.3)	16.4(3.3)	17.1(0.5)
100	18.7(4.2)	17.4(3.8)	17.1(3.8)	18.8(0.6)

SPRING

	ANGLE CLASSES 1	2	3	ALL
5	5.9(1.5)	8.3(1.5)	7.9(1.5)	8.4(0.8)
10	7.1(2.0)	10.2(2.0)	9.8(2.0)	10.3(1.0)
20	8.3(2.5)	12.2(2.5)	11.0(2.5)	12.3(1.3)
50	9.1(3.0)	13.8(3.0)	12.6(3.0)	13.9(1.6)
100	9.4(3.5)	15.0(3.5)	13.4(3.5)	15.1(1.8)

SUMMER

	ANGLE CLASSES 1	2	3	ALL
5	6.9(1.6)	8.2(1.6)	2.6(1.6)	8.2(0.4)
10	8.5(2.1)	8.9(2.1)	4.6(2.1)	9.0(0.6)
20	9.8(2.7)	9.5(2.7)	6.2(2.7)	9.9(0.7)
50	11.2(3.3)	10.2(3.3)	7.5(3.3)	11.3(0.9)
100	11.8(3.8)	10.8(3.8)	8.5(3.8)	11.9(1.0)

FALL

	ANGLE CLASSES 1	2	3	ALL
5	10.8(1.5)	15.7(1.5)	14.1(1.5)	16.1(0.6)
10	12.8(2.0)	16.7(2.0)	16.7(2.0)	17.4(0.8)
20	14.4(2.5)	17.4(2.5)	18.4(2.5)	18.5(1.0)
50	16.1(3.0)	18.0(3.0)	20.3(3.0)	20.4(1.3)
100	17.1(3.5)	18.7(3.5)	21.3(3.5)	21.4(1.5)

(Continued)

TABLE OF EXTREMES ESTIMATES
GRID LOCATION 3, 5 LAT=45.75 LON=83.70 WEST END DRUMMOND ISLAND MI

SHORELINE GRID POINT 26

WINTER

	ANGLE CLASSES 1	2	3	ALL
5	10.8(1.6)	15.1(1.6)	13.4(1.6)	15.4(0.2)
10	13.8(2.1)	15.7(2.1)	14.8(2.1)	16.1(0.3)
20	15.7(2.7)	16.4(2.7)	15.7(2.7)	16.4(0.4)
50	18.0(3.3)	16.7(3.3)	16.4(3.3)	18.1(0.5)
100	19.4(3.8)	17.1(3.8)	17.1(3.8)	19.5(0.6)

SPRING

	ANGLE CLASSES 1	2	3	ALL
5	6.3(1.5)	7.9(1.5)	7.5(1.5)	8.0(0.7)
10	7.1(2.0)	10.2(2.0)	9.4(2.0)	10.3(1.0)
20	7.9(2.5)	11.8(2.5)	11.0(2.5)	11.9(1.2)
50	8.7(3.0)	13.8(3.0)	12.6(3.0)	13.9(1.5)
100	9.1(3.5)	15.0(3.5)	13.4(3.5)	15.1(1.8)

SUMMER

	ANGLE CLASSES 1	2	3	ALL
5	6.9(1.6)	7.5(1.6)	3.0(1.6)	7.5(0.5)
10	8.5(2.1)	8.5(2.1)	4.9(2.1)	8.5(0.7)
20	9.8(2.7)	9.5(2.7)	6.2(2.7)	9.9(0.9)
50	11.2(3.3)	10.2(3.3)	7.5(3.3)	11.3(1.1)
100	11.8(3.8)	10.8(3.8)	8.2(3.8)	11.9(1.2)

FALL

	ANGLE CLASSES 1	2	3	ALL
5	11.2(1.5)	14.8(1.5)	13.4(1.5)	15.4(0.6)
10	13.1(2.0)	16.4(2.0)	16.1(2.0)	17.1(0.8)
20	14.8(2.5)	17.4(2.5)	18.0(2.5)	18.1(1.0)
50	16.4(3.0)	18.4(3.0)	19.7(3.0)	19.8(1.3)
100	17.4(3.5)	18.7(3.5)	21.0(3.5)	21.1(1.5)

(Continued)

TABLE OF EXTREMES ESTIMATES
GRID LOCATION 3, 6 LAT=45.75 LON=83.50 FALSE DETOUR CHANNEL

SHORELINE GRID POINT 27

WINTER

	ANGLE CLASSES 1	2	3	ALL
5	12.5(1.6)	16.1(1.6)	13.4(1.6)	16.4(0.4)
10	14.8(2.1)	17.4(2.1)	14.8(2.1)	17.4(0.5)
20	16.4(2.7)	18.0(2.7)	15.7(2.7)	18.1(0.6)
50	18.0(3.3)	18.7(3.3)	16.7(3.3)	18.8(0.7)
100	19.0(3.8)	19.0(3.8)	17.4(3.8)	19.1(0.9)

SPRING

	ANGLE CLASSES 1	2	3	ALL
5	6.7(1.5)	9.1(1.5)	7.9(1.5)	9.2(0.7)
10	7.5(2.0)	11.4(2.0)	9.8(2.0)	11.5(0.9)
20	7.9(2.5)	13.0(2.5)	11.0(2.5)	13.1(1.2)
50	8.7(3.0)	15.0(3.0)	12.6(3.0)	15.1(1.4)
100	8.7(3.5)	15.7(3.5)	13.4(3.5)	15.8(1.7)

SUMMER

	ANGLE CLASSES 1	2	3	ALL
5	6.9(1.6)	7.9(1.6)	3.0(1.6)	7.9(0.5)
10	8.9(2.1)	8.9(2.1)	4.9(2.1)	9.2(0.7)
20	10.5(2.7)	9.5(2.7)	6.6(2.7)	10.6(0.9)
50	11.8(3.3)	10.5(3.3)	7.9(3.3)	11.9(1.1)
100	12.8(3.8)	10.8(3.8)	8.9(3.8)	12.9(1.2)

FALL

	ANGLE CLASSES 1	2	3	ALL
5	14.1(1.5)	15.4(1.5)	13.1(1.5)	16.1(0.7)
10	15.7(2.0)	17.4(2.0)	16.4(2.0)	17.7(1.0)
20	17.1(2.5)	18.7(2.5)	18.7(2.5)	19.0(1.2)
50	18.4(3.0)	20.0(3.0)	21.0(3.0)	21.1(1.5)
100	19.0(3.5)	20.7(3.5)	22.3(3.5)	22.4(1.8)

(Continued)

Table E1 (Concluded)

TABLE OF EXTREMES ESTIMATES
GRID LOCATION 3, 7 LAT=45.75 LON=83.30 COCKBURN ISLAND MI

SHORELINE GRID POINT 28

WINTER

	ANGLE CLASSES 1	2	3	ALL
5	13.8(1.6)	17.1(1.6)	12.8(1.6)	17.1(0.4)
10	15.4(2.1)	18.0(2.1)	14.1(2.1)	18.1(0.6)
20	16.7(2.7)	18.7(2.7)	15.1(2.7)	18.8(0.7)
50	17.7(3.3)	19.4(3.3)	16.1(3.3)	19.4(0.9)
100	18.7(3.8)	19.7(3.8)	16.4(3.8)	19.7(1.0)

SPRING

	ANGLE CLASSES 1	2	3	ALL
5	7.1(1.5)	9.1(1.5)	7.5(1.5)	9.2(0.7)
10	7.9(2.0)	11.0(2.0)	9.1(2.0)	11.1(0.9)
20	8.7(2.5)	12.6(2.5)	10.2(2.5)	12.7(1.2)
50	9.1(3.0)	14.2(3.0)	11.4(3.0)	14.3(1.4)
100	9.4(3.5)	15.4(3.5)	12.2(3.5)	15.5(1.7)

SUMMER

	ANGLE CLASSES 1	2	3	ALL
5	7.9(1.6)	8.5(1.6)	2.0(1.6)	8.9(0.7)
10	9.5(2.1)	10.2(2.1)	3.3(2.1)	10.2(0.9)
20	10.8(2.7)	11.2(2.7)	4.3(2.7)	11.2(1.1)
50	11.8(3.3)	12.5(3.3)	5.2(3.3)	12.6(1.4)
100	12.5(3.8)	13.1(3.8)	5.9(3.8)	13.2(1.6)

FALL

	ANGLE CLASSES 1	2	3	ALL
5	14.8(1.5)	16.4(1.5)	12.5(1.5)	16.7(0.5)
10	16.1(2.0)	17.7(2.0)	16.1(2.1)	18.0(0.7)
20	17.1(2.5)	18.7(2.5)	18.7(2.6)	18.8(0.9)
50	18.0(3.0)	19.7(3.0)	21.3(3.2)	21.4(1.1)
100	18.7(3.5)	20.3(3.5)	23.0(3.7)	23.1(1.2)

Table E2

WAVE HEIGHTS FOR APPROACH DIRECTIONS AND SEASONS COMBINED

SITE	RETURN PERIODS				
	5	10	20	50	100
1	20.2	20.7	21.1	21.7	22.1
2	19.1	19.7	20.3	21.5	22.5
3	15.5	16.4	17.3	18.5	19.4
4	16.3	17.3	18.4	19.9	21.0
5	12.0	12.0	12.0	21.2	22.3
6	17.6	18.7	19.8	21.2	22.3
7	18.8	19.7	20.8	22.3	23.4
8	19.1	20.1	21.1	22.4	23.5
9	19.2	20.1	21.0	22.2	23.2
10	19.7	20.8	21.9	23.4	24.5
11	20.4	21.1	21.8	23.5	25.1
12	19.5	20.4	21.4	23.0	24.5
13	19.2	20.1	21.3	23.1	24.8
14	20.2	21.0	21.8	23.0	24.0
15	20.1	21.0	21.9	23.3	24.5
16	20.1	21.1	22.1	23.7	25.0
17	20.0	21.1	22.3	24.0	25.5
18	19.6	20.7	21.8	23.5	25.0
19	17.1	18.1	19.1	20.6	21.8
20	15.2	16.1	17.1	18.5	19.5
21	16.3	17.2	18.0	19.2	20.0
22	15.3	16.1	16.9	17.9	18.8
23	13.9	14.5	15.1	15.9	16.5
24	17.6	18.6	19.7	21.2	22.3
25	16.5	17.7	18.9	20.5	21.7
26	16.2	17.5	18.8	20.5	21.8
27	17.7	18.5	19.5	21.1	22.5
28	18.3	19.0	19.7	21.4	23.1

Table E3

GRID LOCATION 22,12 LAT=43.02 LON=82.33 PORT HURON MI

GRID POINT NUMBER 1

SIGNIFICANT PERIOD BY ANGLE CLASS AND WAVE HEIGHT

WAVE HEIGHT (FT)	ANGLE CLASS		
	1	2	3
1	1.6	1.6	2.0
2	3.2	2.8	3.2
3	4.4	3.9	4.3
4	5.3	4.7	5.2
5	6.0	5.4	5.7
6	6.2	5.7	5.9
7	6.4	6.1	6.2
8	6.7	6.4	6.4
9	6.9	6.7	6.7
10	7.1	7.1	6.9
11	7.3	7.4	7.1
12	7.5	7.7	7.4
13	7.8	8.0	7.6
14	8.0	8.4	7.9
15	8.2	8.7	8.1
16	8.4	9.0	8.3
17	8.6	9.4	8.6
18	8.9	9.7	8.8
19	9.1	10.0	9.1
20	9.3	10.4	9.3
21	9.5	10.7	9.5
22	9.7	11.0	9.8
23	10.0	11.3	10.0
24	10.2	11.7	10.3
25	10.4	12.0	10.5

(Continued)

Table E3 (Continued)

GRID LOCATION 21,12 LAT=43.16 LON=82.33 LAKEPORT MI

GRID POINT NUMBER 2

SIGNIFICANT PERIOD BY ANGLE CLASS AND WAVE HEIGHT

WAVE HEIGHT (FT)	ANGLE CLASS		
	1	2	3
1	3.0	2.8	2.3
2	4.4	4.2	3.6
3	5.2	5.0	4.5
4	5.6	5.6	5.4
5	5.8	6.0	6.0
6	5.9	6.3	6.3
7	6.0	6.5	6.7
8	6.1	6.8	7.0
9	6.2	7.0	7.3
10	6.3	7.3	7.6
11	6.4	7.5	8.0
12	6.5	7.8	8.3
13	6.6	8.0	8.6
14	6.7	8.3	9.0
15	6.8	8.5	9.3
16	6.9	8.8	9.6
17	7.0	9.0	10.0
18	7.1	9.3	10.3
19	7.2	9.5	10.6
20	7.3	9.8	10.9
21	7.4	10.0	11.3
22	7.5	10.3	11.6
23	7.6	10.5	11.9
24	7.7	10.8	12.3
25	7.8	11.0	12.6

(Continued)

Table E3 (Continued)

GRID LOCATION 20,12 LAT=43.31 LON=82.33 LEXINGTON MI

GRID POINT NUMBER 3

SIGNIFICANT PERIOD BY ANGLE CLASS AND WAVE HEIGHT

WAVE HEIGHT (FT)	ANGLE CLASS		
	1	2	3
1	3.4	3.3	1.4
2	4.8	4.4	3.2
3	5.6	5.0	4.6
4	6.1	5.5	5.8
5	6.5	6.0	6.6
6	6.7	6.3	6.9
7	6.9	6.5	7.2
8	7.2	6.8	7.6
9	7.4	7.0	7.9
10	7.6	7.3	8.2
11	7.8	7.6	8.5
12	8.0	7.8	8.8
13	8.3	8.1	9.2
14	8.5	8.3	9.5
15	8.7	8.6	9.8
16	8.9	8.9	10.1
17	9.1	9.1	10.4
18	9.4	9.4	10.8
19	9.6	9.6	11.1
20	9.8	9.9	11.4
21	10.0	10.2	11.7
22	10.2	10.4	12.0
23	10.5	10.7	12.4
24	10.7	10.9	12.7
25	10.9	11.2	13.0

(Continued)

Table E3 (Continued)

GRID LOCATION 19,11 LAT=43.45 LON=82.52 PORT SANILAC MI

GRID POINT NUMBER 4

SIGNIFICANT PERIOD BY ANGLE CLASS AND WAVE HEIGHT

WAVE HEIGHT (FT)	ANGLE CLASS		
	1	2	3
1	3.6	2.8	1.8
2	5.0	4.2	3.4
3	5.6	5.0	4.5
4	6.0	5.5	5.5
5	6.2	5.9	6.2
6	6.3	6.1	6.5
7	6.5	6.4	6.8
8	6.6	6.6	7.0
9	6.8	6.9	7.3
10	6.9	7.1	7.6
11	7.0	7.3	7.9
12	7.2	7.6	8.2
13	7.3	7.8	8.4
14	7.5	8.1	8.7
15	7.6	8.3	9.0
16	7.7	8.5	9.3
17	7.9	8.8	9.6
18	8.0	9.0	9.8
19	8.2	9.3	10.1
20	8.3	9.5	10.4
21	8.4	9.7	10.7
22	8.6	10.0	11.0
23	8.7	10.2	11.2
24	8.9	10.5	11.5
25	9.0	10.7	11.8

(Continued)

Table E3 (Continued)

GRID LOCATION 18,11 LAT=43.59 LON=82.52 FORESTVILLE MI

GRID POINT NUMBER 5

SIGNIFICANT PERIOD BY ANGLE CLASS AND WAVE HEIGHT

WAVE HEIGHT (FT)	ANGLE CLASS		
	1	2	3
1	3.2	3.0	1.6
2	4.7	4.4	3.4
3	5.6	5.3	4.6
4	6.0	5.7	5.6
5	6.4	6.1	6.4
6	6.6	6.3	6.7
7	6.8	6.5	6.9
8	7.0	6.8	7.2
9	7.2	7.0	7.4
10	7.4	7.2	7.7
11	7.6	7.4	8.0
12	7.8	7.6	8.2
13	8.0	7.9	8.5
14	8.2	8.1	8.7
15	8.4	8.3	9.0
16	8.6	8.5	9.3
17	8.8	8.7	9.5
18	9.0	9.0	9.8
19	9.2	9.2	10.0
20	9.4	9.4	10.3
21	9.6	9.6	10.6
22	9.8	9.8	10.8
23	10.0	10.1	11.1
24	10.2	10.3	11.3
25	10.4	10.5	11.6

(Continued)

Table E3 (Continued)

GRID LOCATION 17,11 LAT=43.74 LON=82.52 HELENA MI

GRID POINT NUMBER 6

SIGNIFICANT PERIOD BY ANGLE CLASS AND WAVE HEIGHT

WAVE HEIGHT (FT)	ANGLE CLASS		
	1	2	3
1	3.2	2.4	2.6
2	4.7	4.0	4.2
3	5.6	4.8	5.0
4	6.2	5.4	5.6
5	6.5	5.8	6.1
6	6.6	6.1	6.4
7	6.8	6.3	6.7
8	6.9	6.6	6.9
9	7.1	6.8	7.2
10	7.3	7.1	7.5
11	7.4	7.3	7.8
12	7.6	7.5	8.1
13	7.7	7.8	8.3
14	7.9	8.0	8.6
15	8.0	8.3	8.9
16	8.1	8.5	9.2
17	8.3	8.8	9.5
18	8.5	9.0	9.7
19	8.6	9.3	10.0
20	8.8	9.5	10.3
21	8.9	9.8	10.6
22	9.1	10.0	10.9
23	9.2	10.3	11.1
24	9.4	10.5	11.4
25	9.5	10.8	11.7

(Continued)

Table E3 (Continued)

GRID LOCATION 16,11 LAT=43.88 LON=82.52 HARBOR BEACH MI

GRID POINT NUMBER 7

SIGNIFICANT PERIOD BY ANGLE CLASS AND WAVE HEIGHT

WAVE HEIGHT (FT)	ANGLE CLASS		
	1	2	3
1	2.8	3.6	2.8
2	4.3	5.0	4.4
3	5.4	5.7	5.4
4	6.2	6.1	6.1
5	6.4	6.5	6.5
6	6.5	6.7	6.8
7	6.7	6.9	7.0
8	6.8	7.2	7.3
9	7.0	7.4	7.5
10	7.1	7.6	7.8
11	7.2	7.8	8.0
12	7.4	8.0	8.3
13	7.5	8.3	8.5
14	7.7	8.5	8.8
15	7.8	8.7	9.0
16	7.9	8.9	9.3
17	8.1	9.1	9.5
18	8.2	9.4	9.8
19	8.4	9.6	10.0
20	8.5	9.8	10.3
21	8.6	10.0	10.5
22	8.8	10.2	10.8
23	8.9	10.5	11.0
24	9.1	10.7	11.3
25	9.2	10.9	11.5

(Continued)

Table E3 (Continued)

GRID LOCATION 15,10 LAT=44.03 LON=82.71 HURON CITY MI

GRID POINT NUMBER 8

SIGNIFICANT PERIOD BY ANGLE CLASS AND WAVE HEIGHT

WAVE HEIGHT (FT)	ANGLE CLASS		
	1	2	3
1	2.4	2.8	2.4
2	4.0	4.2	3.8
3	5.0	5.0	4.7
4	5.8	5.5	5.2
5	6.2	6.0	5.7
6	6.4	6.3	6.0
7	6.7	6.5	6.3
8	6.9	6.8	6.6
9	7.2	7.0	6.9
10	7.4	7.3	7.2
11	7.6	7.6	7.5
12	7.9	7.8	7.8
13	8.1	8.1	8.1
14	8.4	8.3	8.4
15	8.6	8.6	8.7
16	8.8	8.9	9.0
17	9.1	9.1	9.3
18	9.3	9.4	9.6
19	9.6	9.6	9.9
20	9.8	9.9	10.2
21	10.0	10.2	10.5
22	10.3	10.4	10.8
23	10.5	10.7	11.1
24	10.8	10.9	11.4
25	11.0	11.2	11.7

(Continued)

Table E3 (Continued)

GRID LOCATION 15, 8 LAT=44.03 LON=83.11 PORT CRESCENT MI

GRID POINT NUMBER 9

SIGNIFICANT PERIOD BY ANGLE CLASS AND WAVE HEIGHT

WAVE HEIGHT (FT)	ANGLE CLASS		
	1	2	3
1	3.0	3.0	3.2
2	4.4	4.3	4.4
3	5.4	5.0	5.2
4	5.8	5.4	5.6
5	6.3	5.8	6.0
6	6.6	6.1	6.2
7	6.8	6.4	6.5
8	7.1	6.6	6.7
9	7.4	6.9	6.9
10	7.7	7.2	7.1
11	7.9	7.5	7.4
12	8.2	7.8	7.6
13	8.5	8.0	7.8
14	8.7	8.3	8.1
15	9.0	8.6	8.3
16	9.3	8.9	8.5
17	9.5	9.2	8.8
18	9.8	9.4	9.0
19	10.1	9.7	9.2
20	10.4	10.0	9.4
21	10.6	10.3	9.7
22	10.9	10.6	9.9
23	11.2	10.8	10.1
24	11.4	11.1	10.4
25	11.7	11.4	10.6

(Continued)

Table E3 (Continued)

GRID LOCATION 15, 7 LAT=44.03 LON=83.30 ENTRANCE SAGINAW BAY MI

GRID POINT NUMBER 10

SIGNIFICANT PERIOD BY ANGLE CLASS AND WAVE HEIGHT

WAVE HEIGHT (FT)	ANGLE CLASS		
	1	2	3
1	2.4	3.2	2.8
2	4.0	4.4	4.2
3	5.0	5.0	4.8
4	5.7	5.4	5.3
5	6.1	5.8	5.6
6	6.4	6.1	5.9
7	6.6	6.3	6.1
8	6.9	6.6	6.4
9	7.1	6.9	6.6
10	7.4	7.2	6.9
11	7.7	7.4	7.2
12	7.9	7.7	7.4
13	8.2	8.0	7.7
14	8.4	8.2	7.9
15	8.7	8.5	8.2
16	9.0	8.8	8.5
17	9.2	9.0	8.7
18	9.5	9.3	9.0
19	9.7	9.6	9.2
20	10.0	9.9	9.5
21	10.3	10.1	9.8
22	10.5	10.4	10.0
23	10.8	10.7	10.3
24	11.0	10.9	10.5
25	11.3	11.2	10.8

(Continued)

Table E3 (Continued)

GRID LOCATION 14, 7 LAT=44.17 LON=83.30 TAWAS CITY MI

GRID POINT NUMBER 11

SIGNIFICANT PERIOD BY ANGLE CLASS AND WAVE HEIGHT

WAVE HEIGHT (FT)	ANGLE CLASS		
	1	2	3
1	3.6	3.5	3.1
2	4.8	4.5	4.1
3	5.3	5.0	4.8
4	5.7	5.3	5.3
5	6.1	5.9	5.8
6	6.3	6.2	6.1
7	6.6	6.5	6.4
8	6.8	6.7	6.7
9	7.1	7.0	7.0
10	7.3	7.3	7.3
11	7.5	7.6	7.6
12	7.8	7.9	7.9
13	8.0	8.1	8.2
14	8.3	8.4	8.5
15	8.5	8.7	8.8
16	8.7	9.0	9.1
17	9.0	9.3	9.4
18	9.2	9.5	9.7
19	9.5	9.8	10.0
20	9.7	10.1	10.3
21	9.9	10.4	10.6
22	10.2	10.7	10.9
23	10.4	10.9	11.2
24	10.7	11.2	11.5
25	10.9	11.5	11.8

(Continued)

Table E3 (Continued)

GRID LOCATION 13, 8 LAT=44.31 LON=83.11 OSCODA AU SABLE MI

GRID POINT NUMBER 12

SIGNIFICANT PERIOD BY ANGLE CLASS AND WAVE HEIGHT

WAVE HEIGHT (FT)	ANGLE CLASS		
	1	2	3
1	3.6	3.4	2.6
2	4.8	4.4	4.0
3	5.4	5.0	4.8
4	5.8	5.4	5.3
5	6.1	5.8	5.8
6	6.3	6.1	6.1
7	6.5	6.3	6.4
8	6.7	6.6	6.6
9	6.9	6.8	6.9
10	7.1	7.1	7.2
11	7.2	7.4	7.5
12	7.4	7.6	7.8
13	7.6	7.9	8.0
14	7.8	8.1	8.3
15	8.0	8.4	8.6
16	8.2	8.7	8.9
17	8.4	8.9	9.2
18	8.6	9.2	9.4
19	8.8	9.4	9.7
20	9.0	9.7	10.0
21	9.1	10.0	10.3
22	9.3	10.2	10.6
23	9.5	10.5	10.8
24	9.7	10.7	11.1
25	9.9	11.0	11.4

(Continued)

Table E3 (Continued)

GRID LOCATION 12, 8 LAT=44.46 LON=83.11 GREENBUSH MI

GRID POINT NUMBER 13

SIGNIFICANT PERIOD BY ANGLE CLASS AND WAVE HEIGHT

WAVE HEIGHT (FT)	ANGLE CLASS		
	1	2	3
1	3.2	3.2	3.6
2	4.4	4.3	4.8
3	5.2	5.0	5.4
4	5.6	5.3	5.8
5	6.0	5.6	6.4
6	6.2	5.8	6.7
7	6.4	6.0	6.9
8	6.7	6.2	7.2
9	6.9	6.4	7.4
10	7.1	6.7	7.7
11	7.3	6.9	8.0
12	7.5	7.1	8.2
13	7.8	7.3	8.5
14	8.0	7.5	8.7
15	8.2	7.7	9.0
16	8.4	7.9	9.3
17	8.6	8.1	9.5
18	8.9	8.3	9.8
19	9.1	8.5	10.0
20	9.3	8.8	10.3
21	9.5	9.0	10.6
22	9.7	9.2	10.8
23	10.0	9.4	11.1
24	10.2	9.6	11.3
25	10.4	9.8	11.6

(Continued)

Table E3 (Continued)

GRID LOCATION 11, 8 LAT=44.60 LON=83.11 HARRISVILLE MI

GRID POINT NUMBER 14

SIGNIFICANT PERIOD BY ANGLE CLASS AND WAVE HEIGHT

WAVE HEIGHT (FT)	ANGLE CLASS		
	1	2	3
1	3.4	3.2	3.2
2	4.8	4.4	4.4
3	5.5	5.2	5.1
4	6.0	5.6	5.6
5	6.4	6.0	6.0
6	6.6	6.3	6.3
7	6.9	6.6	6.6
8	7.1	6.8	6.9
9	7.3	7.1	7.2
10	7.6	7.4	7.5
11	7.8	7.7	7.8
12	8.0	8.0	8.1
13	8.2	8.2	8.4
14	8.5	8.5	8.7
15	8.7	8.8	9.0
16	8.9	9.1	9.3
17	9.2	9.4	9.6
18	9.4	9.6	9.9
19	9.6	9.9	10.2
20	9.9	10.2	10.5
21	10.1	10.5	10.8
22	10.3	10.8	11.1
23	10.5	11.0	11.4
24	10.8	11.3	11.7
25	11.0	11.6	12.0

(Continued)

Table E3 (Continued)

GRID LOCATION 10, 8 LAT=44.74 LON=83.11 BLACK RIVER MI

GRID POINT NUMBER 15

SIGNIFICANT PERIOD BY ANGLE CLASS AND WAVE HEIGHT

WAVE HEIGHT (FT)	ANGLE CLASS		
	1	2	3
1	3.6	3.2	3.5
2	5.0	4.6	4.6
3	5.7	5.4	5.2
4	6.2	5.9	5.6
5	6.6	6.2	6.1
6	6.8	6.4	6.4
7	7.0	6.7	6.6
8	7.3	6.9	6.9
9	7.5	7.1	7.2
10	7.7	7.4	7.4
11	7.9	7.6	7.7
12	8.1	7.8	8.0
13	8.4	8.0	8.3
14	8.6	8.3	8.5
15	8.8	8.5	8.8
16	9.0	8.7	9.1
17	9.2	9.0	9.3
18	9.5	9.2	9.6
19	9.7	9.4	9.9
20	9.9	9.6	10.1
21	10.1	9.9	10.4
22	10.3	10.1	10.7
23	10.6	10.3	11.0
24	10.8	10.6	11.2
25	11.0	10.8	11.5

(Continued)

Table E3 (Continued)

GRID LOCATION 9, 8 LAT=44.89 LON=83.11 OSSINEKE MI

GRID POINT NUMBER 16

SIGNIFICANT PERIOD BY ANGLE CLASS AND WAVE HEIGHT

WAVE HEIGHT (FT)	ANGLE CLASS		
	1	2	3
1	4.0	3.6	3.4
2	5.2	4.9	4.8
3	5.7	5.5	5.5
4	6.1	6.0	6.0
5	6.5	6.4	6.4
6	6.8	6.6	6.6
7	7.0	6.9	6.9
8	7.3	7.1	7.1
9	7.5	7.3	7.4
10	7.8	7.6	7.6
11	8.0	7.8	7.9
12	8.3	8.0	8.1
13	8.5	8.2	8.4
14	8.8	8.5	8.6
15	9.0	8.7	8.9
16	9.3	8.9	9.1
17	9.5	9.2	9.4
18	9.8	9.4	9.6
19	10.0	9.6	9.9
20	10.3	9.9	10.1
21	10.5	10.1	10.4
22	10.8	10.3	10.6
23	11.0	10.5	10.9
24	11.3	10.8	11.1
25	11.5	11.0	11.4

(Continued)

Table E3 (Continued)

GRID LOCATION 8, 8 LAT=45.04 LON=83.11 NORTH POINT MI

GRID POINT NUMBER 17

SIGNIFICANT PERIOD BY ANGLE CLASS AND WAVE HEIGHT

WAVE HEIGHT (FT)	ANGLE CLASS		
	1	2	3
1	3.2	2.6	3.0
2	4.7	4.0	4.4
3	5.7	5.0	5.4
4	6.3	5.4	6.0
5	6.6	5.8	6.4
6	6.8	6.1	6.6
7	7.1	6.4	6.9
8	7.3	6.6	7.1
9	7.6	6.9	7.4
10	7.8	7.2	7.6
11	8.0	7.5	7.8
12	8.3	7.8	8.1
13	8.5	8.0	8.3
14	8.8	8.3	8.6
15	9.0	8.6	8.8
16	9.2	8.9	9.0
17	9.5	9.2	9.3
18	9.7	9.4	9.5
19	10.0	9.7	9.8
20	10.2	10.0	10.0
21	10.4	10.3	10.2
22	10.7	10.6	10.5
23	10.9	10.8	10.7
24	11.2	11.1	11.0
25	11.4	11.4	11.2

(Continued)

Table E3 (Continued)

GRID LOCATION 7, 7 LAT=45.18 LON=83.30 ROCKPORT MI

GRID POINT NUMBER 18

SIGNIFICANT PERIOD BY ANGLE CLASS AND WAVE HEIGHT

WAVE HEIGHT (FT)	ANGLE CLASS		
	1	2	3
1	3.0	3.4	3.2
2	4.4	4.5	4.4
3	5.2	5.0	4.9
4	5.6	5.5	5.3
5	6.0	5.9	5.7
6	6.3	6.2	5.9
7	6.5	6.4	6.1
8	6.8	6.7	6.4
9	7.0	7.0	6.6
10	7.3	7.3	6.8
11	7.6	7.5	7.0
12	7.8	7.8	7.2
13	8.1	8.1	7.5
14	8.3	8.3	7.7
15	8.6	8.6	7.9
16	8.9	8.9	8.1
17	9.1	9.1	8.3
18	9.4	9.4	8.6
19	9.6	9.7	8.8
20	9.9	10.0	9.0
21	10.2	10.2	9.2
22	10.4	10.5	9.4
23	10.7	10.8	9.7
24	10.9	11.0	9.9
25	11.2	11.3	10.1

(Continued)

Table E3 (Continued)

GRID LOCATION 6, 7 LAT=45.32 LON=83.30 STONE PORT MI

GRID POINT NUMBER 19

SIGNIFICANT PERIOD BY ANGLE CLASS AND WAVE HEIGHT

WAVE HEIGHT (FT)	ANGLE CLASS		
	1	2	3
1	3.8	2.8	3.2
2	5.0	4.0	4.4
3	5.4	4.8	5.0
4	5.9	5.2	5.5
5	6.4	6.1	6.0
6	6.7	6.3	6.3
7	6.9	6.6	6.6
8	7.2	6.8	6.9
9	7.4	7.1	7.2
10	7.7	7.3	7.5
11	8.0	7.5	7.8
12	8.2	7.8	8.1
13	8.5	8.0	8.4
14	8.7	8.3	8.7
15	9.0	8.5	9.0
16	9.3	8.7	9.3
17	9.5	9.0	9.6
18	9.8	9.2	9.9
19	10.0	9.5	10.2
20	10.3	9.7	10.5
21	10.6	9.9	10.8
22	10.8	10.2	11.1
23	11.1	10.4	11.4
24	11.3	10.7	11.7
25	11.6	10.9	12.0

(Continued)

Table E3 (Continued)

GRID LOCATION 5, 6 LAT=45.46 LON=83.50 ADAMS POINT MI

GRID POINT NUMBER 20

SIGNIFICANT PERIOD BY ANGLE CLASS AND WAVE HEIGHT

WAVE HEIGHT (FT)	ANGLE CLASS		
	1	2	3
1	3.6	3.4	2.8
2	4.8	4.4	4.2
3	5.3	5.0	5.0
4	5.7	5.5	5.4
5	6.1	5.9	5.8
6	6.4	6.2	6.1
7	6.6	6.4	6.4
8	6.9	6.7	6.6
9	7.1	7.0	6.9
10	7.4	7.3	7.2
11	7.6	7.5	7.5
12	7.9	7.8	7.8
13	8.1	8.1	8.0
14	8.4	8.3	8.3
15	8.6	8.6	8.6
16	8.9	8.9	8.9
17	9.1	9.1	9.2
18	9.4	9.4	9.4
19	9.6	9.7	9.7
20	9.9	10.0	10.0
21	10.1	10.2	10.3
22	10.4	10.5	10.6
23	10.6	10.8	10.8
24	10.9	11.0	11.1
25	11.1	11.3	11.4

(Continued)

Table E3 (Continued)

GRID LOCATION 5, 5 LAT=45.46 LON=83.70 ROGERS CITY MI

GRID POINT NUMBER 21

SIGNIFICANT PERIOD BY ANGLE CLASS AND WAVE HEIGHT

WAVE HEIGHT (FT)	ANGLE CLASS		
	1	2	3
1	3.4	3.4	2.6
2	4.6	4.5	4.0
3	5.2	5.0	4.8
4	5.6	5.4	5.3
5	6.0	5.8	5.7
6	6.3	6.1	6.0
7	6.5	6.3	6.3
8	6.8	6.6	6.6
9	7.0	6.8	6.9
10	7.3	7.1	7.2
11	7.6	7.3	7.5
12	7.8	7.5	7.8
13	8.1	7.8	8.1
14	8.3	8.0	8.4
15	8.6	8.3	8.7
16	8.9	8.5	9.0
17	9.1	8.8	9.3
18	9.4	9.0	9.6
19	9.6	9.3	9.9
20	9.9	9.5	10.2
21	10.2	9.8	10.5
22	10.4	10.0	10.8
23	10.7	10.3	11.1
24	10.9	10.5	11.4
25	11.2	10.8	11.7

(Continued)

Table E3 (Continued)

GRID LOCATION 4, 4 LAT=45.61 LON=83.90 HAMMOND BAY MI

GRID POINT NUMBER 22

SIGNIFICANT PERIOD BY ANGLE CLASS AND WAVE HEIGHT

WAVE HEIGHT (FT)	ANGLE CLASS		
	1	2	3
1	3.6	3.6	3.3
2	4.7	4.6	4.5
3	5.2	5.1	5.2
4	5.7	5.6	5.6
5	6.2	6.0	6.0
6	6.5	6.2	6.3
7	6.8	6.5	6.5
8	7.0	6.7	6.8
9	7.3	7.0	7.0
10	7.6	7.2	7.3
11	7.9	7.4	7.6
12	8.2	7.7	7.8
13	8.4	7.9	8.1
14	8.7	8.2	8.3
15	9.0	8.4	8.6
16	9.3	8.6	8.9
17	9.6	8.9	9.1
18	9.8	9.1	9.4
19	10.1	9.4	9.6
20	10.4	9.6	9.9
21	10.7	9.8	10.2
22	11.0	10.1	10.4
23	11.2	10.3	10.7
24	11.5	10.6	10.9
25	11.8	10.8	11.2

(Continued)

GRID LOCATION 3, 3 LAT=45.75 LON=84.09 CORDWOOD POINT MI

GRID POINT NUMBER 23

SIGNIFICANT PERIOD BY ANGLE CLASS AND WAVE HEIGHT

WAVE HEIGHT (FT)	ANGLE CLASS		
	1	2	3
1	3.8	2.6	3.6
2	4.7	4.0	4.4
3	5.2	4.8	5.0
4	5.7	5.5	5.5
5	6.2	6.0	5.9
6	6.5	6.3	6.2
7	6.8	6.5	6.4
8	7.0	6.8	6.7
9	7.3	7.1	7.0
10	7.6	7.4	7.3
11	7.9	7.6	7.5
12	8.2	7.9	7.8
13	8.4	8.2	8.1
14	8.7	8.4	8.3
15	9.0	8.7	8.6
16	9.3	9.0	8.9
17	9.6	9.2	9.1
18	9.8	9.5	9.4
19	10.1	9.8	9.7
20	10.4	10.1	10.0
21	10.7	10.3	10.2
22	11.0	10.6	10.5
23	11.2	10.9	10.8
24	11.5	11.1	11.0
25	11.8	11.4	11.3

(Continued)

Table E3 (Continued)

GRID LOCATION 2, 3 LAT=45.89 LON=84.09 POINT DOLOMITE MI

GRID POINT NUMBER 24

SIGNIFICANT PERIOD BY ANGLE CLASS AND WAVE HEIGHT

WAVE HEIGHT (FT)	ANGLE CLASS		
	1	2	3
1	3.8	3.8	3.7
2	4.8	4.6	4.8
3	5.3	5.1	5.3
4	5.7	5.6	5.8
5	6.1	6.1	6.2
6	6.4	6.4	6.5
7	6.6	6.7	6.7
8	6.9	7.0	7.0
9	7.1	7.3	7.2
10	7.4	7.6	7.5
11	7.6	7.8	7.8
12	7.9	8.1	8.0
13	8.1	8.4	8.3
14	8.4	8.7	8.5
15	8.6	9.0	8.8
16	8.9	9.3	9.1
17	9.1	9.6	9.3
18	9.4	9.9	9.6
19	9.6	10.2	9.8
20	9.9	10.5	10.1
21	10.1	10.7	10.4
22	10.4	11.0	10.6
23	10.6	11.3	10.9
24	10.9	11.6	11.1
25	11.1	11.9	11.4

(Continued)

Table E3 (Continued)

GRID LOCATION 2, 4 LAT=45.89 LON=83.90 DETOUR REEF MI

GRID POINT NUMBER 25

SIGNIFICANT PERIOD BY ANGLE CLASS AND WAVE HEIGHT

WAVE HEIGHT (FT)	ANGLE CLASS		
	1	2	3
1	3.9	3.4	3.6
2	4.8	4.6	4.8
3	5.3	5.3	5.3
4	5.6	5.7	5.8
5	5.9	6.2	6.2
6	6.1	6.5	6.5
7	6.3	6.8	6.8
8	6.5	7.0	7.0
9	6.7	7.3	7.3
10	6.9	7.6	7.6
11	7.0	7.9	7.9
12	7.2	8.2	8.2
13	7.4	8.4	8.4
14	7.6	8.7	8.7
15	7.8	9.0	9.0
16	8.0	9.3	9.3
17	8.2	9.6	9.6
18	8.4	9.8	9.8
19	8.6	10.1	10.1
20	8.8	10.4	10.4
21	8.9	10.7	10.7
22	9.1	11.0	11.0
23	9.3	11.2	11.2
24	9.5	11.5	11.5
25	9.7	11.8	11.8

(Continued)

Table E3 (Continued)

GRID LOCATION 3, 5 LAT=45.75 LON=83.70 WEST END DRUMMOND ISLAND MI

GRID POINT NUMBER 26

SIGNIFICANT PERIOD BY ANGLE CLASS AND WAVE HEIGHT

WAVE HEIGHT (FT)	ANGLE CLASS		
	1	2	3
1	3.8	3.6	3.6
2	4.8	4.8	4.6
3	5.2	5.4	5.2
4	5.6	5.8	5.7
5	6.0	6.3	6.2
6	6.2	6.5	6.5
7	6.4	6.7	6.7
8	6.6	6.9	7.0
9	6.8	7.1	7.2
10	7.0	7.4	7.5
11	7.2	7.6	7.8
12	7.4	7.8	8.0
13	7.6	8.0	8.3
14	7.8	8.2	8.5
15	8.0	8.4	8.8
16	8.2	8.6	9.1
17	8.4	8.8	9.3
18	8.6	9.0	9.6
19	8.8	9.2	9.8
20	9.0	9.4	10.1
21	9.2	9.7	10.4
22	9.4	9.9	10.6
23	9.6	10.1	10.9
24	9.8	10.3	11.1
25	10.0	10.5	11.4

(Continued)

Table E3 (Continued)

GRID LOCATION 3, 6 LAT=45.75 LON=83.50 FALSE DETOUR CHANNEL MI

GRID POINT NUMBER 27

SIGNIFICANT PERIOD BY ANGLE CLASS AND WAVE HEIGHT

WAVE HEIGHT (FT)	ANGLE CLASS		
	1	2	3
1	3.6	3.5	3.6
2	4.8	4.6	4.6
3	5.4	5.2	5.0
4	5.8	5.6	5.5
5	6.2	6.0	5.9
6	6.4	6.3	6.2
7	6.7	6.5	6.5
8	6.9	6.8	6.7
9	7.2	7.0	7.0
10	7.4	7.3	7.3
11	7.6	7.6	7.6
12	7.9	7.8	7.9
13	8.1	8.1	8.1
14	8.4	8.3	8.4
15	8.6	8.6	8.7
16	8.8	8.9	9.0
17	9.1	9.1	9.3
18	9.3	9.4	9.5
19	9.6	9.6	9.8
20	9.8	9.9	10.1
21	10.0	10.2	10.4
22	10.3	10.4	10.7
23	10.5	10.7	10.9
24	10.8	10.9	11.2
25	11.0	11.2	11.5

(Continued)

Table E3 (Concluded)

GRID LOCATION 3, 7 LAT=45.75 LON=83.30 COCKBURN ISLAND MI

GRID POINT NUMBER 28

SIGNIFICANT PERIOD BY ANGLE CLASS AND WAVE HEIGHT

WAVE HEIGHT (FT)	ANGLE CLASS		
	1	2	3
1	3.6	3.8	3.7
2	4.6	4.7	4.5
3	5.2	5.1	5.0
4	5.6	5.6	5.5
5	6.0	6.0	5.9
6	6.3	6.3	6.2
7	6.5	6.6	6.4
8	6.8	6.9	6.7
9	7.0	7.2	6.9
10	7.3	7.4	7.2
11	7.6	7.7	7.5
12	7.8	8.0	7.7
13	8.1	8.3	8.0
14	8.3	8.6	8.2
15	8.6	8.9	8.5
16	8.9	9.2	8.8
17	9.1	9.5	9.0
18	9.4	9.8	9.3
19	9.6	10.1	9.5
20	9.9	10.4	9.8
21	10.2	10.6	10.1
22	10.4	10.9	10.3
23	10.7	11.2	10.6
24	10.9	11.5	10.8
25	11.2	11.8	11.1

Table E4

Azimuths of Normal Shoreline Vectors*

Shoreline Point	Azimuth	Shoreline Point	Azimuth
1	180	15	270
2	240	16	270
3	270	17	270
4	270	18	240
5	270	19	210
6	270	20	210
7	240	21	210
8	210	22	210
9	180	23	210
10	210	24	330
11	300	25	0
12	300	26	0
13	300	27	0
14	270	28	0

* See Figure 21.

APPENDIX F: NOTATION

a	Regression constant (Equation 2), and Phillips equilibrium constant (Equation B9)
a_ℓ, a_s	Regression coefficients relating wind speeds at different elevations (ℓ = above 20 ft, s = at 20 ft)
a_n	Parameter in asymptotic distribution of extreme values
b	Regression constant
b_n	Parameter in asymptotic distribution of extreme values
B	Linear constant for log-linear wind profile (Appendix A), and coefficient of energy transfer and function of propagation direction relative to wind direction and wind speed (Appendix B)
B_ℓ, B_s	Regression coefficients relating wind speeds at different elevations (ℓ = above 20 ft, s = at 20 ft)
C_f	Coefficient of bottom friction
C_G	Group velocity
d	Water depth
d_j	Distance between j^{th} wind station and interpolation point
e	Napierian base = 2.71828...
E	Total wave energy
$E(f)$	One-dimensional representation of wave spectrum
$E_\infty(f)$	Fully developed wave spectrum
f	Frequency
f_{max}	Frequency associated with maximum spectral density
f_1, f_2	Lowest and highest frequency, respectively, in the model
F	Land-bounded fetch (Equation 10), and wave component (Equation B15)
$F(f,\theta)$	Two-dimensional representation of wave spectrum
$F(x)$	Cumulative probability function of x
$F(\vec{x},\vec{k},t)$	Five-dimensional representation of wave spectrum
$F(H)$	Cumulative probability function of H
$F(L)$	Ice-limited fetch
$F(\omega)$	One-dimensional spectral energy density and function of ω
g	Function (Equation 10) and gravitational acceleration
G	Geostrophic wind velocity (Parts I-IV) and function (Equation A1)

$h(\theta)$	Spreading factor
H	Wave height
H'	Wave height transformed by fetch reduction (Equation 11), and wave height as hindcast by model (Equation D9)
H^*	Reduced wave height variate
H_L	Ice-limited wave height
$H_{1/3}$	Significant wave height
i	Conventional summation over all dimensions
k	Parameter denoting curvature in extremal distribution (Equation 5), and KEYPS function constant (Equation A13)
$\vec{k}$	Wave number vector
K	Von Karman constant
ℓ_i	Series product of distances between wind stations and interpolation point
L'	Stability length
n	Number of independent observations within a season or year
N	Number of years in a sample (Figure 23), and number of wind stations (Appendix C)
NORM	Sum of multiple products ℓ_i
$p(H)$	Probability of a particular wave height occurring at a site
$p'(H)$	Probability of a particular wave height occurring estimated from hindcasts not considering ice cover
$p(\varepsilon)$	Probability of no ice at the site
q	Ratio of energy density in spectrum to that in fully developed spectrum
R	Ratio of lake-wind speed to land-wind speed (Equations 1 and 2), and angular spreading function in Barnett model (Equation B11)
S	Sum of all exterior sources and sinks of energy transfer into spectrum (Equation B7), and standard deviation of annual maxima (Equation D8)
S_B	Sum of sources in Barnett model
S_I	Sum of sources in Inoue model
S_ℓ	Sum of linear source terms
S_x	Standard deviation of the estimate
$S_{n\ell}$	Sum of nonlinear source terms
S_1-S_4	Sources involving weak interactions between winds and waves

S_1'-S_4'	Sources involving weak interactions between currents and waves
S_5	Source involving weak interactions among different spectral components of waves
S_6	Source involving weak interactions between bottom and waves
S_7	Unknown dissipation function due to breaking
t	Time (Equation B1), and wind duration (Equation A3)
T	Return period or recurrence interval (Equation 6), and nondimensional time factor (Equation A1)
T'	Return period as modified by ice cover
T_a	Air temperature
T_ℓ	Recurrence interval at elevation above 20 ft
T_s	Lake surface temperature (Figures 9 and 11), and recurrence interval at 20-ft elevation (Equation A6)
T_w	Water temperature
T_1,T_2	Transfer functions dependent on coupling coefficients between spectral components involved in the interactions
u	Wind speed (Equation A4), fluid velocity relative to the bottom (Equation B26), and parameter of the double-exponential distribution (Equation D1)
u_*	Friction velocity
U	East-west wind component
U_ℓ	Wind speed over land
U_w	Wind speed over water
V	Anemometer-level wind (Figure 11), and north-south wind component (Appendix C)
V_o	Wind velocity (Equation A9)
W_i	Weighting of interpolation function on i^{th} wind station
x	Actual fetch (Equation A2)
$\vec{x}$	Location vector
x_o	Parameter of extremal distribution
X	Nondimensional fetch factor
X_ℓ	Distance inland from lake-land interface
y	Reduced variate in distribution of extremes
Z	Elevation (Equation A4), and parameter of the combined double-exponential and Gaussian distribution (Equation D15)
Z_o	Roughness height

α Parameter of extremal distribution (Equation 5), energy transfer due to interaction between turbulent pressure fluctuations and waves--Phillips' mechanism (Equation B7), and parameter of double-exponential distribution (Equation D1)

β Energy transfer due to interaction between mean wind profile and waves--Miles' mechanism (Equation B9), and inverse of α (Equation D20)

γ Function of $\vec{k},\vec{k}'$ in Equation B7

Γ Parameter of wave-wave interactions

δ Integration variable

δ_* Land boundary layer thickness

δ_{ij} Kronecker delta

Δt Increment of time in numerical equation

ε Nondimensional wind shear (Equation A12), and function of $\vec{k},\vec{k}'$ (Equation B7)

θ Direction of wave propagation

θ_w Direction of wind heading

θ_1,θ_2 Limiting angles for wave propagation toward the shore

ν Dynamic viscosity of air

ν_{ij} Viscosity tensor

π 3.1416

Π Nondimensional wave height

σ Circular frequency associated with F (Equation B4), and standard deviation of the errors in hindcast wave heights (Equation D11)

σ^2 Variance of surface in a wave spectrum (related to total energy)

τ Parameter of wave-wave interactions

ϕ Modification function of Z/L' for wind profile due to thermal effects (Equation A10), and limiting function for wind input in Barnett model (Equation B10)

Φ Effect of ice cover at site on return periods (Equation 8), and probability integral (Equation D16)

$\Phi(f,\theta)$ Frictional dissipation function

Φ_n Normalized function dependent on air-sea temperature difference (Equation 2)

Ψ Function of Z, which relates estimated wave height distribution to actual wave height distribution

ψ_v Velocity-dependent function (Equation 2)

ω Angular frequency

ω_o Wind frequency

In accordance with letter from DAEN-RDC, DAEN-ASI dated 22 July 1977, Subject: Facsimile Catalog Cards for Laboratory Technical Publications, a facsimile catalog card in Library of Congress MARC format is reproduced below.

Resio, Donald T
Design wave information for the Great Lakes; Report 4: Lake Huron / by Donald T. Resio, Charles L. Vincent. Vicksburg, Miss. : U. S. Waterways Experiment Station, 1977.
49, ₍104₎ p. : ill. ; 27 cm. (Technical report - U. S. Army Engineer Waterways Experiment Station ; H-76-1, Report 4)
Prepared for U. S. Army Engineer Division, North Central, Chicago, Illinois.
References: p. 45-49.

1. Design wave. 2. Great Lakes. 3. Lake Huron. 4. Water waves. I. Vincent, Charles L., joint author. II. United States. Army. Corps of Engineers. North Central Division. III. Series: United States. Waterways Experiment Station, Vicksburg, Miss. Technical report ; H-76-1, Report 4.
TA7.W34 no.H-76-1 Report 4